(12) INTERNATIONAL APPLICATION PUBLISHED UNDER THE PATENT COOPERATION TREATY (PCT)

(19) World Intellectual Property Organization
International Bureau

(43) International Publication Date
20 September 2018 (20.09.2018)

WIPO | PCT

(10) International Publication Number
WO 2018/170152 A1

(51) International Patent Classification:
A61K 38/54 (2006.01) *C07K 19/00* (2006.01)
A61K 38/43 (2006.01)

(21) International Application Number:
PCT/US2018/022471

(22) International Filing Date:
14 March 2018 (14.03.2018)

(25) Filing Language: English

(26) Publication Language: English

(30) Priority Data:
1704071.8 14 March 2017 (14.03.2017) GB

(71) Applicant: **GEMINI THERAPEUTICS** [US/US]; 36 Irving Street, No. 3, Cambridge, MA 02138 (US).

(72) Inventors: **KAVANAGH, David**; Framlington Place, Newcastle-upon-Tyne NE2 4HH (GB). **MARCHBANK, Kevin**; Framlington Place, Newcastle-upon-Tyne NE2 4HH (GB).

(74) Agent: **VARMA, Anita** et al.; White & Case LLP, 75 State Street, Boston, MA 02109 (US).

(81) Designated States *(unless otherwise indicated, for every kind of national protection available)*: AE, AG, AL, AM, AO, AT, AU, AZ, BA, BB, BG, BH, BN, BR, BW, BY, BZ, CA, CH, CL, CN, CO, CR, CU, CZ, DE, DJ, DK, DM, DO, DZ, EC, EE, EG, ES, FI, GB, GD, GE, GH, GM, GT, HN, HR, HU, ID, IL, IN, IR, IS, JO, JP, KE, KG, KH, KN, KP, KR, KW, KZ, LA, LC, LK, LR, LS, LU, LY, MA, MD, ME, MG, MK, MN, MW, MX, MY, MZ, NA, NG, NI, NO, NZ, OM, PA, PE, PG, PH, PL, PT, QA, RO, RS, RU, RW, SA, SC, SD, SE, SG, SK, SL, SM, ST, SV, SY, TH, TJ, TM, TN, TR, TT, TZ, UA, UG, US, UZ, VC, VN, ZA, ZM, ZW.

(84) Designated States *(unless otherwise indicated, for every kind of regional protection available)*: ARIPO (BW, GH, GM, KE, LR, LS, MW, MZ, NA, RW, SD, SL, ST, SZ, TZ, UG, ZM, ZW), Eurasian (AM, AZ, BY, KG, KZ, RU, TJ, TM), European (AL, AT, BE, BG, CH, CY, CZ, DE, DK, EE, ES, FI, FR, GB, GR, HR, HU, IE, IS, IT, LT, LU, LV, MC, MK, MT, NL, NO, PL, PT, RO, RS, SE, SI, SK, SM, TR), OAPI (BF, BJ, CF, CG, CI, CM, GA, GN, GQ, GW, KM, ML, MR, NE, SN, TD, TG).

Published:
— *with international search report (Art. 21(3))*
— *with sequence listing part of description (Rule 5.2(a))*

(54) Title: RECOMBINANT MATURE COMPLEMENT FACTOR I

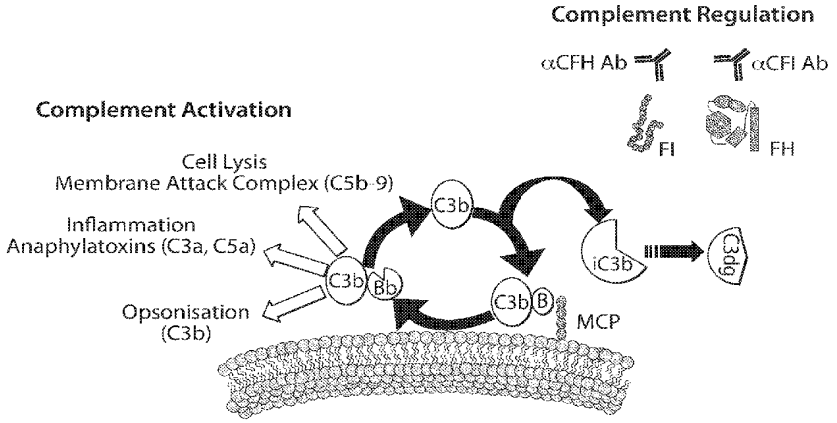

Figure 1

(57) Abstract: The disclosure provides, in part, compositions comprising mature recombinant mature Complement Factor I (CFI) protein and methods of making and using those compositions.

WO 2018/170152 A1

RECOMBINANT MATURE COMPLEMENT FACTOR I

Cross-Reference to Related Application

This application claims the benefit of priority from Great Britain Patent Application No. 1704071.8, filed on March 14, 2017. The foregoing application is incorporated herein by reference in its entirety.

Technical Field

Aspects of the present invention relate to a recombinant mature Complement Factor I protein, compositions comprising such proteins and methods of manufacture and uses thereof. Also included herein are methods of treating a complement-mediated disorder comprising administering a composition comprising a recombinant mature Complement Factor I protein to a patient in need thereof.

Background to the Invention

The complement system is a part of the innate immune system which is made up of a large number of discrete plasma proteins that react with one another to opsonize pathogens and induce a series of inflammatory responses that help to fight infection. A number of complement proteins are proteases that are themselves activated by proteolytic cleavage. There are three ways in which the complement system protects against infection. First, it generates large numbers of activated complement proteins that bind covalently to pathogens, opsonizing them for engulfment by phagocytes bearing receptors for complement. Second, the small fragments of some complement proteins act as chemo-attractants to recruit more phagocytes to the site of complement activation, and also to activate these phagocytes. Third, the terminal complement components damage certain bacteria by creating pores in the bacterial membrane.

Complement Factor I, also known as C3b/C4b inhibitor, is a serine proteinase that is essential for regulating the complement cascade. It is expressed in numerous tissues but principally by liver hepatocytes. The encoded preproprotein is cleaved to produce both heavy and light chains, which are linked by disulfide bonds to form a heterodimeric glycoprotein. This heterodimer can cleave and inactivate the complement components C4b and C3b, and it prevents the assembly of the C3 and C5 convertase enzymes. Defects in this gene cause complement factor I deficiency, an autosomal recessive disease associated with a susceptibility to pyogenic infections.

Mutations in this gene have been associated with a predisposition to atypical hemolytic uremic syndrome, a disease characterized by acute renal failure, microangiopathic hemolytic anemia and thrombocytopenia. Recently low levels of circulating CFI have been identified in individuals with very rare CFI variant genes and these individuals associated with advanced Age-Related Macular Degeneration (AMD) supporting the role of CFI in risk of AMD (Kavanagh et al (2015). AMD is the most common cause of vision loss in those aged over 50 and currently there are few treatment options. This research suggests that enhancing CFI activity in these individuals may have some therapeutic benefit.

Currently, efforts to produce compositions comprising a high percentage of recombinant mature CFI have had limited success. Typically, prior art methods result in incomplete cleavage of the proform to form the mature CFI protein. Thus, the prior art typically results in compositions comprising significant amounts of uncleaved proform protein. Furthermore, previous efforts have resulted in compositions which have reduced activity as compared to plasma-derived Complement Factor I.

It is therefore an aim of certain embodiments of the present invention to at least partially mitigate the problems associated with the prior art.

It is an aim of certain embodiments of the present invention to provide a method for producing a composition which comprises a high concentration of recombinant mature Complement Factor I.

It is an aim of certain embodiments to provide a composition comprising recombinant mature Complement Factor I for use in the treatment of complement-mediated disorders.

Summary of the Disclosure

Unless defined otherwise, all technical and scientific terms used herein have the same meaning as commonly understood by a person skilled in the art to which to this invention belongs.

Certain aspects of the present invention provide an isolated recombinant mature Complement Factor I.

The term "isolated" as used herein refers to a biological component (such as a nucleic acid molecule or protein) that has been substantially separated or purified away from other biological components in the cell of the organism in which the component naturally occurs, i.e., other chromosomal and extra chromosomal DNA and RNA, and proteins. Nucleic acids and proteins that have been "isolated" include nucleic acids and proteins purified by standard purification methods. The term also embraces nucleic acids and proteins prepared by recombinant expression in a host cell as well as chemically synthesized nucleic acids, proteins and peptides.

It is considered that the present inventors have devised a method of producing an isolated recombinant mature CFI protein which is substantially isolated from other cellular components including for example a recombinant precursor CFI protein. It is considered that prior art methods of producing a recombinant CFI protein have resulted in incomplete processing of a precursor CFI protein such that a recombinant mature CFI protein has not been substantially isolated.

In a first aspect of the present invention, there is provided a composition comprising a recombinant mature Complement Factor I (CFI) protein, wherein the recombinant mature CFI protein comprised in the composition represents greater than about 50% by weight of a total CFI protein content of the composition.

Thus, certain embodiments of the present invention relate to a recombinant mature Complement Factor I (CFI), compositions comprising recombinant mature Complement Factor I and methods of obtaining such a protein.

As used herein, the term "protein" can be used interchangeably with "peptide" or "polypeptide", and means at least two covalently attached alpha amino acid residues linked by a peptidyl bond. The term protein encompasses purified natural products, or chemical products, which may be produced partially or wholly using recombinant or synthetic techniques. The term protein may refer to a complex of more than one polypeptide, such as a dimer or other multimer, a fusion protein, a protein variant, or derivative thereof. The term also includes modified proteins, for example, a protein modified by glycosylation, acetylation, phosphorylation, pegylation, ubiquitination, and so forth. A protein may comprise amino acids not encoded by a nucleic acid codon.

Complement Factor I is an important complement regulator. It is expressed in numerous tissues but principally by liver hepatocytes. CFI is a heterodimer in which the two chains are

linked together by disulphide bond. The heavy chain contains the Factor I module, a CD5 domain and two low density lipoprotein receptor domains (LDLr). The light chain comprises a serine protease domain, the active site of which consists of a triad of His380, Asp439 and Ser525. A CFI heavy chain amino acid sequence is shown in SEQ ID. No. 1 and a CFI light chain amino acid sequence is shown in SEQ ID. No. 2 (Figure 2).

When CFI is synthesised, it is initially made as a single chain precursor (precursor CFI protein), in which a four residue linker peptide (RRKR) connects the heavy chain to the light chain. Thus, as used herein, the term "precursor CFI protein" is used to refer to a single chain precursor Complement Factor I protein which comprises a four residue linker peptide (RRKR). Aptly, the precursor CFI protein is substantially inactive and has essentially no C3 C3b-inactivating or iC3b-degradation activity. In certain embodiments, the recombinant precursor CFI protein comprises an amino acid sequence as set forth in SEQ. ID. No. 3 (Figure 2).

During processing, the precursor CFI protein is cleaved by a calcium-dependent serine endoprotease, furin, leaving the heavy chain and light chain of full length mature FI held together by a single disulphide bond. This protein is referred to herein as a mature CFI protein.

Thus, as used herein, the term "mature CFI protein" refers to a CFI protein which is or has been cleaved at or adjacent to a RRKR linker sequence e.g. by furin. In certain embodiments, the mature CFI protein lacks an RRKR linker sequence as compared to a precursor CFI protein, wherein the precursor CFI protein comprises a RRKR linker sequence at positions 318 to 321. In other embodiments, the mature CFI protein is cleaved adjacent to the RRKR linker sequence and therefore the mature CFI protein may comprise a light chain and a heavy chain, one or both of which comprises one or more amino acid residues of the linker sequence. In certain embodiments, the recombinant precursor CFI protein is a non-human mammalian CFI protein.

In certain embodiments, a mature CFI protein comprises a disulphide bond and wherein the recombinant mature CFI protein is cleavable into a heavy chain and a light chain upon reduction of the disulphide bond. In certain embodiments, the mature CFI protein comprises a heavy chain comprising a Factor I module, a CD5 module, an LDLr module, LDLr module and a light chain comprising a serine protease domain. In certain embodiments, the mature CFI protein is glycosylated.

As used herein, the term "recombinant precursor CFI protein" is used to refer to a precursor CFI protein as described above which is obtained using recombinant methods.

As used herein, the term "total CFI protein content" refers to a total content of the combination of recombinant mature CFI protein and a recombinant precursor CFI protein present in a single composition.

Aptly, a "recombinant mature CFI protein" is a mature CFI protein defined above which is made by recombinant expression, i.e. it is not naturally occurring or derived from plasma. Aptly, a wild-type mature CFI protein comprises two chains, each chain undergoing glycosylation which results in a total of six N-linked glycosylation sites which adds up to 3kDa of carbohydrate to the predicted molecular weight of 85kDa.

The recombinant mature CFI protein may have a different glycosylation pattern to a naturally-derived i.e. plasma-derived mature CFI protein.

The terms "recombinant" and "recombinant expression" are well-known in the art. The term "recombinant expression", as used herein, relates to transcription and translation of an exogenous gene in a host organism. Exogenous DNA refers to any deoxyribonucleic acid that originates outside of the host cell. The exogenous DNA may be integrated in the genome of the host or expressed from a non-integrating element.

A recombinant protein includes any polypeptide expressed or capable of being expressed from a recombinant nucleic acid. Thus, a recombinant mature CFI protein is expressed by a recombinant DNA sequence. Aptly, the recombinant mature CFI protein has undergone post-expression processing to be cleaved at or adjacent to a RRKR linker sequence to leave a heterodimer as described herein.

In certain embodiments, the recombinant mature CFI protein represents greater than about 60% by weight of the total CFI protein content of the composition. In certain embodiments, the recombinant mature CFI protein represents greater than about 70% by weight of the total CFI protein content of the composition. In one embodiment, the recombinant mature CFI protein represents greater than about 80% by weight of the total CFI protein content of the composition.

In certain embodiments, the recombinant mature CFI protein represents greater than about 90% by weight of the total CFI protein content of the composition. Aptly, the recombinant

mature CFI protein represents greater than about 95% by weight of the total CFI protein content of the composition.

In certain embodiment, the composition further comprises a recombinant precursor Complement Factor I protein, wherein the ratio of recombinant mature CFI: recombinant precursor CFI in the composition is from greater than 50:50 to 100:0.

In a second aspect of the present invention, there is provided a composition comprising a recombinant mature Complement Factor I (CFI) protein and optionally a recombinant precursor Complement Factor I protein, wherein the ratio of recombinant mature CFI: recombinant precursor CFI in the composition is from greater than 50:50 to 100:0.

In certain embodiments, the ratio of recombinant mature CFI: recombinant precursor CFI in the composition is from 60:40 to 100:0. In certain embodiments, the ratio of recombinant mature CFI: recombinant precursor CFI in the composition is from 70:30 to 100:0. In certain embodiments, the ratio of recombinant mature CFI: recombinant precursor CFI in the composition is from 80:20 to 100:0, for example from about 90:10 to 100:0, for example from 95:05 to 100:0.

In certain embodiments, the recombinant CFI protein is a human CFI protein. In certain embodiments, the recombinant mature CFI protein comprises a first amino acid molecule comprising an amino acid sequence as set forth in SEQ. ID. No. 1. In certain embodiments, the recombinant mature CFI protein comprises a first amino acid molecule comprising an amino acid sequence which has at least 80% sequence identity to the amino acid sequence as set forth in SEQ. ID. No. 1. Aptly, the % sequence identity is over the entire length of the amino acid sequence set forth in SEQ. ID. No. 1.

In certain embodiments, the recombinant mature CFI protein comprises a first amino acid sequence that is at least 90% identical to the amino acid sequence as set forth in SEQ ID NO: 1, e.g. at least 91%, 92%, 93% or 94%. In certain embodiments, the recombinant mature CFI protein comprises a first amino acid molecule comprising an amino acid sequence that is at least 95% identical to the amino acid sequence as set forth in SEQ ID NO: 1, e.g. 96%, 97%, 98%, 99% or 100% identical.

In certain embodiments, the recombinant mature CFI protein comprises a further amino acid molecule comprising an amino acid sequence as set forth in SEQ. ID. No. 2, wherein the first and further amino acid sequence are linked by a disulphide bond.

In certain embodiments, the recombinant mature CFI protein comprises a further amino acid molecule comprising an amino acid sequence which has at least 80% sequence identity to the amino acid sequence as set forth in SEQ. ID. No. 2 wherein the first and further amino acid sequence are linked by a disulphide bond. In certain embodiments, the recombinant mature CFI protein comprises an amino acid sequence that is at least 90% identical to the amino acid sequence as set forth in SEQ ID NO: 1, e.g. at least 91%, 92%, 93% or 94% identical.

In certain embodiments, the recombinant mature CFI protein comprises a further amino acid molecule comprising an amino acid sequence that is at least 95% identical to the amino acid sequence as set forth in SEQ ID NO: 2, e.g. at least 96%, 97%, 98%, 99% or 100% identical.

Thus, in certain embodiments, proteins having minor modifications in the sequence may be equally useful, provided they are functional. The terms "sequence identity", "percent identity" and "sequence percent identity" in the context of two or more nucleic acids or polypeptides, refer to two or more sequences or subsequences that are the same or have a specified percentage of nucleotides or amino acid residues that are the same, when compared and aligned (introducing gaps, if necessary) for maximum correspondence, not considering any conservative amino acid substitutions as part of the sequence identity. The percent identity can be measured using sequence comparison software or algorithms or by visual inspection. Various algorithms and software are known in the art that can be used to obtain alignments of amino acid or nucleotide sequences.

Suitable programs to determine percent sequence identity include for example the BLAST suite of programs available from the U.S. government's National Center for Biotechnology Information BLAST web site (http://blast.ncbi.nlm.nih.gov/Blast.cgi). Comparisons between two sequences can be carried using either the BLASTN or BLASTP algorithm. BLASTN is used to compare nucleic acid sequences, while BLASTP is used to compare amino acid sequences. ALIGN, ALIGN-2 (Genentech, South San Francisco, California) or MegAlign, available from DNASTAR, are additional publicly available software programs that can be used to align sequences. One skilled in the art can determine appropriate parameters for maximal alignment by particular alignment software. In certain embodiments, the default parameters of the alignment software are used.

In certain embodiments, the recombinant mature CFI protein may comprise an amino acid sequence comprising one or more mutations as compared to a reference sequence. In certain embodiments, the reference sequence is as shown in SEQ. ID. No. 1 and 2. In certain embodiments, the mutation may be an insertion, a deletion, or a substitution.

Substitutional variants of proteins are those in which at least one amino acid residue in the amino acid sequence has been removed and a different amino acid residue inserted in its place. The mature recombinant CFI protein of certain embodiments of the present invention can contain conservative or non-conservative substitutions.

The term "conservative substitution" as used herein relates to the substitution of one or more amino acid residues for amino acid residues having similar biochemical properties. Typically, conservative substitutions have little or no impact on the activity of a resulting protein. Screening of variants of the CFI proteins described herein can be used to identify which amino acid residues can tolerate an amino acid residue substitution. In one example, the relevant biological activity of a modified protein is not decreased by more than 25%, preferably not more than 20%, especially not more than 10%, compared with CFI when one or more conservative amino acid residue substitutions are effected.

In certain embodiments, the composition is essentially free of a furin protein or fragments thereof. Furin is a subtilisin-like proprotein convertase which cleaves protein *in vivo* at a minimal cleavage site of Arg-X-X-Arg. A human furin protein comprises an amino acid sequence as set forth in SEQ. ID. 4.

In certain embodiments, the composition is a pharmaceutical composition. The pharmaceutical composition further comprises one or more pharmaceutically acceptable excipients. Further details of pharmaceutical compositions are provided herein.

In a further aspect of the present invention, there is provided a method of preparing a composition comprising a recombinant mature Complement Factor I (CFI) protein, wherein the recombinant mature CFI protein represents greater than 50% by weight of a total CFI protein content of the composition, the method comprising:

a. contacting a recombinant precursor CFI protein with a furin protein or fragment thereof; and
b. incubating the recombinant precursor CFI protein with the furin protein or fragment thereof for a predetermined period of time, whereby the furin protein or fragment thereof cleaves the recombinant precursor CFI protein at or

adjacent to a RRKR linker sequence site to form the recombinant mature Complement Factor I protein.

In certain embodiments, the recombinant precursor CFI protein is a human precursor CFI protein. the recombinant precursor CFI protein comprises an amino acid sequence as set forth in SEQ. ID. No: 3. In certain embodiments, the recombinant precursor CFI protein is as described herein.

In certain embodiments, the recombinant precursor CFI protein comprises a tag. In certain embodiments, the tag is a His-tag.

In certain embodiments, the method comprises expressing the recombinant precursor CFI protein prior to step (a). In certain embodiments, the method comprises expressing the recombinant precursor CFI protein in a eukaryotic cell.

In certain embodiments, the method comprises expressing the recombinant precursor CFI protein in a prokaryotic cell. Aptly, the prokaryotic cell is *Escherichia coli*.

In certain embodiments, the eukaryotic cell is selected from an insect, a plant, a yeast or a mammalian cell.

Suitable host cells for cloning or expressing the DNA encoding a CFI protein include prokaryote, yeast, or higher eukaryote cells. Suitable prokaryotes for this purpose include eubacteria, such as Gram-negative or Gram-positive organisms, for example, Enterobacteriaceae such as Escherichia, e.g., *E. coli*, Enterobacter, Erwinia, Klebsiella, Proteus, Salmonella, e.g., *Salmonella typhimurium*, Serratia, e.g., *Serratia marcescans*, and Shigella, as well as Bacilli such as B. subtilis and B. licheniformis, Pseudomonas such as P. aeruginosa, and Streptomyces.

In addition to prokaryotes, eukaryotic microbes such as filamentous fungi or yeast may be suitable cloning or expression hosts for CFI-encoding vectors. Saccharomyces cerevisiae, or common baker's yeast, is the most commonly used among lower eukaryotic host microorganisms although others may be useful.

In certain embodiments, the host cell is a mammalian host cell e.g. monkey kidney CV1 line transformed by SV40 (e.g. COS-7); human embryonic kidney line (e.g. 293 or 293 cells); baby hamster kidney cells (e.g. BHK); Chinese hamster ovary cells/-DHFR (CHO), mouse

sertoli cells (e.g. TM4); monkey kidney cells (e.g. CV1); African green monkey kidney cells (e.g. VERO-76); human cervical carcinoma cells (e.g. HELA); canine kidney cells (e.g. MDCK); buffalo rat liver cells (e.g. BRL 3A); human lung cells (e.g. W138); human liver cells (e.g. Hep G2); mouse mammary tumor (MMT 060562); TRI cells, MRC 5 cells and FS4 cells. In certain embodiments, the mammalian cell is a CHO cell.

Host cells are transformed with the above-described expression or cloning vectors for antibody production and cultured in conventional nutrient media modified as appropriate for inducing promoters, selecting transformants, or amplifying the genes encoding the desired sequences.

In certain embodiments, the method comprises transforming the cell with a nucleic acid molecule encoding a precursor CFI protein. Aptly, the method comprises transforming the cell with a vector which encodes a precursor CFI protein as described herein.

"Nucleic acid molecule' or 'nucleic acid sequence", as used herein, refers to a polymer of nucleotides in which the 3' position of one nucleotide sugar is linked to the 5' position of the next by a phosphodiester bridge. In a linear nucleic acid strand, one end typically has a free 5' phosphate group, the other a free 3' hydroxyl group. Nucleic acid sequences may be used herein to refer to oligonucleotides, or polynucleotides, and fragments or portions thereof, and to DNA or RNA of genomic or synthetic origin that may be single- or double-stranded, and represent the sense or antisense strand.

The term "vector" as used herein means a nucleic acid sequence containing an origin of replication. A vector may be a viral vector, bacteriophage, bacterial artificial chromosome or yeast artificial chromosome. A vector may be a DNA or RNA vector. A vector may be a self-replicating extrachromosomal vector, and aptly, is a DNA plasmid.

Aptly, the vector may further comprise a promoter. The term "promoter" as used herein means a synthetic or naturally-derived molecule which is capable of conferring, activating or enhancing expression of a nucleic acid in a cell. A promoter may comprise one or more specific transcriptional regulatory sequences to further enhance expression and/or to alter the spatial expression and/or temporal expression of same. A promoter may also comprise distal enhancer or repressor elements, which may be located as much as several thousand base pairs from the start site of transcription. A promoter may regulate the expression of a gene component constitutively, or differentially with respect to cell, the tissue or organ in which expression occurs or, with respect to the developmental stage at which expression

occurs, or in response to external stimuli such as physiological stresses, pathogens, metal ions, or inducing agents.

In certain embodiments, the method comprises isolating the expressed recombinant precursor CFI protein prior to step (a). In certain embodiments, step (a) comprises adding the furin protein or fragment thereof to a solution comprising the expressed recombinant precursor CFI protein.

In certain embodiments, step (b) comprises incubating the furin protein or fragment thereof with the recombinant precursor CFI protein at a temperature of between about 25°C to about 42°C.

In certain embodiments, step (b) comprises incubating the furin protein or fragment thereof with the recombinant precursor CFI protein at a temperature of between about 30°C to about 42°C.

In certain embodiments, step (b) comprises incubating the furin protein or fragment thereof with the recombinant precursor CFI protein at a temperature of between about 35°C to about 38°C.

In certain embodiments, step (b) comprises incubating the furin protein or fragment thereof with the recombinant precursor CFI protein in a solution having a pH of between about 5 and 7.

In certain embodiments, step (b) comprises incubating the furin protein or fragment thereof with the recombinant precursor CFI protein in a solution having a pH of between about 5 and 6.

In certain embodiments, the solution comprises calcium ions. In certain embodiments, the solution comprises calcium ions at a concentration of between about 1mM to about 5mM. In certain embodiments, the solution further comprises potassium ions.

In certain embodiments, step (b) comprises incubating the furin protein or fragment thereof with the recombinant precursor CFI protein for between about 5 hours and about 48 hours.

In certain embodiments, step (b) comprises incubating the furin protein or fragment thereof with the recombinant precursor CFI protein for between about 8 hours and about 20 hours.

In certain embodiments, the furin protein is a human furin protein or fragment thereof. In certain embodiments, the furin protein is a fragment of a mature furin protein. Aptly, the furin protein is a truncated furin protein which is terminated before the transmembrane domain. Aptly the truncated furin protein comprises at least one or more amino acid residues at a position at or between 595-791 that is involved in the catalytic activity of furin e.g. to cleave at a RRKR linker sequence.

In certain embodiments, the furin protein or fragment thereof is glycosylated. Aptly, the furin protein or fragment thereof is glycosylated at one or more amino acid residues selected from Asn387, Asn440 and Asn553.

In certain embodiments, the furin protein or fragment thereof has a molecular weight of 60 kDa or greater. Aptly, the furin protein or fragment thereof has a molecular weight of between about 65 to 85 kDa. In certain embodiments, the furin protein or fragment thereof comprises a tag e.g. a His tag.

In certain embodiments, the furin protein or fragment thereof comprises the amino acid sequence as set forth in SEQ. ID. No.4 or a fragment thereof. In certain embodiments, the furin protein fragment comprises at least amino acid residues 108 to 715 of a protein comprising the amino acid sequence as set forth in SEQ. ID. No: 4.

In certain embodiments, the furin protein is a protein having at least 80%, e.g. at least 85%, 90%, 91%, 92%, 93%, 94%, 95%, 96%, 97%, 98%, 99% or 100% sequence identity with a protein having a sequence as depicted in SEQ. ID. No. 4. Aptly, the % sequence identity is over the entire length of the amino acid sequence set forth in SEQ. ID. No. 4. In certain embodiments, the furin protein is a protein having at least 80% at least 85%, 90%, 91%, 92%, 93%, 94%, 95%, 96%, 97%, 98%, 99% or 100% sequence identity with the sequence consisting of amino acid residues 108 to 715 of SEQ. ID. No. 4.

In certain embodiments, the furin protein or fragment thereof is expressed in a mammalian cell. Aptly, the method comprises obtaining a furin protein or fragment thereof which has been expressed in a mammalian cell.

In certain embodiments, the method further comprises isolating the recombinant mature CFI protein. In certain embodiments, the method further comprises purifying the isolated

recombinant mature CFI protein. In certain embodiments, the recombinant mature CFI protein is as described herein.

In a further aspect of the present invention, there is a composition obtainable from the method described herein.

In a further aspect of the present invention, there is provided a composition according to aspects of the present invention for use in the treatment of a complement-mediated disorder. In certain embodiments, the composition is for use in the treatment of a C3 myopathy.

In certain embodiments, the composition is for use in the treatment of a complement-mediated disorder. In certain embodiments, the composition is for use in the treatment of a disorder associated with Complement Factor I deficiency. Such disorders may be characterised by severe and often recurrent infections.

In a further aspect of the present invention, there is provided a method of treating a complement-mediated disorder, the method comprising:

a) administering a therapeutically effective amount of a composition as described herein to a subject in need thereof.

In certain embodiments, the method is a method of treating a C3 myopathy.

In certain embodiments, the composition is for use in the treatment of a disorder associated with Complement Factor I deficiency. Such disorders may be characterised by severe and often recurrent infections.

In certain embodiments, the complement-mediated disorder is selected from age-related macular degeneration (AMD), Alzheimer's Disease, atypical haemolytic uraemic syndrome (aHUS), membranoproliferative glomerulonephritis Type 2 (MPGN2), atherosclerosis (in particular, accelerated atherosclerosis) and chronic cardiovascular disease.

In certain embodiments, the composition is for use in the treatment of a complement-associated eye condition, for example, age-related macular degeneration (AMD), choroidal neovascularization (CNV), uveitis, diabetic and other ischemia-related retinopathies, diabetic macular edema, pathological myopia, von Hippel-Lindau disease, histoplasmosis of the eye, Central Retinal Vein Occlusion (CRVO), corneal neovascularization, and retinal neovascularization.

In certain embodiments, the composition is for use in the treatment of age-related macular degeneration. Age-related Macular Degeneration (AMD) is the leading cause of blindness in the elderly worldwide. AMD is characterized by a progressive loss of central vision attributable to degenerative and neovascular changes in the macula, a highly specialized region of the ocular retina responsible for fine visual acuity. In certain embodiments, the group of complement-associated eye conditions includes age-related macular degeneration (AMD), including non-exudative (wet) and exudative (dry or atrophic) AMD, choroidal neovascularization (CNV), diabetic retinopathy (DR), and endophthalmitis.

AMD is age-related degeneration of the macula, which is the leading cause of irreversible visual dysfunction in individuals over the age of 60. Two types of AMD exist, non-exudative (dry) and exudative (wet) AMD. The dry, or nonexudative, form involves atrophic and hypertrophic changes in the retinal pigment epithelium (RPE) underlying the central retina (macula) as well as deposits (drusen) on the RPE. Patients with nonexudative AMD can progress to the wet, or exudative, form of AMD, in which abnormal blood vessels called choroidal neovascular membranes (CNVMs) develop under the retina, leak fluid and blood, and ultimately cause a blinding disciform scar in and under the retina. Nonexudative AMD, which is usually a precursor of exudative AMD, is more common. The presentation of nonexudative AMD varies; hard drusen, soft drusen, RPE geographic atrophy, and pigment clumping can be present. Complement components are deposited on the RPE early in AMD and are major constituents of drusen.

In certain embodiments, the composition described herein is for use to treat a subject. "Treatment" is an approach for obtaining beneficial or desired clinical results. For the purposes of the present disclosure, beneficial or desired clinical results include, but are not limited to, alleviation of symptoms, diminishment of extent of disease, stabilized (i.e., not worsening) state of disease, delay or slowing of disease progression, amelioration or palliation of the disease state, and remission (whether partial or total), whether detectable or undetectable. "Treatment" can also mean prolonging survival as compared to expected survival if not receiving treatment.

"Treatment" is an intervention performed with the intention of preventing the development or altering the pathology of a disorder. Accordingly, "treatment" refers to both therapeutic treatment and prophylactic or preventative measures in certain embodiments. Those in need of treatment include those already with the disorder as well as those in which the disorder is to be prevented. By treatment is meant inhibiting or reducing an increase in

pathology or symptoms when compared to the absence of treatment, and is not necessarily meant to imply complete cessation of the relevant condition.

The terms "patient", "subject" and "individual" may be used interchangeably and refer to either a humans or non-human mammal. Aptly, the subject is a human.

As used herein an "effective" amount or a "therapeutically effective amount" of a protein refers to a nontoxic but sufficient amount of the protein to provide the desired effect. The amount that is "effective" will vary from subject to subject, depending on the age and general condition of the individual, mode of administration, and the like. An appropriate "effective" amount in any individual case may be determined by one of ordinary skill in the art using routine experimentation.

An effective dosage and treatment protocol may be determined by conventional means, starting with a low dose in laboratory animals and then increasing the dosage while monitoring the effects, and systematically varying the dosage regimen as well. Numerous factors may be taken into consideration by a clinician when determining an optimal dosage for a given subject. Such considerations are known to the person skilled in the art.

Aptly, a pharmaceutical composition as described herein may contain one or more pharmaceutically acceptable excipients or carriers. In some embodiments, the composition is substantially pyrogen free or is pyrogen free. In some embodiments, the composition is sterile.

Various literature references are available to facilitate the selection of pharmaceutically acceptable carriers or excipients. See, e.g., Remington's Pharmaceutical Sciences and US Pharmacopeia: National Formulary, Mack Publishing Company, Easton, PA (1984); Hardman et al. (2001) Goodman and Gilman's The Pharmacological Basis of Therapeutics, McGraw-Hill, New York, NY; Gennaro (2000) Remington: The Science and Practice of Pharmacy, Lippincott, Williams, and Wilkins, New York, NY; Avis et al. (Eds.) (1993); Pharmaceutical Dosage Forms: Parenteral Medications, Marcel Dekker, NY; Lieberman, et al. (Eds.) (1990) Pharmaceutical Dosage Forms: Tablets, Marcel Dekker, New York, NY; Lieberman, et al. (Eds.) (1990) Pharmaceutical Dosage Forms: Disperse Systems, Marcel Dekker, NY; Weiner, Wang, E, Int. J. Pharm. 185: 129-188 (1999) and Wang W. Int. J.;Pharm. 203: 1-60 (2000), and Kotkoskie (2000) Excipient Toxicity and Safety, Marcel Dekker, New York, NY.

The term "pharmaceutically acceptable salt" refers to a salt of the CFI protein of embodiments of the invention. Salts include pharmaceutically acceptable salts such as acid addition salts and basic salts. Examples of acid addition salts include hydrochloride salts, citrate salts and acetate salts. Examples of basis salts include salts where the cation is selected from alkali metals, such as sodium and potassium, alkaline earth metals, such as calcium, and ammonium ions $^{+}N(R^3)_3(R^4)$, where R^3 and R^4 independently designates optionally substituted C_{1-6}-alkyl, optionally substituted C_{2-6}-alkenyl, optionally substituted aryl, or optionally substituted heteroaryl.

The term "solvate" in the context of the present disclosure refers to a complex of defined stoichiometry formed between a solute (e.g., a protein or pharmaceutically acceptable salt thereof according to the present disclosure) and a solvent. The solvent in this connection may, for example, be water, ethanol or another pharmaceutically acceptable, typically small-molecular organic species, such as, but not limited to, acetic acid or lactic acid. When the solvent in question is water, such a solvate is normally referred to as a hydrate.

The pharmaceutical compositions for use in the treatment of a complement-mediated disorder can be in unit dosage form. In such form, the composition is divided into unit doses containing appropriate quantities of the active component. the unit dosage form can be a packaged preparation, the package containing discrete quantities of the preparations, for example, packeted tablets, capsules, and powders in vials or ampoules. The unit dosage form can also be a capsule, cachet, or tablet itself, or it can be the appropriate number of any of these packaged forms. It may be provided in single dose injectable form, for example in the form of a pen. In certain embodiments, packaged forms include a label or insert with instructions for use. Compositions may be formulated for any suitable route and means of administration. Pharmaceutically acceptable carriers or diluents include those used in formulations suitable for oral, rectal, nasal, topical (including buccal and sublingual), vaginal or parenteral (including subcutaneous, intramuscular, intravenous, intradermal, and transdermal) administration. The formulations may conveniently be presented in unit dosage form and may be prepared by any of the methods well known in the art of pharmacy.

In vitro Uses

The bioactivity of recombinant CFI proteins and the compositions comprising such proteins can be measured in vitro using a suitable bioassay. Suitable bioassays are described below in detail, and include using surface plasmon resonance (SPR) to measure binding of the

protein to CFH and measuring the ability of protein-bound CFH to interact with other relevant complement components (e.g. binding to C3b or C3d, or inducing decay of C3b.Bb).

In certain embodiments, the composition and/or recombinant mature CFI of embodiments of the present invention may be used in *in vitro* assays to analyse genetic variants of the CFI protein. In certain embodiments, in order to target therapy to those who will most likely receive benefit, the importance of functionally significant rare genetic variants of CFI would be advantageous. This is achieved through assays of recombinant mutant proteins compared to the wild-type protein. Overexpression of *CFI* in cell lines results in incomplete processing. As the precursor form of FI is not active, varying rates of processing in individual cell lines could decrease the validity of the results. Thus, the recombinant mature CFI protein of certain embodiments of the invention could be utilized in such assays.

It will be clear to a person skilled in the art that features described in relation to any of the embodiments described above can be applicable interchangeably between the different embodiments. The embodiments described above are examples to illustrate various features of the invention.

Throughout the description and claims of this specification, the words "comprise" and "contain" and variations of them mean "including but not limited to", and they are not intended to (and do not) exclude other components, integers or steps. Throughout the description and claims of this specification, the singular encompasses the plural unless the context otherwise requires. In particular, where the indefinite article is used, the specification is to be understood as contemplating plurality as well as singularity, unless the context requires otherwise.

Features, integers or characteristics described in conjunction with a particular aspect, embodiment or example of the invention are to be understood to be applicable to any other aspect, embodiment or example described herein unless incompatible therewith. All of the features disclosed in this specification (including any accompanying claims, abstract and drawings), and/or all of the steps of any method or process so disclosed, may be combined in any combination, except combinations where at least some of such features and/or steps are mutually exclusive.

The invention is not restricted to the details of any foregoing embodiments. The invention extends to any novel one, or any novel combination, of the features disclosed in this specification (including any accompanying claims, abstract and drawings), or to any novel

one, or any novel combination, of the steps of any method or process so disclosed. The reader's attention is directed to all papers and documents which are filed concurrently with or previous to this specification in connection with this application and which are open to public inspection with this specification, and the contents of all such papers and documents are incorporated herein by reference.

Brief Description of the Drawings

Embodiments of the invention are further described hereinafter with reference to the accompanying drawings, in which:

Figure 1 depicts an overview of certain aspects of the complement system;

Figure 2 depicts the amino acid sequences of proteins described herein. Particularly:

SEQ. ID. No. 1 is an amino acid sequence of human heavy chain of a mature Complement Factor I;

SEQ. ID. No. 2 is an amino acid sequence of human light chain of a mature Complement Factor I;

SEQ. ID. No. 3 is an amino acid sequence of human precursor Complement Factor I;

SEQ. ID. No. 4 is an amino acid sequence of a human furin protein; and

SEQ. ID. No. 7 is an amino acid sequence of a linker sequence of human Complement Factor I.

Figure 3 depicts AKTA purification of WT Factor I (FI). FI was detected by measuring UV absorbance at 280nm, as demonstrated by the blue trace. The green trace represents the imidazole gradient. The red circle highlights the point at which FI was eluted from the column. Samples of fractions corresponding to this area and surrounding fractions were run under reduced conditions on a western. There is a single band at 88kDa and this corresponds to the proform of FI only.

Figure 4 is a representation of the processing of recombinant human FI in mammalian cell lines. Pro-FI undergoes processing before secretion. When *CFI* is expressed in cell lines, incomplete processing of the protein results in the secretion of both Pro-FI with an intact RRKR linker, and the mature FI in which the heavy and the light chain is linked only by a disulfide bond.

Figure 5 shows appearance of FI on a Western blot. Diagram shows how different forms of FI appear on both non-reduced and reduced Western blots. Pro-FI will appear at 88 kDa under reduced and non-reduced conditions. Mature FI will appear at 88 kDa under non-reducing conditions, but when reduced will appear at 50 kDA due to breakage of the disulphide bond. FI broken down into its two constituent chains will always appear at 50 kDa under both reduced and non-reduced conditions. The light chain is not often detected on a western blot as antibodies used for detection predominantly detect heavy chain epitopes.

Figure 6 shows Western blots to show effect of adding furin to pro-FI in sodium acetate (pH 5.0) buffer and Pro-FI in HEPES (pH 7.0) buffer. All reactions had a final concentration of 100mM buffer and 5mM $CaCl_2$. All samples were incubated for 15 hours at 37□C unless stated otherwise. Lane 1 contains purified Pro-FI before exchange into different buffers, non--incubated. Lane 2 contains Pro-FI alone in sodium acetate buffer. Lane 3 contains Pro-FI in sodium acetate buffer with furin. Lane 4 contains Pro-FI alone in HEPES buffer. Lane 3 contains Pro-FI in HEPES buffer with furin.

Figure 7 shows a Western blot (reduced and non-reduced) to determine the minimum concentration of furin required to achieve full cleavage of Pro-FI at the RRKR linker. All reactions had a final concentration of 100mM sodium acetate (pH 5) and 5mM $CaCl_2$. Lane 1 contains Pro-FI and buffer only. Lane 2 contains Pro-FI in buffer with half of the concentration of furin in lane 1. Concentration of furin is halved a further 3 times in lanes 4, 5 and 6. Non-reduced Western confirms the nature of FI in cleavage reactions is cleaved FI.

Figure 8 shows a Western blot (reduced) which shows the effect of changing concentration of calcium ions and potassium ions on furin efficacy. All reactions had a final concentration of 1/32 furin compared to previous experiments and 100mM sodium acetate (pH 5) buffer. All reactions were incubated at 37□C for a period of 16 hours. The first lanes contain Pro-FI in a buffer containing 5mM $CaCl_2$. The second lanes contain pro-CFI in a buffer containing 5mM CaCl2 with furin. The third lanes contain pro-CFI in a buffer containing 1mM $CaCl_2$. The fourth lanes contain Pro-FI in a buffer containing 1mM CaCl2 with furin. All four lanes in the bottom western also contain 20mM KCl. The first lanes contain Pro-FI in a buffer containing 5mM $CaCl_2$. The second lanes contain pro--CFI in a buffer containing 5mM CaCl2 with furin. The third lanes contain pro-CFI in a buffer containing 1mM $CaCl_2$. The

fourth lanes contain Pro-FI in a buffer containing 1mM $CaCl_2$ with furin. All four lanes in the bottom western also contain 20mM KCl.

Figure 9 shows the results of a C3b cofactor assay to determine the activity of Pro-FI compared to mature FI. All reactions were incubated at 37□C for 20 min. Two separate exposures are used due to low intensity of the lower bands, and too high intensity of the bands above 50 kDa. Lane 1 contains iC3b (cleaved C3b), positive control. Lane 2 contains uncleaved C3b, negative control. Lane 3 contains C3b and previously non-incubated pro-FI. Lane 4 is empty. Lane 5 contains C3b and Pro---FI. Lane 6 contains C3b and furin only, to demonstrate furin does not cleave C3b, Lane 7 contains furin alone, to demonstrate antibodies used do no cross react with furin. Lane 8 contains C3b, Pro-FI and furin (therefore cleaved FI). Appearance of α2 band in lane 1 and lane 8 only suggests cleavage of C3b took place in these lanes only. Therefore, this data suggests that only cleaved FI has activity, and Pro-FI is inactive.

Figure 10 illustrates a western blot to determine the activity of pro-FI to mature FI. Equal samples were available for lane 4 and lane 7, which allowed a valid comparison between the activity of pro-CFI and cleaved CFI to be made. All reactions were incubated at 37□C for 20 min. Lane 1 uncleaved C3b, negative control. Lane 2 contains C3b and previously non-incubated Pro-FI. Lane 3 is empty. Lane 4 contains C3b and pro-CFI. Lane 5 contains C3b and furin only, to demonstrate furin does not cleave C3b, Lane 6 contains furin alone, to demonstrate antibodies used do no cross react with furin. Lane 7 contains C3b, Pro-FI and furin (therefore cleaved FI).

Methods and materials

Mutagenesis

The pDR2 E1F vector used for expression of recombinant pro-CFI (pro-rCFI), was provided by Dr Kevin Marchbank (Institute of Cellular Medicine Newcastle University). Site-directed mutagenesis was performed using the QuikChange site directed mutagenesis kit (Stratagene, La Jolla, CA) (Cat #200523) to add a 6x histidine tag to CFI cDNA in pDR2 EF1 to form pDR2 EF1α. Primers used for the mutagenesis are shown in Table 1. Full length Maxiprep sequencing was undertaken to ensure fidelity of both the wild-type and mutant vectors.

Reverse	GAGATCACAATTTTAATGATGATGATGATGATGCTTATCGTCATCGT CTACATTGTACTGAGAAATAAAAGG (SEQ. ID. NO 5)
Forward	CCTTTTATTTCTCAGTACAATGTAGACGATGACGATAAGCATCATC ATCATCATCATTAAAATTGTGATCTC (SEQ. ID. NO 6)

Table 1: Mutagenesis primers

Cell culture

Chinese hamster ovary cells (CHO) cells were maintained in DMEM:F12 mixture (Lonza Group Ltd) supplemented with L-Glutamine (final concentration 4.5 mM, Life Technologies), penicillin and streptomycin (100 U/ml each, Life technologies) and 10% heat inactivated Fetal Bovine Serum (FBS) (Biosera). Transient transfection of CHO cells was performed using a jetPEI DNA transfection protocol.

Cell transfection

Cells were counted with a haemocytometer and diluted to 75,000 cells/ml. A 6 well culture plate had 2 ml of cells added per well (150,000 cells per well). 3 µg of DNA encoding the pro-CFI cDNA was diluted with sodium chloride (NaCl) to a final concentration of DNA in a volume of 100 µl. 6µL of jetPEI reagent (Polyplus) was diluted in NaCl to a final concentration in a volume of 100ul. The jetPEI solution was added in its entirety to the DNA solution, and this mixture was incubated for 30 minutes at room temperature. 200 µL of jetPEI/DNA mix was added per well to the cells in 1ml of serum containing medium. Plates were then incubated at 37°C for 24 hours. After 24 hours, the supernatant was removed from the flasks and checked for expression of CFI using a nickel pulldown assay.

Nickel pulldown

Hygromycin was added to incubated cells to remove non-transfected cells. Single clones were then isolated using limited dilution. Growth of cells was monitored and wells which contained a single colony of cells were established. These were transferred to separate flasks and supernatant removed to perform western blot analysis using nickel-Sepharose beads (Ni Sepharose Excel, GE Healthcare Life Sciences) to establish the best expressers of FI. 50 µL of bead slurry was placed in phosphate buffered saline (PBS) and centrifuged at 300 xg to precipitate the beads, before removal of the PBS. 1 ml of cell culture supernatant was then added to the beads. The cell culture supernatant and bead mix was then incubated for 2 hours at room temperature end over end or at 4°C overnight. After incubation the samples were centrifuged at 300 xg and supernatant was removed gently so as to not disturb the pellet which should be bound to the His-tagged protein. The pellet was then washed with 20-40 mM imidazole to remove non-specifically bound proteins. After washing, samples were spun at 300 xg and supernatant was removed, leaving the pellet. Pelleted nickel beads and bound protein were then subjected to western blot analysis to check for expression of pro-CFI.

The protocol followed is as follows:

1. Using 1.5 ml V bottomed tubes wash 50ul aliquots of bead slurry (~25ul of beads + 25ul 20% EtOH) in PBS (each 50ul is enough to pull down 1ml of supernatant)
2. Spin beads at 300xg, remove PBS
3. Add 1ml supernatant
4. Incubate for 2hr @ RT end over end (or o/n at 4 degrees)
5. Spin at 300xg and gently remove supernatant
6. Wash with 20--40mM Imidazole to remove non-specific binders
7. Spin at 300xg and gently remove supernatant
8. Wash with PBS
9. Spin at 300xg and gently remove supernatant leaving approx 35ul of PBS
10. Add relevant volume of loading buffer for western ~10ul 5x loading buffer to account for buffer between beads
11. Boil as normal
12. Spin at 300xg remove sample and load ~35ul on western

Protein purification

Supernatant of rCFI expressing cells was collected and purified on an AKTA purifier (GE Healthcare, Piscataway, NJ) using a 1ml His-Trap column. A 0-0.5 M imidazole gradient in 20mM phosphate was used to disrupt interaction of the His-tagged pro-rCFI with the His-Trap column, eluted fractions were collected. Western blots were conducted in order to determine which fractions contained pro-CFI. The fractions containing pro-rCFI were then pooled together.

SDS Polyacrylamide Gel electrophoresis (SDS-PAGE) and Western Blot Analysis

25µL of sample to be studied was added to 1.5 mL tubes which contained 6.25 µL of reducing sample buffer (Thermo Scientific, 39000) or non-reducing sample buffer (Thermo Scientific, 39001). All samples were heated at 95°C for 8 minutes before centrifugation at a speed of 13,200 rpm for 2 seconds. 10% Tris-glycine gels were made according to manufacturer's instructions (Novex, Life Sciences, EC6075BOX). Once set, gels were placed in XCell SureLock Mini-Cells (Novex, Life technologies. E10002) and the mini-cells were filled with 1x running buffer (25mM Tris base, 192 mM Glycine, 0.1% SDS, deionised Water, pH 8.3) in both compartments. 22 µL of sample was loaded into each well of the gel. When required 14 µL of Factor I standard was loaded into a well of the gel (Comptech, A138) and used as a marker. 7 µL of MW ladder (Biolabs, P7708s) was added to at least one well of each gel. The XCell SureLock Mini-Cell was connected to a Powerpac (Bio-rad, 300V, 400mA, 75W) and ran for 35 minutes at 190 volts. After running, gels were transferred onto nitrocellulose membrane (Invitrogen, Life technologies, LC2001) using chilled (4°C) 1x Tris-Glycine transfer buffer (12mM Tris base, 96mM Glycine, DI Water, pH 8.3, 20% Methanol). Transfer was performed by a transfer blotter run for 60 minutes at 100 volts. After transfer was complete, membranes were washed briefly with deionised water before staining with Ponceau S solution (Sigma, P7170) to determine success of transfer. Membranes were de-stained in trays placed on a rotating table. All membranes were blocked overnight at 4°C, or for 1 hour at room temperature using a solution of 5% non-fat milk powder in 1 x TBST (50mM Tris. HCl, pH 7.4, 150 mM NaCl, 0.05% Tween 20). The following antibodies were used;

For detecting pro-CFI and mature CFI: Primary antibody, sheep polyclonal Factor I (Abcam, Cambridge, MA, ab8843) was applied at a concentration of 2.37 µg/ml for 1hr at room temperature. Membranes were washed with Tris buffered saline tween (TBST) buffer (137 mM NaCl, 2.7 mM KCl, Tris base 19 mM, Tween) three times for 10 minutes. Secondary antibody, Rabbit polyclonal secondary antibody to sheep IgG conjugated to horse radish peroxidase (HRP) (Abcam, Cambridge, MA), was applied at a concentrations of 2.37 µg/ml

for 1 hour at room temperature or overnight at 4°C. Blots were then washed three times for 10 min in TBST. Supersignal Chemilumiescent Substrate (Pierce, Rockford, IL) was applied to membranes for 1 minute before exposure to an X-ray film for varying time periods before they were developed using standard film developing techniques.

For detecting C3b and iC3b: Primary antibody, rabbit polyclonal anti-C3 antibody (Abcam) at a concentration of 1:5000 before the use of goat anti-rabbit IgG HRP antibody

Pro-CFI cleavage by furin *in vitro*

Experiments to optimise the *in vitro* cleavage of pro-rCFI by furin were carried out as detailed herein.

Purified pro-rCFI was buffer exchanged from elution buffer into 1 x cleavage buffer (100mM HEPES pH 5.2, 0.5% Triton X-100, and 1mM $CaCl_2$) using a PD-10 desalting column (GE Healthcare) with a bed volume of 8.3 ml.

Furin was obtained from R & D Systems. Properties of the furin protein are provided in Table 2

Table 2

Supplier	**R & D Systems**
Storage buffer pH	9
Presence of tag(s)	C-terminal 10 his-tag
Protein structure	Truncated (amino acid residues 108-715)
Molecular Weight	The calculated molecular weight of truncated human furin is 65 kDa. its apparent molecular weight in SDS-PAGE gels is 65-85 kDa.
Source	Mouse myeloma cell line,
Unit definition	Measured by its ability to cleave the fluorogenic peptide substrate pER TKRAMC (Catalog # ES013). The specific activity is >125 pmol/min/µg.

Pro-rFI was buffer exchanged from elution buffer into 1 x cleavage buffer (100mM HEPES pH 5.2, 0.5% Triton X---100, and 1mM $CaCl_2$) using a PD-10 desalting column (GE Healthcare) with a bed volume of 8.3 ml.

Cleavage reactions using furin-RD were made up as detailed in Table 3 below.

Table 3

Sample	Furin-RD (µL)	Pro-rCFI (µL)	Cleavage buffer (µL)	Total volume (µL)
1A (pro-CFI only)	0	234	141	375
2A (pro-CFI only	0	234	141	375
3A (pro-CFI + furin)	0	234	126	375
1B (pro-CFI only)	0	31.2	18.8	50
2B (pro-CFI only	0	31.2	18.8	50
3B (pro-CFI + furin)	2	31.2	16.8	50
4B (Furin only)	2	0	48	50

Optimisation of cleavage reaction pH

In order to test the optimum pH for cleavage of pro-CFI a number of buffers with different pH values were tested. Firstly the purified pro-rCFI was exchanged from elution buffer into three buffers of differing pH using PD MidiTrap G-25 columns (GE Healthcare). Columns were equilibrated using 15 ml in total of the respective buffer which was 100mM (sodium acetate, pH 5.0 or HEPES, pH 7 or Tris-base pH 9). 0.93 ml pro-rCFI in elution buffer was added to each column before centrifugation at 1000 x g for 2 minutes. To establish whether buffer exchange was successful, 30 µL of pro-rCFI exchanged at each pH was subjected to western blot analysis as described previously. Exact quantities of reaction mixes are shown in Table 4 below.

Sample	Pro-rCFI (µL)	1 M corresponding stock buffer (µL)	50 mM $CaCl_2$ (µL)	DI H_2O (µL)	Total (µL)
pH 5	30	2	5	13	50
pH 7	30	2	5	13	50
pH 9	30	2	5	13	50

Table 4: Volumes used for buffer exchange.

Furin cleavage reactions were then set up containing 30 µL of pro-rCFI in the respective buffer and 2 µL of furin. In order to ensure the concentrations of the buffer to which the pro-rCFI had been exchanged to 2µL of 1 M stock solution of each respective buffer was added to samples before making samples up to 50µL with deionised water. Control reactions without furin were set up for each pH buffer. Reactions were incubated at 37□C for 15 hours. Non-incubated samples of pre-exchange, purified pro-rCFI were also set up. Quantities of each reaction are shown in Table 5.

Sample	**Incubated**	**Pro-–Factor I (of the appropriate pH) (ul)**	**Furin (ul)**	**1M stock buffer (at the appropriate pH) (ul)**	**50mM CaCl2 (ul)**	**H2O (ul)**	**Total (ul)**
Previously purified Batch Pro-CFI	No	30µL(previously purified WT CFI)	0	2	5	13	50
Newly purified batch Pro-rCFI (before desalting)	No	30µL(newly purified CCFI before desalting)	0	2	5	13	50
pH 5 Pro-rCFI only	Yes	30µL(pH 5)	0	2	5	13	50
pH 5 Pro-rCFI and furin	Yes	30µL(pH 5)	2	2	5	11	50
pH 7 Pro-rCFI only	Yes	30µL(pH 7)	0	2	5	13	50
pH 7 Pro-rCFI and furin	Yes	30µL(pH 7)	2	2	5	11	50
pH 9 Pro-rCFI only	No	30µL(pH 9)	0	2	5	13	50
pH 9 Pro-rCFI only	Yes	30µL(pH 9)	0	2	5	13	50
pH 9 Pro-rCFI and furin	Yes	30µL(pH 9)	2	2	5	11	50

Table 5: Volumes for pH optimisation of pro-rCFI cleavage by furin.

After incubation the samples were subjected to western blot analysis as described previously to assess the level of conversion of pro-CFI to mature CFI by detection of the constitute bands of each.

Testing effect of furin concentration on pro-CFI cleavage

In order to test the minimal amount of furin needed for relatively high rates of cleavage of pro-rCFI serial dilutions of furin were made up: 1:2, 1:4, 1:8 and 1:16. The diluted furin was used for cleavage reactions set up as shown in Table 6. Samples were incubated at 37°C for 16 hours.

Sample	pro-rCFI exchanged into 100 mM sodium acetate pH 5 (µL)	Furin (µL)	Furin dilution factor	1M stock sodium acetate pH 5 buffer (µL)	50mM $CaCl_2$ (µL)	H_2O (µL)	Total (µL)
1	30	0	0	2	5	13	50
2	30	10	1:1	2	5	3	50
3	30	10	1:2	2	5	3	50
4	30	10	1:4	2	5	3	50
5	30	10	1:8	2	5	3	50
6	30	10	1:16	2	5	3	50

Table 6: Volumes of reactions to test furin concentration effect on cleavage rate.

After incubation samples were subjected to western blot analysis as described previously.

Testing effect of ion concentration on furin cleavage of pro-CFI

In order to test the effect that ion concentration had on the cleavage of pro-rCFI by furin differing potassium and calcium concentrations were tested. Furin was diluted to 1/32 of the original concentration before use in reaction mixes as detailed in Table 7 below.

Sample	Pro-rCFI	Furin diluted	1M stock	10 mM	50mM $CaCl_2$	H_2O (µL)	KCl 250	Total (µL)

	pH5 buffer (µL)	1:16 (µL)	sodium acetate pH 5 buffer (µL)	$CaCl_2$ (µL)	(µL)		mM	
1	15	0	1	0	2.5	6.4	0	25
2	15	2.5	1	0	2.5	4	0	25
3	15	0	1	2.5	0	6.5	0	25
4	15	2.5	1	2.5	0	4	0	25
5	15	0	1	0	2.5	4.5	2	25
6	15	2.5	1	0	2.5	2	2	25
7	15	0	1	2.5	0	4.5	2	25
8	15	2.5	1	2.5	0	2	2	25

Table 7: Ion concentration experiments, reaction volumes.

Optimised pro-CFI digestion reaction volumes

Pro-rCFI digestion was performed using the reaction mixes detailed in Table 8. Pro-rCFI was used in pH5 buffer (100 mM sodium acetate pH 5).

Reactant	Reaction		
	Pro-rCFI + Furin	Pro-rCFI only	Furin only
Pro-CFI	15 µL	15 µL	0 µL
Furin	5 µL	0	5 µL
1M pH 5 stock	1 µL	1 µL	2.5 µL
50mM $CaCl_2$	2.5 µL	2.5 µL	2.5 µL
H_2O	1.5 µL	6.5 µL	15 µL
Total	25 µL	25 µL	25 µL

Table 8: Optimised cleavage reactions.

C3b inactivation assay: Comparison of pro-CFI vs mature FI

A C3b inactivation assay was used to compare the activity of pro-rCFI and mature CFI. A sample of pro-rCFI was cleaved by furin using conditions identified in the optimisation (as

detailed previously). Three control reactions were set up: 2 x Pro-CFI only (incubated and non-incubated) and furin only (incubated) in order to determine whether any C3b cleavage occurred with pro-rCFI that had been cleaved by furin but subjected to the same conditions. All incubated samples were incubated at 37□ for 16 hours.

25 µl reactions were set up with a final concentration of C3b at 0.2 µg/µl. (Comptech). CFH (Comptech) was used as a cofactor and each reaction contained a final CFH concentration of 66.6 ng/µl. A positive control containing C3b and serum CFI (sFI) (Comptech) at a final concentration of 10 ng/µL (Comptech) was made up. A negative control for uncleaved C3b had no CFI and only C3b in. Two further controls of pro-rCFI only (incubated and non-incubated) were set up and also a control of furin only were set up by adding 10 µL of each respective reaction prepared previously. A further control of furin without the presence of CFH, CFI or C3b was also made up. Reactions were made up to the final volume of 25 µL using low salt buffer. The 7 reactions made up are detailed in Table 9.

Sample	**Sample description**	**Reactant**						
		C3b [1.6 µg/µL]	sCFI [11.11 ng/µL]	CFH [333 ng/µL]	Pro-CFI	Furin	Low salt buffer	Total volume (µL)
1	Cleaved C3b control	3 µL	4.5 µL	5 µL	-	-	12.5 µL	25 µL
2	Uncleaved C3b control	3 µL	-	5 µL	10 µL	-	7 µL	25 µL
3	Pro-rCFI ONLY (pre-incubated)	3 µL	-	5 µL	10 µL	-	7 µL	25 µL
4	Cleaved rCFI (pre-incubated)	3 µL	-	5 µL	10 µL	-	7 µL	25 µL
5	Furin control	3 µL	-	5 µL	10 µL	10 µL	7 µL	25 µL
6	Pro-rCFI ONLY (non-	3 µL	-	5 µL	10 µL	-	7 µL	25 µL

	incubated)							
7	Furin ONLY	-	-	-	-	10 µL	15 µL	25 µL
Final Concentration		0.2 µg/µL	2 ng/ µL	66.6 ng/ µL			-	-

Table 9: C3b inactivation assay reaction volumes

A 10 µL aliquot was removed at 20 minutes from each reaction mix. Each aliquot was added to an equal volume of 1 x laemelli buffer and western blot analysis was performed as outlined previously using the antibodies detailed for detecting C3b. Activity of rCFI was determined by generation and intensity of the α1 and α2 bands upon developing of x-ray images.

Also ran on some gels was a sample of inactivated (cleaved) C3b (iC3B) to act as a marker for C3b cleavage products.

Results & Discussion

Factor I purification

Supernatant of rCFI expressing cells was collected and purified as described herein. Collected fractions were run on a polyacrylamide gel under reducing conditions before western blotting of the gel. The presence of rCFI is confirmed by the band at a molecular weight of 88 kDa, corresponding to the MW of pro-rCFI (uncleaved). This is further confirmed by the absence of a band corresponding to a molecular weight of 50 kDa which would be expected from cleaved mature CFI. The concentration of the rCFI was determined by ELISA testing to be 0.6 ng/µL.

Factor I cleavage optimisation

Cleavage of the ^{318}RRKR^{321} cleavage site was optimised by testing a range of conditions, to ensure that the maximum level of cleavage of pro-rCFI to mature rCFI was achieved *in vitro*. All samples were subjected to polyacrylamide gel electrophoresis in reducing and non-reducing conditions to allow the distinction between mature rCFI and the heavy chain alone which may be dissociated due to degradation of the protein.

Under non-reducing conditions, both the pro-rCFI and mature rCFI should have a MW of approximately 88kDa; when Pro-rCFI is reduced, it should remain at 88kDa due to the

existence of the RRKR linker; Mature rCFI should separate into the heavy chain (50 kDa) and light chain (37 kDa) as the di-sulphide bridge between the two chains is reduced. The light chain is not often detected on a western blot as antibodies used for detection predominantly detect heavy chain epitopes. Figure 4 summarizes the processing of CFI in mammalian cells and demonstrates the effect of reduction on the different forms. Figure 5 provides a diagram of how different forms of CFI are expected to appear on a western blot under both reducing and non-reducing conditions.

Optimisation of pH for cleavage of pro-rCFI by furin

After incubation with furin it can be seen from the western blots shown in Figure 5A (reducing conditions) and 5B (non-reducing conditions) that no pro-rCFI or mature rCFI is detectable when the reaction is performed at pH 7 (lanes 4 and 5) as is indicated by the absence of bands at ~88 and/or 50 kDa. When the reaction was performed at pH5 the presence of a band at ~50 kDa in Figure 5A and absence of a band at ~88 kDa indicates that all detectable amounts of the pro-rCFI has been cleaved to the mature CFI form.

A broad pH is provided in the prior art for cleavage of pro-CFI. These experiments show that the pH of the reaction can help maximize the cleavage of pro-rCFI to the mature form. It has been suggested that slightly acidic pH may help to increase the rate of proteolytic cleavage due to conformational change that may help to expose the cleavage site. The data here indicates that a high rate of cleavage occurs at pH 5 but other pH values may also allow for a high rate of cleavage depending on other reaction conditions and reactants that may be used.

Optimisation of furin concentration

It can be seen from Figure 6A and 6B that even at low concentrations furin is able to provide a high rate of cleavage of pro-CFI. This can be seen by the presence of a band in the western blot performed in reducing conditions (Figure 6A) at ~50 kDa which corresponds to cleaved mature rCFI and the absence of a band at ~88 kDa which corresponds to uncleaved pro-CFI. Even when furin is diluted by a factor of 16 a relatively high rate of cleavage is observed.

Cleavage by furin is confirmed by the absence of a band at ~50 kDa in Figure 6A lane1 which corresponds to a pro-rCFI control. If degradation of the protein was the cause of the band seen at ~50 kDa it would be expected to be seen for the pro-rCFI only control as well.

Optimisation of ion concentration

The results indicate that the regardless of potassium ion concentration, calcium ions enhances the rate of cleavage. This can be seen in Figure 7A by the presence of a band at ~50 kDa corresponding to cleaved mature rCFI in lane 2. The corresponding band in lane 4 which shows the products of a cleavage reaction performed with a lower (1 mM $CaCl_2$) calcium ion concentration and is less intense indicating that a higher (5m M $CaCl_2$) calcium ion concentration may increase the cleavage rate.

It can be seen when comparing the western blots shown in Figure 8A and 8B that the presence of potassium ions may help increase the rate of pro-rCFI cleavage by furin by the fact that the bands corresponding to cleaved mature rCFI (~50 kDa) in lanes 2 and 4 of Figure 8B have a greater intensity than that seen in Figure 8A.

It is noted though that for shorter incubation times the presence of potassium ions may help speed up the cleavage reaction allowing for faster cleaving of all of the pro-CFI to mature CFI.

Following the optimisation tests the reaction mix and condition for cleavage of pro-CFI using furin was as given in Table 10:

	Pro-rCFI + Furin
Pro-CFI	15 µL
Furin	5 µL
1M pH 5 stock	1 µL
50mM $CaCl_2$	2.5 µL
H_2O	1.5 µL
Total	25 µL

Table 10: Optimised furin cleavage of pro-FI

Pro-rCFI was first exchanged into 100 mM sodium acetate pH 5. Samples were incubated at 37°C for 16 hours. Potassium ions were not included in the reaction as the effect they had when using the given reaction conditions was considered negligible.

C3b inactivation assay: Comparison of pro-rCFI vs mature CFI

In order to test the*in vitro* activity of the *in vitro* cleaved mature rCFI a C3b inactivation assay was performed. It is expected that if CFI is in the active mature form it will cleave C3b into its inactive state iC3b by cleavage of the α chain to produce two chains with molecular weights of 68 kDa (α1) and 46 kDa (α2) the α2 chain is further cleaved to a final molecular weight of 43 kDa. This change in the structure of C3b can be seen by analysing the products of an C3b inactivation reaction using a western blot and comparing the intensity and occurrence of a band that corresponds to the α chain and the intensity and occurrence of bands that correspond to the α1 and α2 chains. This therefore allows for the activity of the mature CFI to cleave C3b to be accessed.

It can be seen from Figure 9 that when compared to control experiments (lanes 2, 3, 4, 5, 6, and 7) lane 8 which corresponds to a sample containing the i*n vitro* cleaved mature rCFI, is the only sample containing bands that correspond to the α1 and α2 chains. This scan be confirmed by comparing the western blot bands seen for the iC3b cleaved by incubation with mature sCFI.

The separation of the β and α1 bands was not as defined as possible and so a second western blot was performed. Figure 10 shows the western blot analysis with the separation of the β and α1 bands. The activity of the *in vitro* cleaved rCFI can be seen to be comparable to sCFI indicating that the amount of cleavage of pro-CFI to CFI is relatively high.

CLAIMS

1. A composition comprising a recombinant mature Complement Factor I (CFI) protein, wherein the recombinant mature CFI protein comprised in the composition represents greater than about 50% by weight of a total CFI protein content of the composition.
2. The composition according to claim 1, wherein the recombinant mature CFI protein represents greater than about 60% by weight of the total CFI protein content of the composition.
3. The composition according to claim 1 or claim 2, wherein the recombinant mature CFI protein represents greater than about 70% by weight of the total CFI protein content of the composition.
4. The composition according to any preceding claim, wherein the recombinant mature CFI protein represents greater than about 80% by weight of the total CFI protein content of the composition.
5. The composition according to any preceding claim, wherein the recombinant mature CFI protein represents greater than about 90% by weight of the total CFI protein content of the composition.
6. The composition according to any preceding claim, wherein the recombinant mature CFI protein represents greater than about 95% by weight of the total CFI protein content of the composition.
7. The composition according to any preceding claim, which optionally further comprises a recombinant precursor Complement Factor I protein, wherein the ratio of recombinant mature CFI: recombinant precursor CFI in the composition is from greater than 50:50 to 100:0.
8. A composition comprising a recombinant mature Complement Factor I (CFI) protein and optionally a recombinant precursor Complement Factor I protein, wherein the ratio of recombinant mature CFI: recombinant precursor CFI in the composition is from greater than 50:50 to 100:0.
9. The composition according to claim 7 or claim 8, wherein the ratio of recombinant mature CFI: recombinant precursor CFI in the composition is from 60:40 to 100:0.
10. The composition according to any of claims 7 to 9, wherein the ratio of recombinant mature CFI: recombinant precursor CFI in the composition is from 70:30 to 100:0.
11. The composition according to any of claims 7 to 10, wherein the ratio of recombinant mature CFI: recombinant precursor CFI in the composition is from 80:20 to 100:0.

12. The composition according to any of claims 7 to 11, wherein the ratio of recombinant mature CFI: recombinant precursor CFI in the composition is from 90:10 to 100:0.
13. The composition according to any of claims 7 to 12, wherein the ratio of recombinant mature CFI: recombinant precursor CFI in the composition is from 95:05 to 100:0.
14. The composition according to any preceding claim, wherein the recombinant CFI protein is a human CFI protein.
15. The composition according to any preceding claim, wherein the recombinant mature CFI protein comprises a first amino acid molecule comprising an amino acid sequence as set forth in SEQ. ID. No. 1.
16. The composition according to any of claims 1 to 14, wherein the recombinant mature CFI protein comprises a first amino acid molecule comprising an amino acid sequence which has at least 80% sequence identity to the amino acid sequence as set forth in SEQ. ID. No. 1.
17. The composition according to claim 16, wherein the recombinant mature CFI protein comprises a first amino acid sequence that is at least 90% identical to the amino acid sequence as set forth in SEQ ID NO: 1.
18. The composition according to claim 17, wherein the recombinant mature CFI protein comprises a first amino acid molecule comprising an amino acid sequence that is at least 95% identical to the amino acid sequence as set forth in SEQ ID NO: 1.
19. The composition according to any preceding claim, wherein the recombinant mature CFI protein comprises a further amino acid molecule comprising an amino acid sequence as set forth in SEQ. ID. No. 2, wherein the first and further amino acid sequence are linked by a disulphide bond.
20. The composition according to any of claims 1 to 18, wherein the recombinant mature CFI protein comprises a further amino acid molecule comprising an amino acid sequence which has at least 80% sequence identity to the amino acid sequence as set forth in SEQ. ID. No. 2 wherein the first and further amino acid sequence are linked by a disulphide bond.
21. The composition according to claim 20, wherein the recombinant mature CFI protein comprises an amino acid sequence that is at least 90% identical to the amino acid sequence as set forth in SEQ ID NO: 1.
22. The composition according to claim 21, wherein the recombinant mature CFI protein comprises a further amino acid molecule comprising an amino acid sequence that is at least 95% identical to the amino acid sequence as set forth in SEQ ID NO: 2.
23. The composition according to any preceding claim, which is essentially free of a furin protein.

24. The composition according to any preceding claim, which is a pharmaceutical composition.
25. The composition according to claim 20, which further comprises one or more pharmaceutically acceptable excipients.
26. The composition according to any preceding claim for use in the treatment of a complement-mediated disorder.
27. The composition according to claim 22 for use in the treatment of a C3 myopathy.
28. The composition according to claim 22 for use in the treatment of a complement-mediated disorder, wherein the complement-mediated disorder is selected from age-related macular degeneration, Alzheimer's Disease, atypical haemolytic uraemic syndrome, membranoproliferative glomerulonephritis Type 2 (MPGN2), atherosclerosis (in particular, accelerated atherosclerosis) and chronic cardiovascular disease.
29. A method of preparing a composition comprising a recombinant mature Complement Factor I (CFI) protein, wherein the recombinant mature CFI protein represents greater than 50% by weight of a total CFI protein content of the composition, the method comprising:
    a. contacting a recombinant precursor CFI protein with a furin protein or fragment thereof; and
    b. incubating the recombinant precursor CFI protein with the furin protein or fragment thereof for a predetermined period of time, whereby the furin protein or fragment thereof cleaves the recombinant precursor CFI protein at or adjacent to a RRKR linker sequence site to form the recombinant mature Complement Factor I protein.
30. The method according to claim 29, wherein the recombinant precursor CFI protein is a human precursor CFI protein.
31. The method according to claim 29 or claim 30, wherein the recombinant precursor CFI protein comprises a tag.
32. The method of claim 31, wherein the tag is a His-tag.
33. The method according to any of claims 29 to 32, which further comprises expressing the recombinant precursor CFI protein prior to step (a).
34. The method according to claim 33, which comprises expressing the recombinant precursor CFI protein in a eukaryotic cell.
35. The method according to claim 33, which comprises expressing the recombinant precursor CFI protein in a prokaryotic cell.
36. The method of claim 35, wherein the prokaryotic cell is *Escherichia coli*.

37. The method according to claim 34, wherein the eukaryotic cell is selected from an insect, a yeast or a mammalian cell.
38. The method according to claim 37, wherein the mammalian cell is a CHO cell.
39. The method according to any of claims 29 to 38, which comprises isolating the expressed recombinant precursor CFI protein prior to step (a).
40. The method according to any of claims 29 to 39, wherein step (a) comprises adding the furin protein or fragment thereof to a solution comprising the expressed recombinant precursor CFI protein.
41. The method according to any of claims 29 to 40, wherein step (b) comprises incubating the furin protein or fragment thereof with the recombinant precursor CFI protein at a temperature of between about 25°C to about 42°C.
42. The method according to any of claims 29 to 41, wherein step (b) comprises incubating the furin protein or fragment thereof with the recombinant precursor CFI protein at a temperature of between about 30°C to about 42°C.
43. The method according to any of claims 29 to 41, wherein step (b) comprises incubating the furin protein or fragment thereof with the recombinant precursor CFI protein at a temperature of between about 35°C to about 38°C.
44. The method according to any of claims 29 to 43, wherein step (b) comprises incubating the furin protein or fragment thereof with the recombinant precursor CFI protein in a solution having a pH of between about 5 and 7.
45. The method according to claim 44, wherein step (b) comprises incubating the furin protein or fragment thereof with the recombinant precursor CFI protein in a solution having a pH of between about 5 and 6.
46. The method according to claim 44 or claim 45, wherein the solution comprises calcium ions.
47. The method according to claim 46, wherein the solution comprises calcium ions at a concentration of between about 1mM to about 5mM.
48. The method according to any of claims 44 to 47, wherein the solution further comprises potassium ions.
49. The method according to any of claims 29 to 48, wherein step (b) comprises incubating the furin protein or fragment thereof with the recombinant precursor CFI protein for between about 5 hours and about 48 hours.
50. The method according to any of claims 29 to 49, wherein step (b) comprises incubating the furin protein or fragment thereof with the recombinant precursor CFI protein for between about 8 hours and about 20 hours.

51. The method according to any of claims 29 to 50, wherein the furin protein or fragment thereof comprises the amino acid sequence as set forth in SEQ. ID. No.4 or a fragment thereof.
52. The method according to claim 51, wherein the furin protein fragment comprises at least amino acid residues 108 to 715 of a protein comprising the amino acid sequence as set forth in SEQ. ID. No: 4.
53. The method according to any of claims 29 to 52, which further comprises isolating the recombinant mature CFI protein.
54. The method according to claim 53, which further comprises purifying the isolated recombinant mature CFI protein.
55. The method according to any of claims 29 to 53, wherein the recombinant precursor CFI protein comprises an amino acid sequence as set forth in SEQ. ID. No: 3.
56. The method according to any of claims 29 to 54, wherein the recombinant precursor CFI protein comprises an amino acid sequence as set forth in SEQ. ID. No. 3.
57. A composition obtainable from the method of any of claims 29 to 56.
58. A method of treating a complement-mediated disorder, the method comprising:
    a. administering a therapeutically effective amount of a composition according to any of claims 1 to 28 or claim 57 to a subject in need thereof.
59. The method according to claim 58, which is a method of treating a C3 myopathy.
60. The method according to claim 59, which is a method of treating a complement-mediated disorder, wherein the complement-mediated disorder is selected from age-related macular degeneration, Alzheimer's Disease, atypical haemolytic uraemic syndrome, membranoproliferative glomerulonephritis Type 2 (MPGN2), atherosclerosis (in particular, accelerated atherosclerosis) and chronic cardiovascular disease.
61. The method according to claim 60, which is a method of treating age-related macular degeneration.
62. A pharmaceutical composition comprising the composition of any one of claims 1-28, and a pharmaceutically acceptable carrier.
63. The pharmaceutical composition of claim 62, wherein the composition is substantially pyrogen free.
64. The pharmaceutical composition of claim 62 or 63, wherein the composition is sterile.

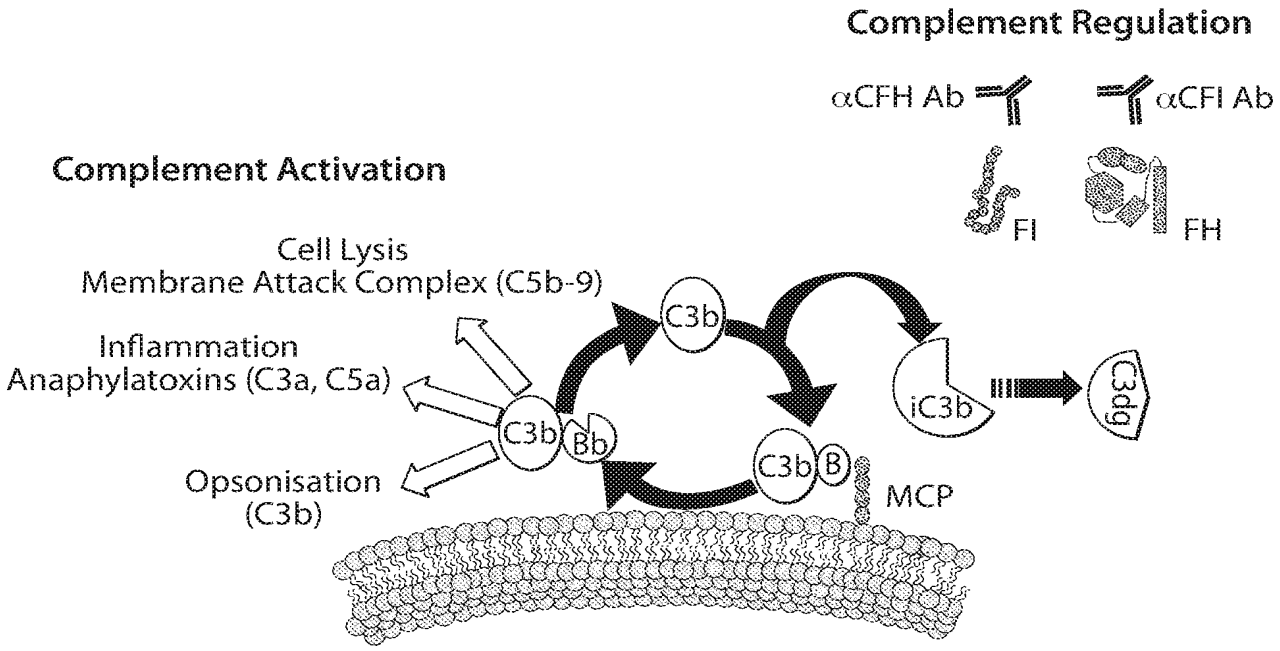
Complement Regulation
αCFH Ab
αCFI Ab
FI
FH
Complement Activation
Cell Lysis
Membrane Attack Complex (C5b-9)
Inflammation
Anaphylatoxins (C3a, C5a)
Opsonisation
(C3b)
C3b
Bb
C3b
B
MCP
iC3b
C3dg

Figure 1

Precursor Complement Factor I (human) (SEQ. ID. No. 3)

MKLLHVFLLFLCFHLRFCKVTYTSQEDLVEKKCLAKKYTHLSCDKVFCQPWQRCIEGTCVCKLPYQC
PKNGTAVCATNRRSFPTYCQQKSLECLHPGTKFLNNGTCTAEGKFSVSLKHGNTDSEGIVEVKLVDQ
DKTMFICKSSWSMREANVACLDLGFQQGADTQRRFKLSDLSINSTECLHVHCRGLETSLAECTFTKR
RTMGYQDFADVVCYTQKADSPMDDFFQCVNGKYISQMKACDGINDCGDQSDELCCKACQGKGFHC
KSGVCIPSQYQCNGEVDCITGEDEVGCAGFASVTQEETEILTADMDAERRRIKSLLPKLSCGVKNRM
HIRRKRIVGGKRAQLGDLPWQVAIKDASGITCGGIYIGGCWILTAAHCLRASKTHRYQIWTTVVDWIHP
DLKRIVIEYVDRIIFHENYNAGTYQNDIALIEMKKDGNKKDCELPRSIPACVPWSPYLFQPNDTCIVSG
WGREKDNERVFSLQWGEVKLISNCSKFYGNRFYEKEMECAGTYDGSIDACKGDSGGPLVCMDANN
VTYVWGVVSWGENCGKPEFPGVYTKVANYFDWISYHVGRPFISQYNV

UniProtKB/Swiss-Prot: P05156.2

>gi|317373341|sp|P05156.2|CFAI_HUMAN RecName: Full=Complement factor I; AltName: Full=C3B/C4B inactivator; Contains: RecName: Full=Complement factor I heavy chain; Contains: RecName: Full=Complement factor I light chain; Flags: Precursor

Heavy Chain (HC): 317 residues (SEQ. ID. No. 1)

KVTYTSQEDL VEKKCLAKKY THLSCDKVFC QPWQRCIEGT CVCKLPYQCP KNGTAVCATN
RRSFPTYCQQ KSLECLHPGT KFLNNGTCTA EGKFSVSLKH GNTDSEGIVE VKLVDQDKTM
FICKSSWSMR EANVACLDLG FQQGADTQRR FKLSDLSINS TECLHVHCRG LETSLAECTF
TKRRTMGYQD FADVVCYTQK ADSPMDDFFQ CVNGKYISQM KACDGINDCG DQSDELCCKA
CQGKGFHCKS GVCIPSQYQC NGEVDCITGE DEVGCAGFAS VAQEETEILT ADMDAERRRI
KSLLPKLSCG VKNRMHI

Calculated MW for non-glycosylated fI heavy chain: 35,286 Dalton

Light Chain (LC): 244 residues (SEQ. ID. No. 2)

IVG GKRAQLGDLP WQVAIKDASG ITCGGIYIGG CWILTAAHCL
RASKTHRYQI WTTVVDWIHP DLKRIVIEYV DRIIFHENYN AGTYQNDIAL IEMKKDGNKK
DCELPRSIPA CVPWSPYLFQ PNDTCIVSGW GREKDNERVF SLQWGEVKLI SNCSKFYGNR
FYEKEMECAG TYDGSIDACK GDSGGPLVCM DANNVTYVWG VVSWGENCGK PEFPGVYTKV
ANYFDWISYH VGRPFISQYN V

CFI Linker Sequence

RRKR (SEQ. ID. No 7)

Figure 2

'Furin' sequence per Wise et al NCBI accession NP_001276753.1 (SEQ. ID. No. 4)

MELRPWLLWVVAATGTLVLLAADAQGQKVFTNTWAVRIPGGPAVANSVARKHGFLNLGQIFGDYYH
FWHRGVTKRSLSPHRPRHSRLQREPQVQWLEQQVAKRRTKRDVYQEPTDPKFPQQWYLSGVTQR
DLNVKAAWAQGYTGHGIVVSILDDGIEKNHPDLAGNYDPGASFDVNDQDPDPQPRYTQMNDNRHGT
RCAGEVAAVANNGVCGVGVAYNARIGGVRMLDGEVTDAVEARSLGLNPNHIHIYSASWGPEDDGKT
VDGPARLAEEAFFRGVSQGRGGLGSIFVWASGNGGREHDSCNCDGYTNSIYTLSISSATQFGNVPW
YSEACSSTLATTYSSGNQNEKQIVTTDLRQKCTESHTGTSASAPLAAGIIALTLEANKNLTWRDMQHL
VVQTSKPAHLNANDWATNGVGRKVSHSYGYGLLDAGAMVALAQNWTTVAPQRKCIIDILTEPKDIGK
RLEVRKTVTACLGEPNHITRLEHAQARLTLSYNRRGDLAIHLVSPMGTRSTLLAARPHDYSADGFND
WAFMTTHSWDEDPSGEWVLEIENTSEANNYGTLTKFTLVLYGTAPEGLPVPPESSGCKTLTSSQACV
VCEEGFSLHQKSCVQHCPPGFAPQVLDTHYSTENDVETIRASVCAPCHASCATCQGPALTDCLSCP
SHASLDPVEQTCSRQSQSSRESPPQQQPPRLPPEVEAGQRLRAGLLPSHLPEVVAGLSCAFIVLVFV
TVFLVLQLRSGFSFRGVKVYTMDRGLISYKGLPPEAWQEECPSDSEEDEGRGERTAFIKDQSAL

Figure 2 (Continued)

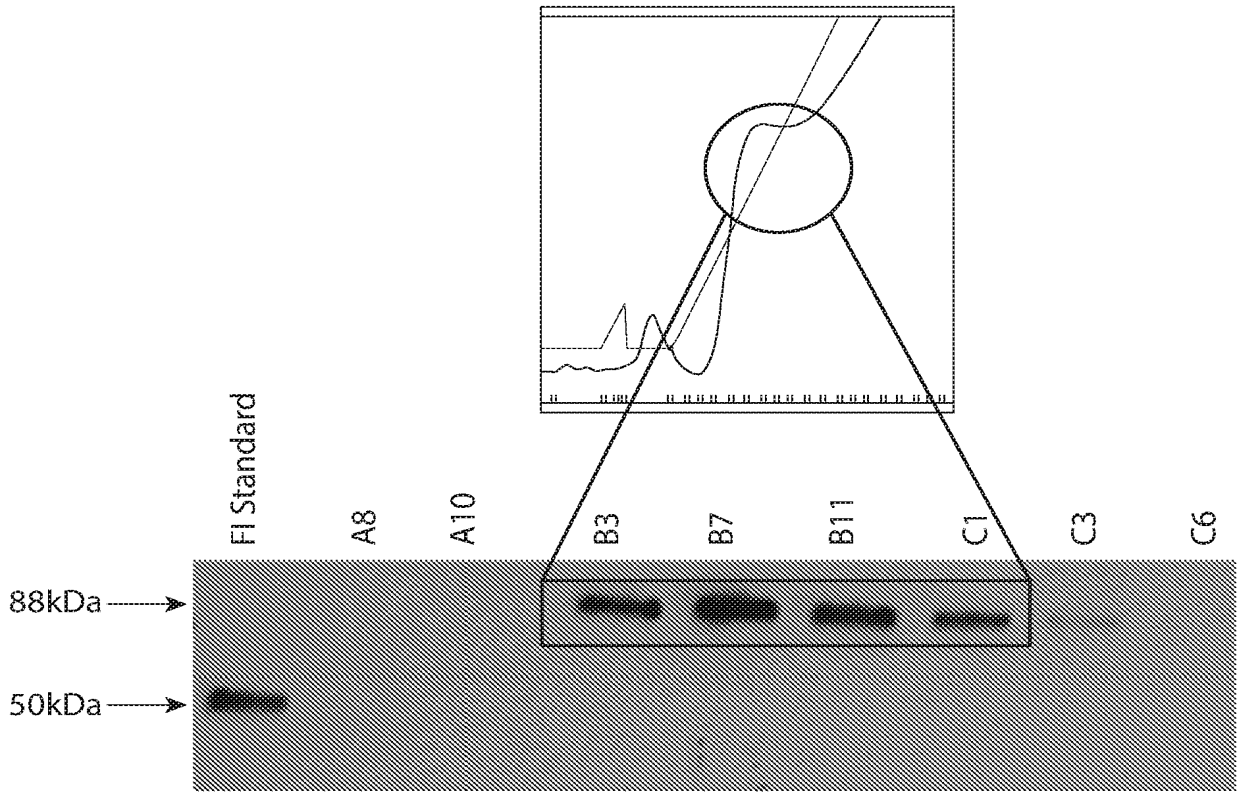

Figure 3

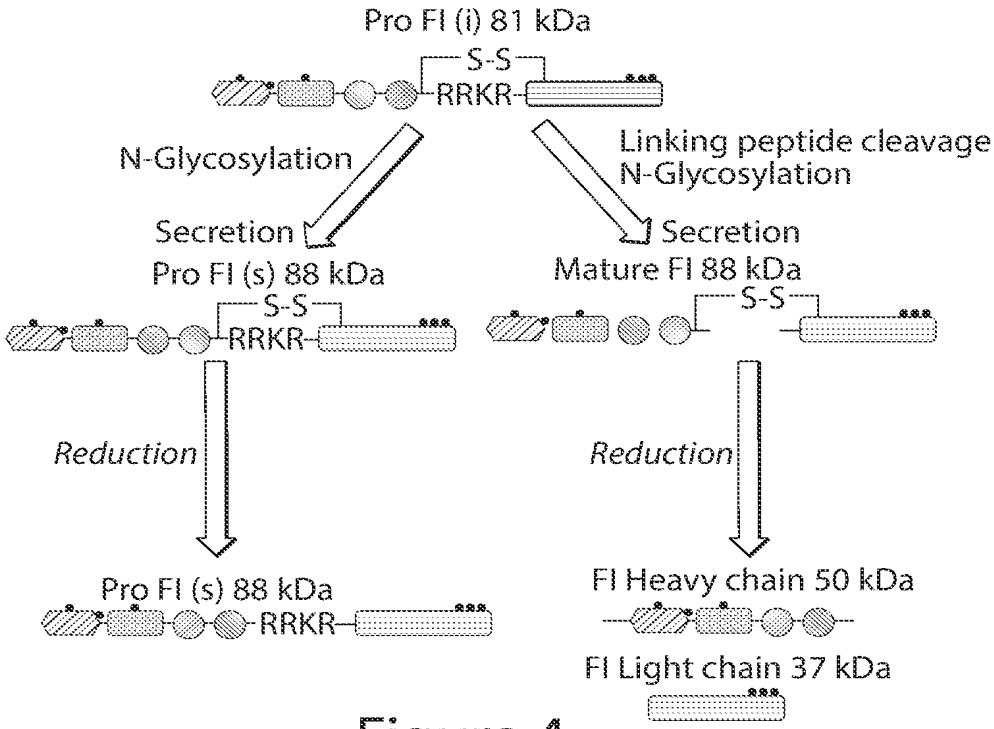

Figure 4

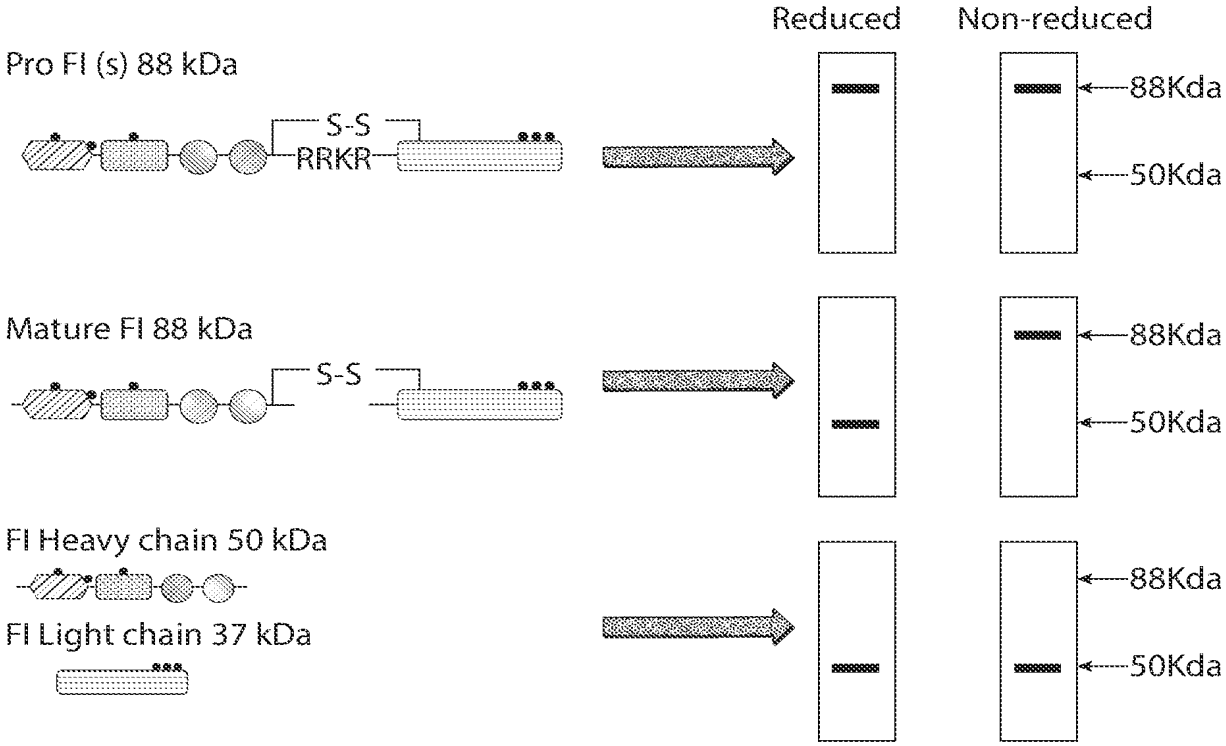

Figure 5

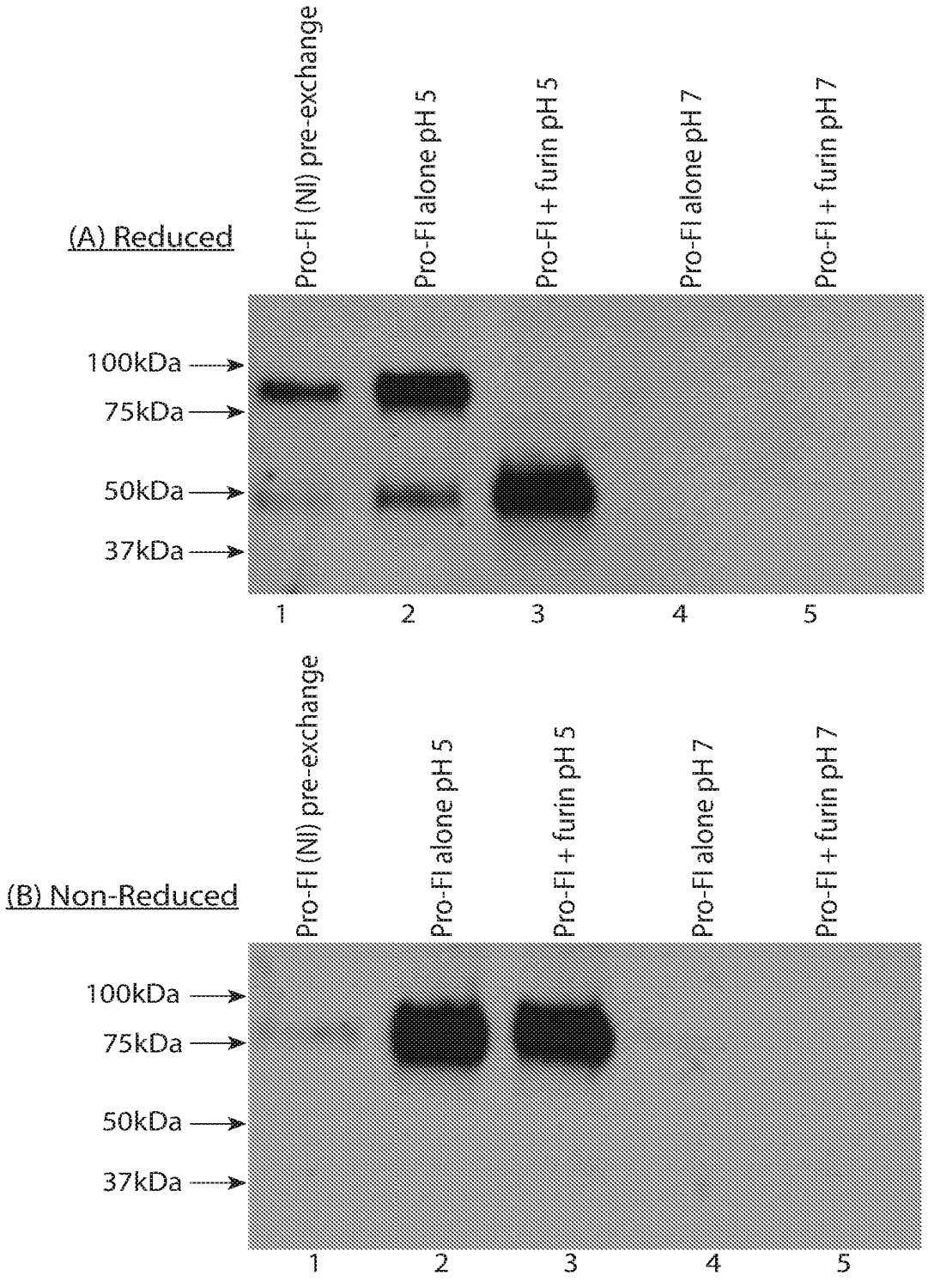
(A) Reduced
Pro-FI (NI) pre-exchange
Pro-FI alone pH 5
Pro-FI + furin pH 5
Pro-FI alone pH 7
Pro-FI + furin pH 7
100kDa
75kDa
50kDa
37kDa
1
2
3
4
5
(B) Non-Reduced
Pro-FI (NI) pre-exchange
Pro-FI alone pH 5
Pro-FI + furin pH 5
Pro-FI alone pH 7
Pro-FI + furin pH 7
100kDa
75kDa
50kDa
37kDa
1
2
3
4
5

Figure 6

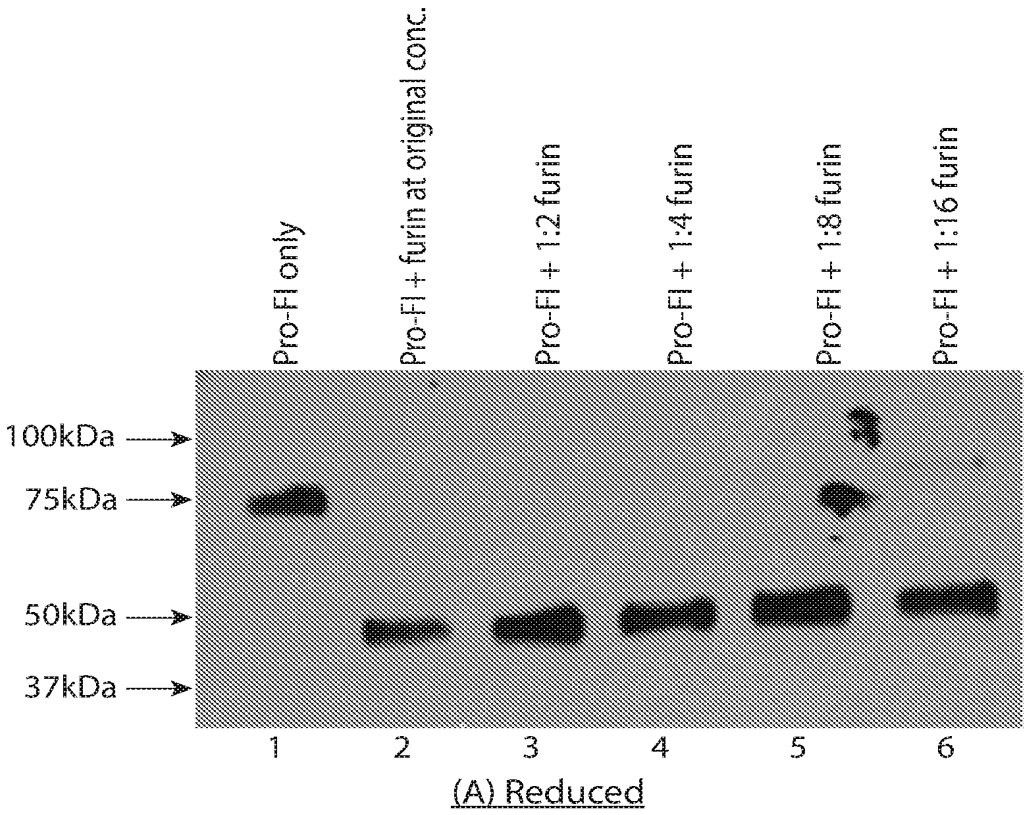
Pro-Fl only
Pro-Fl + furin at original conc.
Pro-Fl + 1:2 furin
Pro-Fl + 1:4 furin
Pro-Fl + 1:8 furin
Pro-Fl + 1:16 furin
100kDa
75kDa
50kDa
37kDa
1
2
3
4
5
6
(A) Reduced

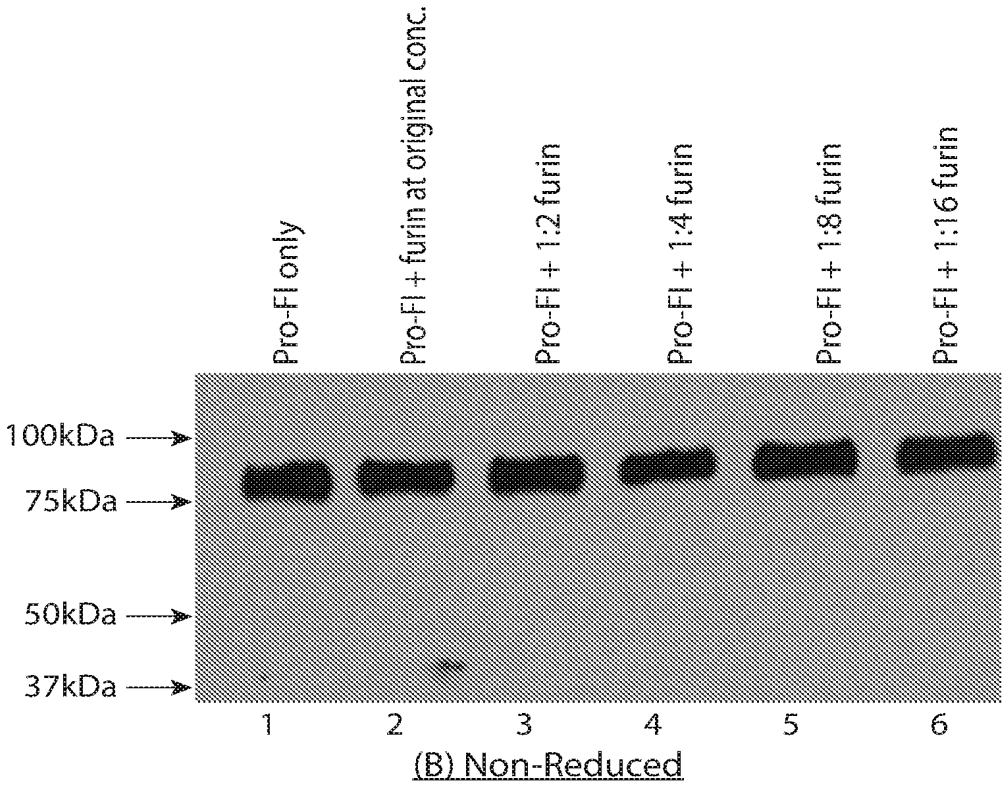
Pro-Fl only
Pro-Fl + furin at original conc.
Pro-Fl + 1:2 furin
Pro-Fl + 1:4 furin
Pro-Fl + 1:8 furin
Pro-Fl + 1:16 furin
100kDa
75kDa
50kDa
37kDa
1
2
3
4
5
6
(B) Non-Reduced

Figure 7

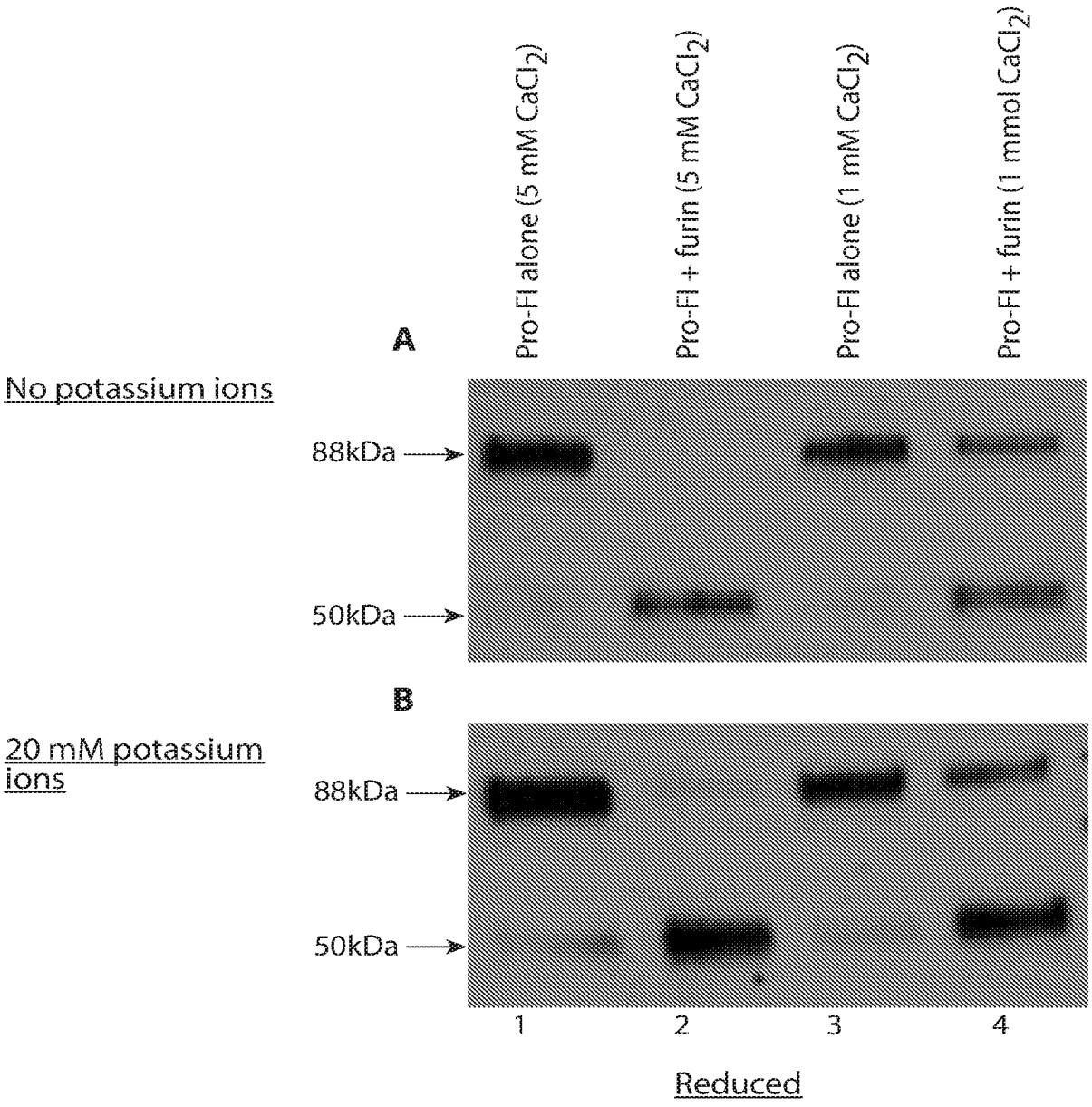
Pro-FI alone (5 mM $CaCl_2$)
Pro-FI + furin (5 mM $CaCl_2$)
Pro-FI alone (1 mM $CaCl_2$)
Pro-FI + furin (1 mmol $CaCl_2$)
A
No potassium ions
88kDa
50kDa
B
20 mM potassium ions
88kDa
50kDa
1
2
3
4
Reduced

Figure 8

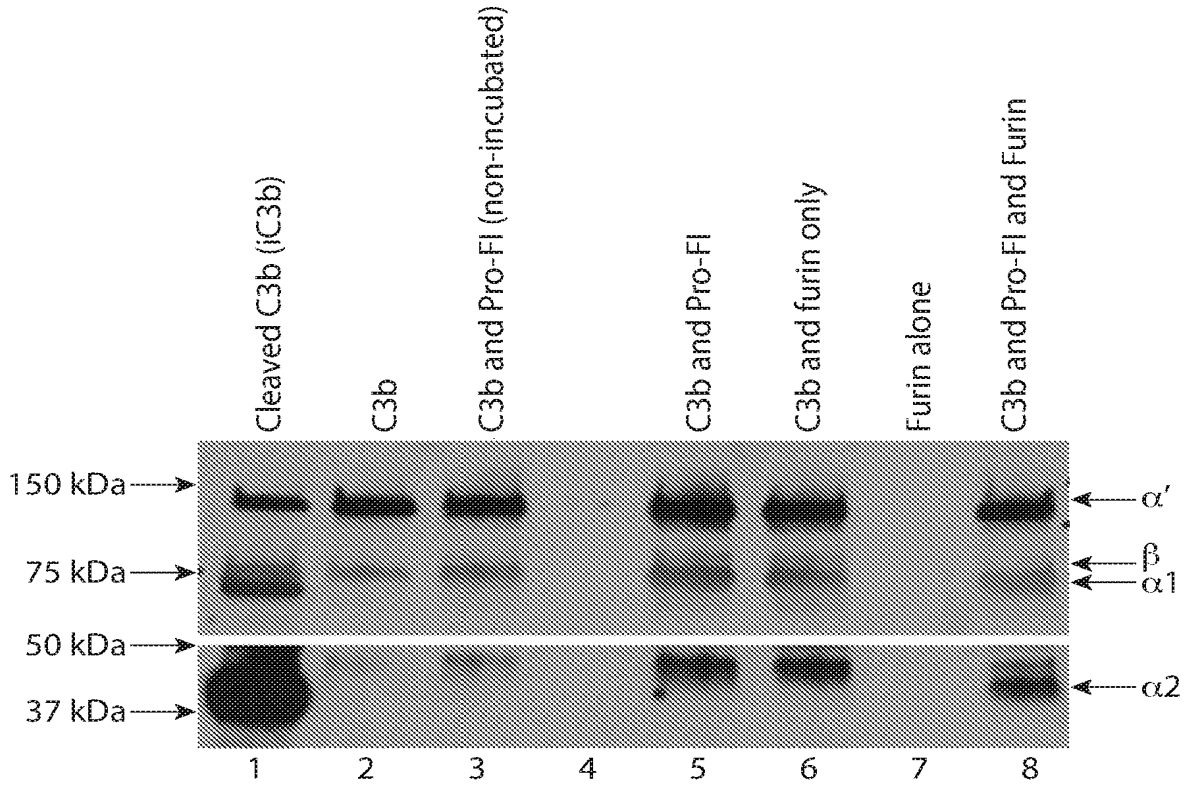

Figure 9

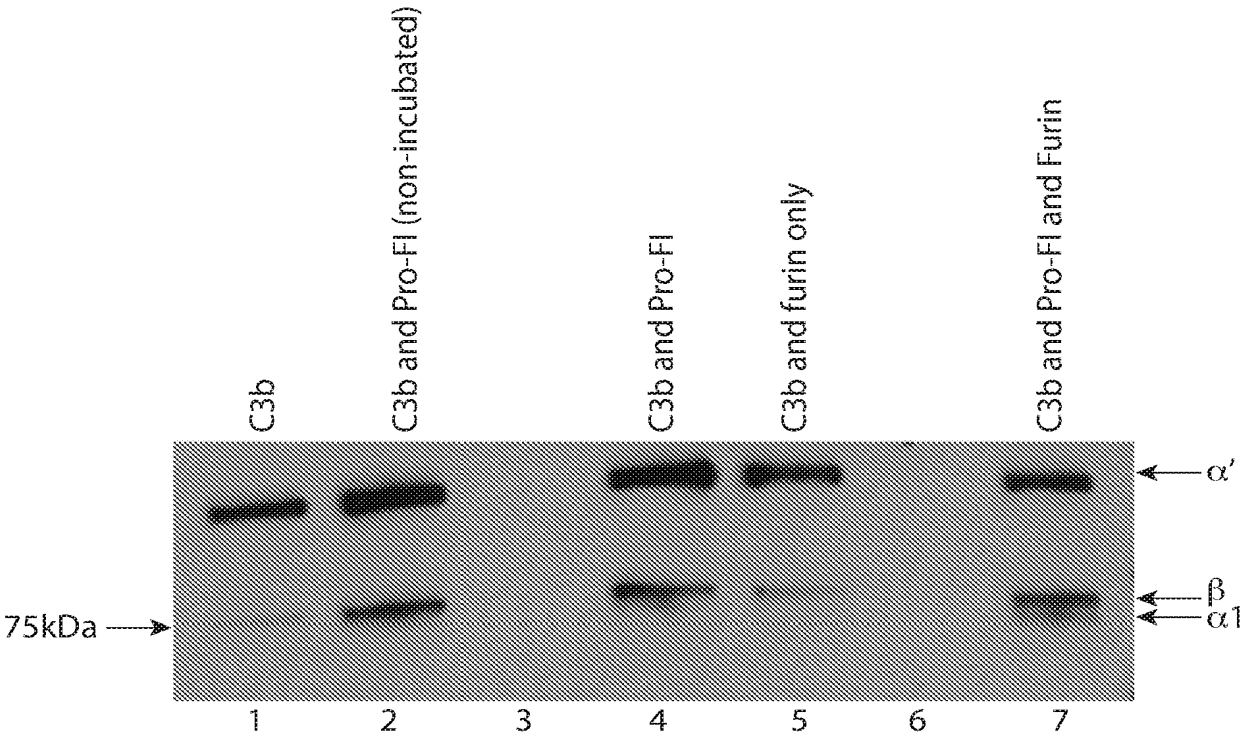

Figure 10

INTERNATIONAL SEARCH REPORT

International application No.
PCT/US2018/022471

A. CLASSIFICATION OF SUBJECT MATTER

A61K 38/54 (2006.01) A61K 38/43 (2006.01) C07K 19/00 (2006.01)

According to International Patent Classification (IPC) or to both national classification and IPC

B. FIELDS SEARCHED

Minimum documentation searched (classification system followed by classification symbols)

Documentation searched other than minimum documentation to the extent that such documents are included in the fields searched

Electronic data base consulted during the international search (name of data base and, where practicable, search terms used)

Databases: PATENW = EPODOC, WPIAP, TXPEA, TXPEB, TXPEC, TXPEE, TXPEF, TXPEH, TXPEI, TXPEP, TXPES, TXPWOEA, TXPUSE0A, TXPUSE1A, TXPUSEA, TXPUSEB, TXPEPEA, TXPEPEB; MEDLINE, BIOSIS, CAPLUS, EMBASE; Google; GenomeQuest, Patent Scope and internal databases.

Search terms: complement factor I, furin, PACE, CFI, recombinant, Kavanagh, David, Marchbank, Kevin, Gemini Therapeutics and similar terms

C. DOCUMENTS CONSIDERED TO BE RELEVANT

Category*	Citation of document, with indication, where appropriate, of the relevant passages	Relevant to claim No.
	Documents are listed in the continuation of Box C	

[X] Further documents are listed in the continuation of Box C

[X] See patent family annex

* Special categories of cited documents:

"A" document defining the general state of the art which is not considered to be of particular relevance

"E" earlier application or patent but published on or after the international filing date

"L" document which may throw doubts on priority claim(s) or which is cited to establish the publication date of another citation or other special reason (as specified)

"O" document referring to an oral disclosure, use, exhibition or other means

"P" document published prior to the international filing date but later than the priority date claimed

"T" later document published after the international filing date or priority date and not in conflict with the application but cited to understand the principle or theory underlying the invention

"X" document of particular relevance; the claimed invention cannot be considered novel or cannot be considered to involve an inventive step when the document is taken alone

"Y" document of particular relevance; the claimed invention cannot be considered to involve an inventive step when the document is combined with one or more other such documents, such combination being obvious to a person skilled in the art

"&" document member of the same patent family

Date of the actual completion of the international search	Date of mailing of the international search report
3 July 2018	03 July 2018
Name and mailing address of the ISA/AU	**Authorised officer**
AUSTRALIAN PATENT OFFICE PO BOX 200, WODEN ACT 2606, AUSTRALIA Email address: pct@ipaustralia.gov.au	Ann Le AUSTRALIAN PATENT OFFICE (ISO 9001 Quality Certified Service) Telephone No. +61262832745

INTERNATIONAL SEARCH REPORT

International application No.
PCT/US2018/022471

Box No. I Nucleotide and/or amino acid sequence(s) (Continuation of item 1.c of the first sheet)

1. With regard to any nucleotide and/or amino acid sequence disclosed in the international application, the international search was carried out on the basis of a sequence listing:

   a. [X] forming part of the international application as filed:

      [ ] in the form of an Annex C/ST.25 text file.

      [X] on paper or in the form of an image file.

   b. [ ] furnished together with the international application under PCT Rule 13ter.1(a) for the purposes of international search only in the form of an Annex C/ST.25 text file.

   c. [ ] furnished subsequent to the international filing date for the purposes of international search only:

      [ ] in the form of an Annex C/ST.25 text file (Rule 13ter.1(a)).

      [ ] on paper or in the form of an image file (Rule 13ter.1(b) and Administrative Instructions, Section 713).

2. [ ] In addition, in the case that more than one version or copy of a sequence listing has been filed or furnished, the required statements that the information in the subsequent or additional copies is identical to that forming part of the application as filed or does not go beyond the application as filed, as appropriate, were furnished.

3. Additional comments:

Category*	Citation of document, with indication, where appropriate, of the relevant passages	Relevant to claim No.
	Buchberger, A.: "The therapeutic utility of Factor I in the treatment of complement dependent pathophysiological processes", May 2016, Department of Infection, Immunity and Inflammation, University of Leicester [online], [retrieved from internet 28 June 2018] <URL:*https://lra.le.ac.uk/bitstream/2381/39850/1/2016BuchbergerAPhD.pdf*> Whole document	
X	see pages 32, 52 58-59, 72-93, 148-149, 184-188 and Figures 3.11 and 3.12	1-64
A	NAKAYAMA, K.: "Furin : a mammalian subtilisin/Kex2p-like endoprotease involved in processing of a wide variety of precursor proteins", Biochem. J. (1997) Vol. *327*, pages 625±635	
A	WO 2007/047995 A2 (CATALYST BIOSCIENCES, INC) 26 April 2007	
A	WO 2010/103291 A2 (CAMBRIDGE ENTERPRISE LIMITED) 16 September 2010	
A	WO 2011/107591 A1 (RIGSHOSPITALET et al.) 09 September 2011	
A	WO 2014/203188 A2 (GLAXOSMITHKLINE INTTELECTUAL PROPERTY (NO.2) LIMITED) 24 December 2014	

INTERNATIONAL SEARCH REPORT Information on patent family members	International application No. **PCT/US2018/022471**

This Annex lists known patent family members relating to the patent documents cited in the above-mentioned international search report. The Australian Patent Office is in no way liable for these particulars which are merely given for the purpose of information.

Patent Document/s Cited in Search Report		Patent Family Member/s	
Publication Number	**Publication Date**	**Publication Number**	**Publication Date**
WO 2007/047995 A2	26 April 2007	WO 2007047995 A2	26 Apr 2007
		AU 2006304804 A1	26 Apr 2007
		AU 2006304804 B2	02 Jun 2011
		CA 2626356 A1	26 Apr 2007
		CN 101340928 A	07 Jan 2009
		CN 101340928 B	21 Dec 2011
		CN 102430117 A	02 May 2012
		EP 1940457 A2	09 Jul 2008
		EP 1940457 B1	12 Dec 2012
		EP 2428218 A1	14 Mar 2012
		EP 2433642 A2	28 Mar 2012
		EP 2433642 B1	07 Dec 2016
		HK 1115815 A1	28 Mar 2013
		IL 190954 A	31 Jul 2017
		JP 2009512451 A	26 Mar 2009
		JP 5219819 B2	26 Jun 2013
		JP 2013013420 A	24 Jan 2013
		JP 5860789 B2	16 Feb 2016
		KR 20080073710 A	11 Aug 2008
		KR 101126423 B1	11 Jul 2012
		KR 20110043772 A	27 Apr 2011
		KR 101393946 B1	12 May 2014
		KR 20140007501 A	17 Jan 2014
		KR 101691692 B1	30 Dec 2016
		MX 2008004693 A	03 Sep 2008
		NO 20081755 A	21 Jul 2008
		NZ 595193 A	27 Sep 2013
		NZ 606504 A	29 Aug 2014
		US 2014242062 A1	28 Aug 2014
		US 9795655 B2	24 Oct 2017
		US 2007093443 A1	26 Apr 2007
		US 2012244139 A1	27 Sep 2012

Due to data integration issues this family listing may not include 10 digit Australian applications filed since May 2001.

INTERNATIONAL SEARCH REPORT Information on patent family members	International application No. **PCT/US2018/022471**

This Annex lists known patent family members relating to the patent documents cited in the above-mentioned international search report. The Australian Patent Office is in no way liable for these particulars which are merely given for the purpose of information.

Patent Document/s Cited in Search Report		Patent Family Member/s	
Publication Number	**Publication Date**	**Publication Number**	**Publication Date**
		ZA 200803384 B	28 Jan 2009
WO 2010/103291 A2	16 September 2010	WO 2010103291 A2	16 Sep 2010
		AU 2010222710 A1	27 Oct 2011
		CA 2755473 A1	16 Sep 2010
		CN 102413836 A	11 Apr 2012
		EP 2405931 A2	18 Jan 2012
		US 2012087905 A1	12 Apr 2012
		US 9066941 B2	30 Jun 2015
		US 2015374804 A1	31 Dec 2015
		US 9782460 B2	10 Oct 2017
		US 2018021416 A1	25 Jan 2018
WO 2011/107591 A1	09 September 2011	WO 2011107591 A1	09 Sep 2011
		AU 2011222883 A1	27 Sep 2012
		AU 2011222883 B2	26 May 2016
		CA 2791841 A1	09 Sep 2011
		EP 2542569 A1	09 Jan 2013
		JP 2013520979 A	10 Jun 2013
		JP 6148013 B2	14 Jun 2017
		US 2015210743 A1	30 Jul 2015
		US 9573984 B2	21 Feb 2017
		US 2013217616 A1	22 Aug 2013
		US 9815876 B2	14 Nov 2017
		US 2017166616 A1	15 Jun 2017
WO 2014/203188 A2	24 December 2014	WO 2014203188 A2	24 Dec 2014
		EP 3011343 A2	27 Apr 2016
		JP 2016529482 A	23 Sep 2016
		US 2016139118 A1	19 May 2016
		US 2017285024 A1	05 Oct 2017

End of Annex

Due to data integration issues this family listing may not include 10 digit Australian applications filed since May 2001.

The goal is to provide authoritative and cutting edge reviews of topical state-of-the-art basic research that is expected to have broad clinical impact in the next few years. This is primarily a "by invitation only" submission type, however, if you have suggestions for topics, please contact Jayakrishna Ambati (jambati@email.uky.edu) the Editor for this section.

Geographic Atrophy

Clinical Features and Potential Therapeutic Approaches

Frank G. Holz, MD,[1] *Erich C. Strauss, MD,*[2] *Steffen Schmitz-Valckenberg, MD,*[1] *Menno van Lookeren Campagne, PhD*[2]

In contrast to wet age-related macular degeneration (AMD), where loss of vision is typically acute and treatment leads to a relatively rapid reduction in retinal fluid and subsequent improvements in visual acuity (VA), disease progression and vision loss in geographic atrophy (GA) owing to AMD are gradual processes. Although GA can result in significant visual function deficits in reading, night vision, and dark adaptation, and produce dense, irreversible scotomas in the visual field, the initial decline in VA may be relatively minor if the fovea is spared. Because best-corrected VA does not correlate well with GA lesions or progression, alternative clinical endpoints are being sought. These include reduction in drusen burden, slowing the enlargement rate of GA lesion area, and slowing or eliminating the progression of intermediate to advanced AMD. Among these considerations, slowing the expansion of the GA lesion area seems to be a clinically suitable primary efficacy endpoint. Because GA lesion growth is characterized by loss of photoreceptors, it is considered a surrogate endpoint for vision loss. Detection of GA can be achieved with a number of different imaging techniques, including color fundus photography, fluorescein angiography, fundus autofluorescence (FAF), near-infrared reflectance, and spectral-domain optical coherence tomography. Previous studies have identified predictive characteristics for progression rates including abnormal patterns of FAF in the perilesional retina. Although there is currently no approved or effective treatment to prevent the onset and progression of GA, potential therapies are being evaluated in clinical studies. *Ophthalmology 2014;121:1079-1091 © 2014 Published by Elsevier Inc. on behalf of the American Academy of Ophthalmology.*

Supplemental material is available at www.aaojournal.org.

Age-related macular degeneration (AMD) is a progressive, degenerative disease of the retina, in which the macula, the area responsible for visual acuity (VA) and color vision, is most affected. The prevalence of AMD increases with age, and it is estimated that in the United States approximately 8 million people ≥55 years old have monocular or binocular intermediate AMD or monocular advanced AMD.[1]

Early signs of AMD include the development of drusen, extracellular deposits between the retinal pigment epithelium (RPE) and Bruch's membrane (Fig 1). In its early and intermediate stages, AMD causes only minimal VA impairment. The advanced stage of dry AMD, geographic atrophy (GA), is characterized by loss of retinal photoreceptors, RPE, and choriocapillaris, and is responsible for approximately 20% of all cases of legal blindness in North America.

Depending on the histopathologic features and stage of the disease, AMD can be divided into several categories. Early AMD is characterized by multiple small (<63 μm) or ≥1 intermediate drusen (≥63 but <125 μm); in intermediate AMD, there may be many intermediate or ≥1 large drusen (≥125 μm), often accompanied by hyper- or hypopigmentation of the RPE; and advanced AMD is characterized by 2 types of late stage lesions: GA (dry) and neovascular (wet) AMD. There is no exclusive dichotomy between GA and wet AMD; both forms of the disease may develop in the same eye. Approximately 10% to 15% of patients with intermediate dry AMD progress to the neovascular form.[2] The average time from entering the Age-related Eye Disease Study (AREDS) to initial appearance of GA has been shown to be approximately 5 to 6 years in the presence of confluent or large (>125 μm) drusen and

ISSN 0161-6420/14/$ - see front matter
http://dx.doi.org/10.1016/j.ophtha.2013.11.023

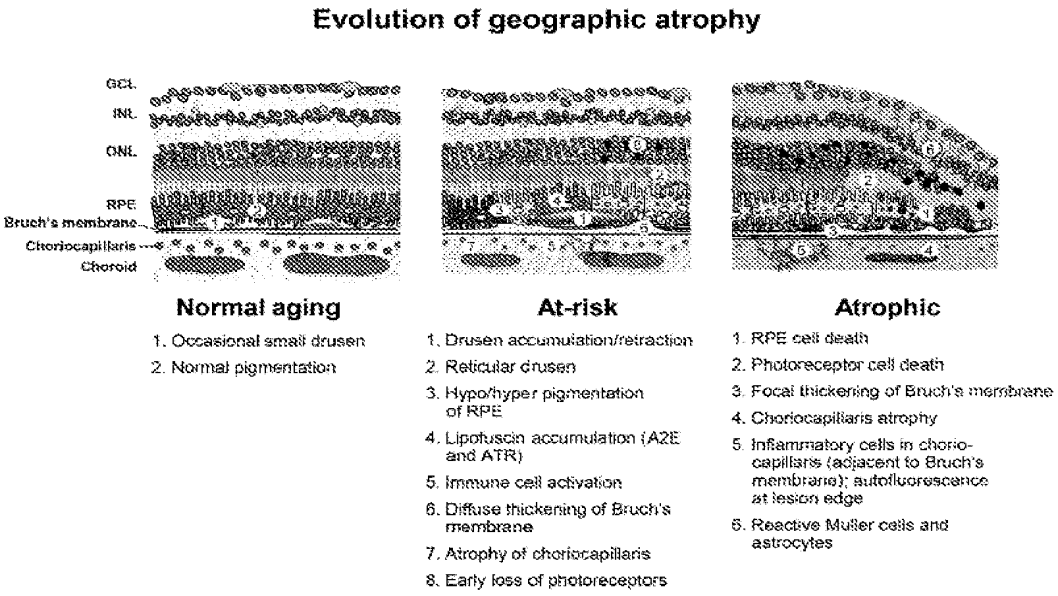

Figure 1. Simplified diagram showing changes in the macula during evolution of geographic atrophy (GA). Three manifestations of retina failure are represented. The course of the disease can vary from case to case. (Modified from Sarks et al., Eye 1988.) A2E = N-retinyl-N-retinylidene ethanolamine; ATR = all-trans retinal; GCL = ganglion cell layer; INL = inner nuclear layer; ONL = outer nuclear layer; RPE = retinal pigment epithelium.

hyperpigmentation, as compared with 2.5 years in the presence of hypopigmentation.[3,4]

The biology of neovascular AMD is better understood than the atrophic form of the disease. This may be because of the availability of better predictive preclinical models for neovascular AMD, although more recently rodent models of atrophic AMD have shown some promise.[5] Because most pathways identified by genetics seem to predispose to both forms of AMD, the current thinking is that both advanced stages are initiated by common pathways that culminate in stress and damage to the RPE, Bruch's membrane, and choroid, and can result in either photoreceptor degeneration or choroidal neovascularization with subsequent degeneration. Based on this principle, early treatment of AMD at the high-risk intermediate AMD stage would be required to prevent both forms of advanced AMD.

Currently, there is no approved or effective treatment to prevent either onset or progression of GA. However, in recent years, significant progress has been made in understanding the pathogenesis of GA, which has led to a number of new potential therapies currently undergoing clinical trial evaluation (Table 1, available at www.aaojournal.org).

Clinical Background on GA

Epidemiology and Risk Factors

In the industrially developed world, AMD is the primary cause of blindness for adults >55 years of age. Patients in the early and intermediate stages of dry AMD generally do not lose central vision, but instead have other functional impairments, such as difficulty reading and limited vision at night or with reduced light.[6] Risk factors for AMD include advanced age, race, smoking, and diet.

With aging, gradual and cumulative damage to the retina occurs through various factors, including oxidative stress. In addition, impairment of normal physiologic function in RPE cells, including the constant degradation of lipid-rich outer photoreceptor discs, can lead to formation of intracellular (lipofuscin) and extracellular debris (drusen). The advanced form of dry AMD, or GA, is responsible for approximately 20% of all legal cases of blindness in North America with increasing incidence and prevalence owing to a higher life expectancy.

Overall, AMD is more common in white patients than in individuals of other ethnic origins. Although drusen are seen with similar frequency in non-white and white people, the latter have been shown to have an increased prevalence of advanced AMD, perhaps a consequence of lower melanin levels. In the Multi-ethnic Study of Atherosclerosis, the prevalence of AMD was 2.4% in blacks, 4.2% in Hispanics, 4.6% in Chinese, and 5.4% in whites.[7]

Cigarette smoking is another risk factor for AMD in many clinical trials. A direct correlation has been reported between the risk of developing the disease and number of cigarettes smoked. In a case-control study of 715 white patients, smoking >40 pack-years of cigarettes was associated with a 3.5-fold higher risk for GA.[8] The mechanisms by which smoking increases the risk for AMD include the reduced generation of antioxidants, induction of hypoxia, generation of reactive oxygen species, and impaired choroidal blood flow.

Finally, there is some evidence for an association between diet, specifically fat intake, and obesity and an increased risk of AMD. Moreover, several studies have demonstrated the protective effect of antioxidants, nuts, fish,

and ω-3 fatty acids. In the AREDS study, a zinc antioxidant oral supplement was reported to slow the progression of AMD to the wet form of AMD, but there was no statistical benefit in GA.[9] In the Blue Mountains Eye Study, it was shown that high dietary lutein and zeaxanthin intake reduced the risk of long-term AMD. However, the AREDS2 study has shown that the addition of lutein plus zeaxanthin or ω-3 polyunsaturated fatty acids (PUFAs; docosahexaenoic acid plus eicosapentaenoic acid), or both, to the AREDS formulation has not significantly reduced the risk of progression to advanced AMD.[10]

Genetics

Both population-based and familial studies have found evidence of sibling correlations, with an estimation that genetic factors can account for between 55% and 57% of the total variability in disease risk.[11] Recent findings on single nucleotide polymorphism in genes coding for complement factors (CF) H, I, and B, and complement components 2 and 3, implicate the complement system in the pathophysiology of both intermediate and advanced AMD.[12] Many association and linkage studies have pointed to chromosomal locus 1q3, linked with the CFH gene, in conferring substantial AMD risk.[13]

Although genetic association of AMD with a single nucleotide polymorphism does not necessarily imply a causative relationship, in the case of CFH there is strong evidence for a link between CFH function as a negative regulator of the alternative complement pathway and AMD. This is based on the finding that a rare penetrant mutation in CFH that results in loss of function of this important negative regulator of the pathway predisposes to AMD showing a strong genetics-based relationship between increased alternative pathway complement activation and AMD.[14] Furthermore, by combining risk and protective alternative pathway variants, a "complotype" was revealed in which C3, fH, and fB variants collaborate to set levels of alternative pathway activity in plasma, thereby influencing risk in complement-dependent diseases.[15] Last, rare, highly penetrant missense mutations in CFI, a negative regulator of the alternative complement pathway, confers high risk of AMD.[16] Hence, a potentially causative relation has been found between alternative complement pathway activation and the incidence of advanced AMD.

Sequencing of chromosome 10q26 identified common variants with large effect sizes near the age-related maculopathy susceptibility 2 (ARMS2) and high temperature requirement A serine peptidase 1 (HTRA1) genes establishing this locus, in addition to the CFH variant on chromosome 1, as a second major AMD susceptibility locus. A total of 15 variants in this locus were in strong linkage disequilibrium leaving statistics-based analyses with insufficient power to discriminate between these variants.[17] Functional dissection of the effects of each risk-associated variant in 10q26 is required to determine which of the 2 genes, ARMS2 or HTRA1, is the true AMD susceptibility gene. Only recently, more detailed genome-wide association studies have investigated whether the 2 subtypes of advanced AMD, choroidal neovascularization (CNV), and GA, segregate separately in families and associate with different disease variants. The variants in the 10q26 locus confer increased risk for both advanced AMD subtypes, but imparts greater risk for CNV than for GA.[11] Other loci were detected with suggestive associations that differ for advanced AMD subtypes and deserve follow-up in additional studies.

A recent, collaborative, genome-wide association study by the AMD Gene Consortium included >17 100 advanced AMD cases and >60 000 controls of European and Asian ancestry.[11] This study identified 19 loci involved in the regulation of complement activity, lipid metabolism, extracellular matrix remodeling and angiogenesis ($P < 5 \times 10^{-8}$), which includes 7 loci with associations reaching $P < 5 \times 10^{-8}$ for the first time near genes *COL8A1-FILIP1L, IER3-DDR1, SLC16A8, TGFBR1, RAD51B, ADAMTS9*, and *B3GALTL*.

The gene for hepatic lipase (LIPC), located on chromosome 15q21.3, was recently found to be associated with AMD in a large, genome-wide association study[13,18]; its findings were confirmed in another genome-wide study where a strong association with alleles at 2 loci previously associated with high-density lipoprotein (HDL) was found.[19] Exploring the relationship between the LIPC genotype and serum lipids, it was found that the TT genotype of the LIPC gene was associated with a reduced risk of both wet and dry AMD.[13] However, despite this genetic link between LIPC and AMD, epidemiologic evidence suggests that this is not mediated through plasma HDL. Future studies elucidating the role of LIPC in the eye are needed.

Imaging Features

Based on stereo biomicroscopy and color fundus photography, there are distinctive features of GA that differ from other forms of dry AMD. The GA areas are visible on funduscopy as sharply demarcated hypopigmented areas, in which larger choroidal vessels may become visible owing to the absence of the RPE and the choriocapillaris. Although crystalline drusen may be present in areas of GA, soft drusen as in intermediate dry AMD are absent. The definition of GA is based on clinicohistopathologic investigations that have shown that clinically visible areas of atrophy are characterized by cell death in the RPE, outer neurosensory retina, and choriocapillaris. With modern in vivo imaging technology, these findings can be confirmed. By spectral-domain optical coherence tomography (SD-OCT) imaging, choroidal signal enhancement owing to the loss of absorbing pigment and thinning of the outer retinal layers, including the outer nuclear layer, are clearly visible at the site of GA. Owing to the atrophy of the RPE and thus loss of fluorophores, atrophic areas in GA exhibit a markedly reduced signal by FAF imaging (Fig 2). Using simultaneous SD-OCT and FAF confocal scanning laser ophthalmoscope imaging, an excellent spatial correlation of typical SD-OCT and FAF findings at the site of atrophic areas could be demonstrated with loss of photoreceptors (Fig 3). Both modalities allow for noninvasive and rapid assessment of GA in the clinical setting. With image analysis software, areas of GA can

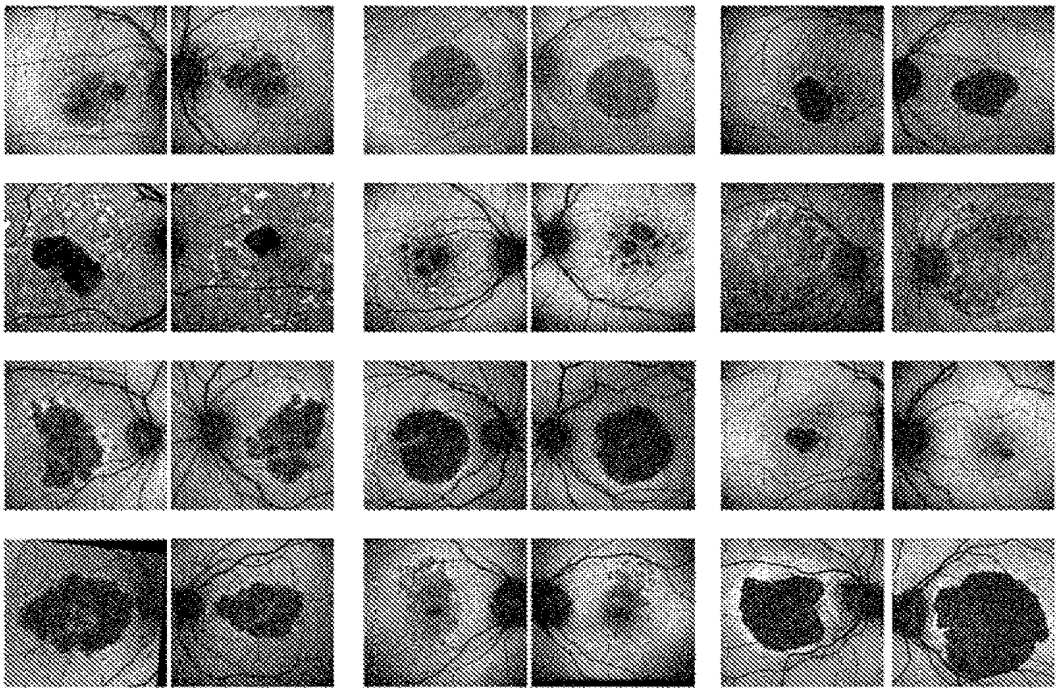

Figure 2. Fundus autofluorescence (FAF) images of both eyes from various patients with unifocal and multifocal geographic atrophy. Note the high degree of intraindividual symmetry between both eyes and interindividual heterogeneity with regard to geographic atrophy size and topography (dark patches reflecting a reduced FAF signal owing to absence of retinal pigment epithelial cells and its fluorophores). This is also seen for the perilesional abnormal patterns of increased FAF signals surrounding the atrophic patches.

be semiautomatically quantified and GA enlargement can be monitored over time. The corresponding functional impact can be demonstrated by microperimetry (Fig 4).

Natural History and Progression

The earliest signs of AMD include the appearance of small drusen, which increase in size over time. Drusen with a diameter of <63 μm, so-called drupelets, are not associated with increased risk of progression and are, therefore, not considered AMD but rather a nonspecific aging change.[3] Intermediate stages are defined by larger, confluent drusen as well as hyper- and hypopigmentation and degeneration, whereas the advanced stage is either GA or CNV. In dry AMD, loss of vision occurs gradually over several years and progresses to GA, a degeneration of the RPE and death of photoreceptor cells, leading to irreversible vision loss. Patients with GA, even in late stages, may maintain good central vision over some time, until the disease progression involves the central fovea. The peripheral spread is typically faster than toward the center for unknown reasons.

Approximately 10% to 15% of patients with intermediate dry AMD progress to the neovascular form. A retrospective analysis of 95 eyes from 2 AREDS studies found that the average time from study entrance to initial appearance of GA was 5 to 6 years in the presence of confluent or large (>125 μm) drusen and hyperpigmentation, compared with 2.5 years in the presence of hypopigmentation.[20] Drusen were found in 100% of patients at the site of later GA development; drusen >125 μm, confluent drusen, and hyperpigmentation were present in >90% of eyes, whereas drusen >250 μm and hypopigmentation were present in >80% eyes.

Longitudinal studies have shown that progression rates vary widely among patients.[21] A mean growth rate of atrophic areas of 1.2 to 2.8 mm^2 per year has been reported from various studies. Some studies have shown that growth rates of atrophic patches depend on size of lesion, with small lesions (disc area [DA] = 0.67 mm^2) growing at approximately 0.5 mm^2 per year, with medium sized lesions (DA = 1.7 mm^2) growing at a rate of 1.5 mm^2 per year[22]; and the largest lesions (DA = 4.2 mm^2) progressing at around 2 to 6 mm^2 per year.[23]

In the Beaver Dam Eye Study, the overall increase in atrophy was 6.4 mm^2 over 5 years. Eyes with multifocal lesions had greater increases (12 mm^2) in atrophy area, and progressed to foveal center more often (83%) compared with eyes with single lesions (2.24 mm^2 increase in atrophy area, 22% progressed to fovea).[4]

Several factors are thought to predict GA progression, such as knowledge of prior rate of atrophic area growth and patterns of abnormal fundus autofluorescence (FAF) detected by confocal scanning laser ophthalmoscopy.[24]

Pathophysiology of AMD

The pathology of AMD is characterized by degenerative changes in the outer portion of the retina, the photoreceptors, the RPE, Bruch's membrane, and the choriocapillaris, leading ultimately to visual loss (Figs 1 and 5). Early

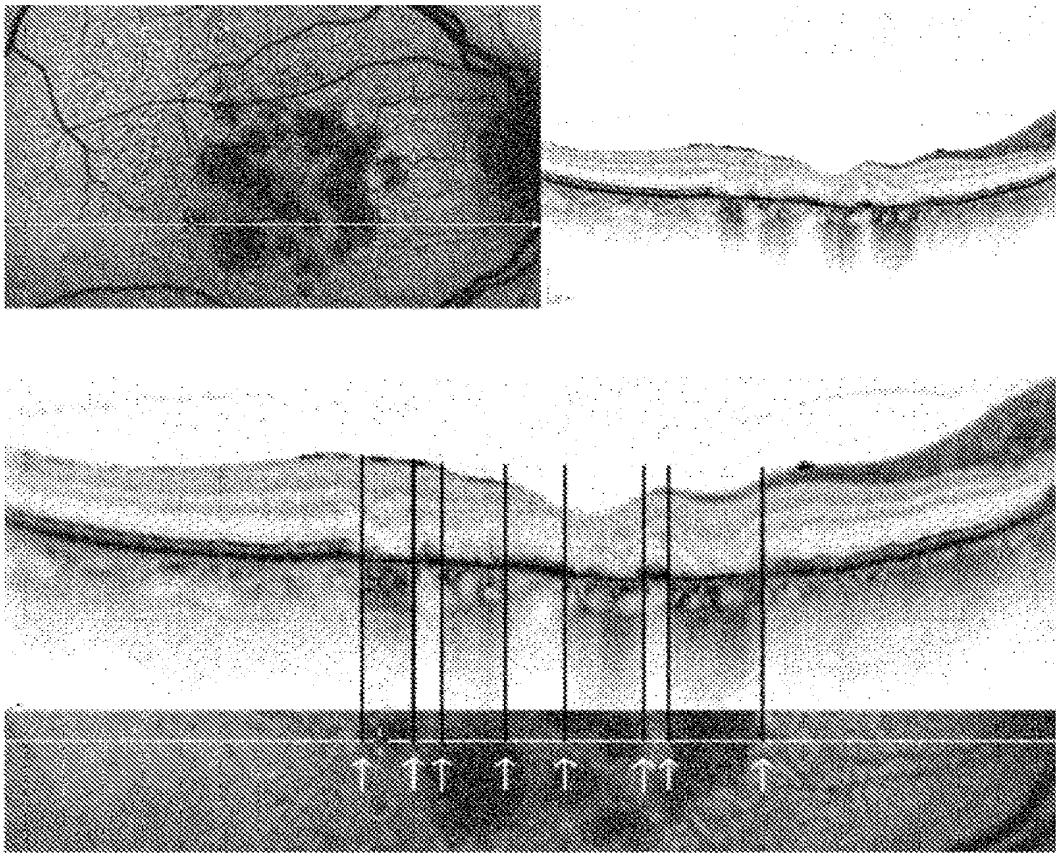

Figure 3. Severely decreased fundus autofluorescence over areas of atrophy is spatially confined to loss of photoreceptors and choroidal signal enhanced by spectral domain optical coherence tomography (SD-OCT) as shown in this representative example of a 77-year-old woman with multifocal atrophic age-related macular degeneration (*upper row*, overview of simultaneous fundus autofluorescence and SD-OCT imaging; *lower row*, at high magnification, the exact correlation of both imaging modalities is illustrated). White arrows and black lines show the loss of the outer retina over areas of decreased fundus autofluorescence, exactly at the site where the SD-OCT B-scan was positioned on the autofluorescence image.

changes include basal laminar and basal linear deposits, thickening and accumulation of lipoidal material in Bruch's membrane, lipofuscin accumulation in the lysosomal compartment of the RPE, and drusen formation beneath the basal lamina of RPE as well as subretinal deposits apical of the RPE cell monolayer (so-called reticular drusen). Both hard and soft drusen are hallmark lesions of AMD. Hard drusen are pinpoint, yellow—white lesions <63 μm in diameter; in small numbers they are not considered a risk factor for AMD, but in larger numbers they independently predict AMD.[23] Soft drusen are larger, have indistinct edges, and tend to become confluent. The presence of large and confluent drusen is a significant risk factor for developing CNV and GA. Reticular drusen are best identified with near-infrared reflectance and/or FAF scanning laser ophthalmoscopy imaging, and are highly prevalent in eyes with GA.[24] Late changes include RPE atrophy, or GA, presenting as well-demarcated areas of RPE cell loss, subsequent to hypopigmentation. This process is followed by degeneration of corresponding photoreceptors, and thinning of the retina.

The pathophysiology of GA remains poorly understood, in part because of its multifactorial etiology, a combination of environmental and genetic risk factors, and a lack of appropriate animal models. Biochemical, histologic, and genetic studies have implicated several pathways, including oxidative damage, chronic inflammation, excessive accumulation of lipofuscin, and malfunctioning of the complement system. These mechanisms may be operative in various phenotypic manifestations of AMD, and it is currently unknown which of these mechanisms are more relevant or perhaps specific for the development of outer retinal atrophy. In addition, the contribution of different mechanisms may vary between patients, which may be reflected in differences in the genotype or clinical characteristics, for example, presence or absence of reticular drusen with GA.

Lipids and Lipid Metabolism

Available evidence from epidemiology, pathology, and genetics studies suggests a potential link between risk factors for cardiovascular disease and AMD, such as smoking, hypertension, and hyperlipidemia. Accumulation of lipids in Bruch's membrane play a vital role in the pathogenesis of AMD and there are similarities between AMD lesions and

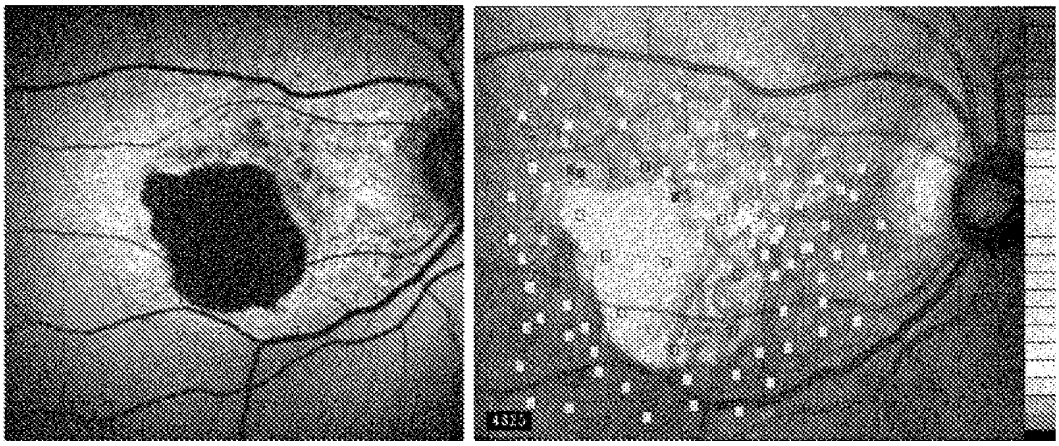

Figure 4. Loss of retinal sensitivity on microperimetry in the area of geographic atrophy. In perilesional areas with increased autofluorescence, signal retinal sensitivity is reduced to variable degrees.

atherosclerotic plaques, although it has been shown that the lipoprotein particles within Bruch's membranes are different from plasma lipoproteins in that they contain free and esterified cholesterol, phosphatidylcholine, and apolipoprotein B100.[27] A number of studies have explored the potential of statins in lowering the incidence and progression of AMD; however, most studies were observational, retrospective, or population based, and the results were inconclusive. A recent Cochrane review identified just 2 randomized, placebo-controlled trials—one with inconclusive results; the other, ongoing.[28]

Inflammation, Complement, and the Inflammasome

In contrast with wet AMD, where CNV is associated with inflammatory cells,[29] the etiology of GA has not been associated with a marked recruitment of leukocytes from the circulation. Rather, GA has been primarily associated with activation of cells constitutively present in the retina, including microglia cells, Muller cells, RPE cells, and occasional macrophages, with peripheral immune cells present in the choroid, mostly consisting of pericapillary macrophages, giant cells and mast cells[30] (Lutty G, Bhutto I,

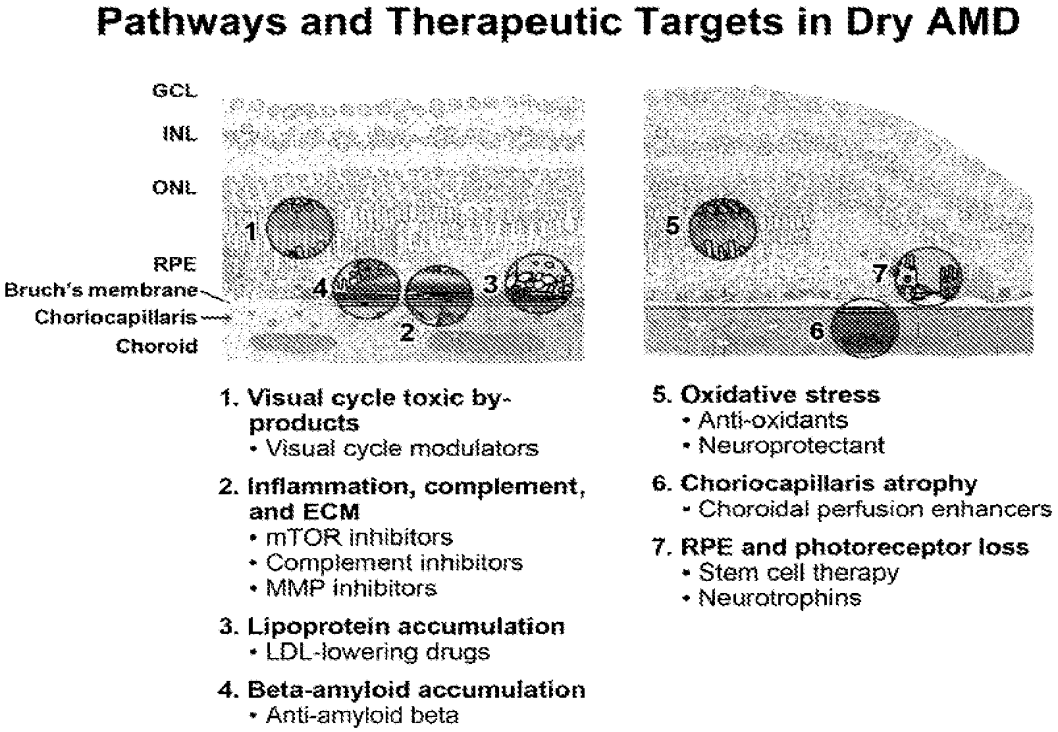

Figure 5. Different targetable pathways involved in the development of GA. AMD = age-related macular degeneration; ECM = extracellular matrix; GA = geographic atrophy; GCL = ganglion cell layer; INL = inner nuclear layer; LDL = low-density lipoprotein; MMP = matrix metalloproteinase; ONL = outer nuclear layer; RPE = retinal pigment epithelium; mTOR = mammalian target of rapamycin.

Seddon J, Mcleod D. Mast cell degranulation in AMD choroid. Presented at the Association for Research in Vision and Ophthalmology [ARVO] Annual Meeting, May 5–9, 2013, Seattle, WA). The appearance of these innate immune cells close to sites of cellular deposits on Bruch's membrane may indicate that the phagocytotic capacity of the declining RPE cells has been exceeded, resulting in attraction of phagocytic cells that in turn have been shown to produce angiogenic factors. Drusen that largely consist of lipoprotein particles and RPE cell remnants also consist of a number of inflammatory proteins, including apolipoprotein E, coagulation proteins, acute phase proteins, immunoglobulin G, complement components, and complement activators. This further supports the hypothesis that local inflammation, induced by lipoprotein accumulation and oxidation, marks the early pathogenesis of AMD.[31] Next to formation of a membrane attack complex on cells, excessive activation of the alternative complement cascade generates a variety of proinflammatory responses and is thought to play a significant role in the progression of AMD.[32] This is supported by findings described under Genetics, that CFH polymorphism increases patients' risk for developing AMD.

Two recent studies[33,34] examined the role of DICER1 deficiency and found that patients with GA have reduced RPE levels of DICER1, an enzyme that cuts long double-stranded RNA into smaller pieces and plays a key role in maintaining RPE cell health. The RPE constantly produces long double-stranded *Alu* RNA and in healthy individuals, DICER processes these toxic RNAs into shorter, nontoxic versions. In patients with GA, DICER1 levels are greatly reduced and this leads to *Alu* RNA accumulation in the RPE. It was found that a DICER1 deficit or *Alu* RNA exposure activates the inflammasome and its components and triggers Toll-like receptor–independent MyD88 signaling via interleukin (IL)-18. Inflammasomes are a group of recently discovered protein complexes composed of a sensor for sterile or pathogen-associated noxious stimuli, such as the NOD-like receptor family, pyrin domain-containing protein 3 (NLRP3), and caspase-1, which are connected through an adapter protein (PYCARD). In contrast with the pathogenic effect of increased inflammasome activation in the absence of DICER1, an independent study[35] has found that NLRP3 has a protective role in neovascular AMD through the induction of IL-18 by drusen components. Hence, although recent observations have confirmed that human GA RPE contains elevated levels of NLRP3, PYCARD, and IL-18,[36] further dissection of a protective versus pathogenic role for the inflammasome and its products is required to provide a rationale for targeting this pathway in GA.

Oxidative Stress and Lipoproteins

The retina is particularly receptive to oxidative damage because of high oxygen tension, marked exposure to irradiation, a high proportion of PUFAs in the photoreceptor outer segments (POS), presence of several chromophores (e.g., lipofuscin, melanin, rhodopsin), and the generation of reactive oxygen intermediates created through phagocytosis of photoreceptors. Increased levels of antioxidant enzymes in the RPE of AMD eyes; advanced glycation end products in soft drusen, basal linear, and laminar deposits; and lipoperoxidation and DNA strand breaks in eyes with GA all add to the growing body of evidence that cumulative oxidative stress contributes to the pathophysiology of AMD. These findings are supported by epidemiologic studies that indicate that smoking, known to cause oxidative damage, is among the main risk factors for AMD, and that a diet rich in antioxidants seems to decrease the risk for AMD. Owing to constant light exposure and exposure to oxidative stress, proteins, lipids, and DNA can undergo lipid peroxidation. Malondialdehyde (MDA) is a common lipid peroxidation product that accumulates in AMD; MDA can in turn modify endogenous molecules, generating novel oxidation-specific epitopes, which are also present on the surface of apoptotic cells and blebs released from them. Many of these oxidation-specific epitopes are recognized as danger signals by innate immune receptors.[37] Of interest, the CFH polymorphism H402, which is strongly associated with AMD, markedly reduces the ability of CFH to bind MDA,[38] further reinforcing a genetic link between disease etiology and inflammation.

One important age-related change in AMD consists of lipid and lipoprotein accumulation in aging Bruch's membrane, basal deposits, and drusen, leading to extracellular deposits.[39] Although the accumulation of lipids alone does not seem to have an adverse effect on RPE function, the combination with oxidative stress over time leads to the formation of lipid peroxidation products. The retina has the highest concentration of ω-3 PUFAs of all tissues, and within the retina, PUFAs are particularly enriched in POS membranes. Owing to their polyunsaturated nature, PUFAs are highly susceptible to oxidative degeneration. The resulting lipid peroxidation products present a physical barrier to POS degradation, forming highly reactive aldehyde intermediates, such as such as MDA, 4-hydroxynonenal, and carboxyethylpyrrole. Accumulation of these advanced lipid peroxidation end products interferes with protein stability and function and can lead to apoptosis. Advanced lipid peroxidation end products have been found in lipofuscin, as well as in drusen and Bruch's membranes of AMD patients.

Lipofuscin, a diverse group of autofluorescent lipid, protein, and retinoid aggregates and a product of autooxidation, may play a role in the pathogenesis of AMD.[40] In the RPE, the lipofuscin concentration is highest in the macula, specifically the parafoveal ring, and is largely derived from impaired POS phagocytosis. It is thought that lipofuscin adversely affects RPE function by mechanically interfering with its cell architecture. *N*-retinyl-*N*-retinylidene ethanolamine (A2E), the major component of lipofuscin and a byproduct of the visual cycle, is synthesized within the POS. The RPE, which acts as a phagocyte, takes up the POS, leading to the accumulation of A2E in the RPE. In vitro, in cell culture, and in animal models, A2E has been shown to have many different effects, including impairment of RPE phagocytosis, inhibition of lysosomal degradation, and induction of detergent effects on the lysosomal membrane, all resulting in RPE apoptosis.[41] Of note, A2E is a condensation product of all-Trans Retinal, which on its own is toxic by stimulating the production of

superoxide via nicotinamide adenine dinucleotide phosphate hydrogen oxidase.[32] However, a recent investigation in flat-mounted RPE and retinal cross-sections from human donors found that the accumulation of A2E was not responsible for the increase in lipofuscin fluorescence observed in the central RPE with aging lipofuscin fluorescence.[33] Furthermore, in a histologic examination of a small number of human donor eyes with GA the increased signal of autofluorescence in perilesional areas may be caused by vertically superimposed cells and cellular fragments and not by increased lipofuscin content of individual cells.[34]

Amyloid

Studies have shown that drusen—abnormal extracellular deposits—contain a number of components that are also commonly found in plaques that characterize other chronic diseases, such as glomerulonephritis, atherosclerosis, and Alzheimer's disease. A number of these agents are inflammatory mediators, immunomodulators, and components of the complement system, suggesting that drusen formation is an inflammatory event aggravated by complement activation. In the human eye, the Alzheimer's amyloid β protein has been identified as a potential activator of the complement system and found to colocalize with activated fragments of complement C3 within drusen.[35] Potentially, amyloid β protein deposition may be a contributor to RPE atrophy, drusen generation, and AMD pathogenesis. More recently, it was shown in a mouse model of AMD that systemic Aβ40 and Aβ42 antibody administration was associated with abrogation of electroretinographic deficits, reduced Aβ levels, and structural preservation of the RPE. These findings implicate Aβ in the pathogenesis of AMD and identify Aβ as a viable therapeutic target for its treatment.[36]

Choroidal Perfusion and Neurodegeneration

The choroid provides oxygen and nourishment to the outer layers of the retina. The juxtaposition of the RPE/Bruch's membrane and choriocapillaris permits the choriocapillaris to provide all of the metabolic needs from serum for the photoreceptors including 90% of the O_2 consumed by the PR in darkness. Because photoreceptors are almost anoxic in the dark, any disruption in choroidal blood flow would be detrimental to these cells.

Clinical studies in subjects with GA have shown that choroidal blood flow and volume may be impaired compared with age-matched control subjects, suggesting that these may be early pathologic changes of AMD. Alterations adjacent to Bruch's membrane, for example, basolateral and basolinear deposits as well as drusen formation, may affect hemodynamic properties of retinal tissue perfusion and suggests that therapies targeting choroidal blood flow may be beneficial in dry AMD. With the advent of SD-OCT imaging, choroidal thickness can be assessed in vivo. Preliminary reports indicate that choroidal thickness may be reduced in certain types of GA. Choriocapillaris malperfusion has also been implicated as a potential contributor to the evolution of reticular drusen.

Rationale for Therapeutic Strategy

The primary goal in treating AMD is to identify the underlying cause and prevent or slow disease progression and loss of vision (Table 1, available at www.aaojournal.org); however, suitable and reliable in vitro systems and/or animal models for testing the efficacy of new therapeutic agents are lacking. Although the main target for GA remains unknown, the pathways described offer some insight into potential therapeutic interventions. Although photoreceptor and RPE loss may be the initial event, intervention at any individual molecular pathway may not be sufficient to completely halt the progression to GA. Pathways currently being evaluated in clinical studies include the preservation of RPE cells and photoreceptors, prevention of oxidative damage, reduction in the accumulation of retinal toxins, and alleviation of inflammatory damage.

Lipid Modulators

Although preclinical research studies have suggested a potential rationale for an antilipid therapeutic strategy in GA,[37] to date, no trials in GA with this target have been identified.

Anti-inflammatory Agents

Fluocinolone. Iluvien (Iluvien; Alimera Sciences, Alpharetta, GA) is a non—bio-erodible polyimide tube containing 180 μg of corticosteroid designed for intravitreal injection. A phase 2 study in patients with bilateral GA is currently under way; the primary endpoint will be the enlargement rate of GA in treated versus untreated eyes.

Glatiramer Acetate. Glatiramer acetate (Copaxone; Teva Pharmaceuticals, Kfar-Saba, Israel) is an immunomodulatory agent that downregulates inflammatory cytokines. It has been tested in a mouse model of Alzheimer's disease, and has been shown to eliminate formation of plaques, namely, amyloid deposits containing inflammatory mediators, suggesting that glatiramer acetate may be effective in dry AMD. A phase 2/3 study is underway to evaluate the efficacy and safety of glatiramer acetate in halting progression of dry AMD, including progression to wet AMD.[37]

Sirolimus. Sirolimus (Rapamycin; Wyeth, Madison, WI) was originally approved as an antifungal and was later assessed in oncology because of its ability to inhibit the mammalian target of rapamycin. It has a broad spectrum of action, inhibiting inflammation, angiogenesis, fibrosis, and hyperpermeability. The anti-inflammatory effects may show benefit in attenuating early complement activation and drusen formation. A phase 1/2 study sponsored by the National Eye Institute assessed whether sirolimus could be safely administered to patients with GA, and if it could preserve vision in these patients. Results show that subconjunctival sirolimus given every 3 months for 2 years did not prevent GA progression in 8 patients (54% increase in study and a 40% increase in the fellow eye) and may be associated with effects detrimental to VA (decrease in study and fellow eye, 21 and 3 letters, respectively).[38] In addition, another phase 1/2 study in patients with bilateral GA is currently active, but no longer

enrolling; it is scheduled to complete in July 2014. A phase 2 study is currently enrolling patients with central GA who have shown progressive worsening over time and is scheduled to complete in December 2014.

LFG316. LFG316 (Novartis Pharmaceutical Corporation, East Hanover, NJ), administered intravitreally in 12 monthly doses, is thought to be an antibody that inhibits activation of complement C5. It is currently being evaluated in a phase 2 study in patients with GA.

POT-4. POT-4 (Appellis Pharmaceuticals, Crestwood, KY and Alcon Research LTD, Fort Worth, TX) is a cyclic 13-amino acid peptide that prevents the conversion of C3 to C3a and C3b, thereby inhibiting all 3 major pathways of complement activation; it is intended as a treatment for dry AMD.[49] A phase 1 safety trial in patients with advanced neovascular lesions has been completed.

Eculizumab. Eculizumab (SOLIRIS, Alexion Pharmaceutials, Cheshire, CT) is a humanized monoclonal antibody that inhibits the complement cascade at C5, preventing the formation and release of the downstream anaphylatoxin C5a and the formation of the cytolytic membrane attack complex. Eculizumab is approved by the US Food and Drug Administration for the intravenous treatment of paroxysmal nocturnal hemoglobinuria, also a complement-mediated condition. A phase 2 trial, the COMPLETE study, assessed the efficacy and safety of IV administration of eculizumab in patients with dry AMD, including manifest GA at baseline. The COMPLETE study failed to demonstrate efficacy with the primary outcome measure at the predefined 6 month endpoint (Yehoshua Z, Alexandre C, Gregori G, et al. Systemic complement inhibition with eculizumab for the treatment of GA in AMD patients: The COMPLETE study. Presented at the 2012 Annual Meeting of the Association for Research in Vision and Ophthalmology [ARVO], May 6–10, 2012, Fort Lauderdale, FL).

ARC-1905. ARC-1905 (Ophthotech, Princeton, NJ) is an anti-C5 pegylated aptamer that inhibits downstream complement activation and is administered as an intravitreal injection. Aptamers are smaller than antibodies and do not generally elicit an immune response. A phase 1 dose escalation study assessed ARC-1905 in combination with ranibizumab. This was a safety, tolerability, and pharmacokinetic study of multiple doses of ARC-1905 intravitreous injection when administered in combination with multiple doses of ranibizumab 0.5 mg per eye, or with 1 induction dose of ranibizumab 0.5 mg per eye in subjects with subfoveal choroidal neovascularization secondary to AMD. This study was completed in June 2012. The status of another phase 1 safety and tolerability study, which evaluated ARC-1905 in patients with drusen and/or GA in both eyes, is currently unknown.

Lampalizumab. Lampalizumab (Genentech/Roche, South San Francisco, CA), previously designated as FCFD4514S, is a recombinant, monoclonal antibody fragment directed against factor D, which is the rate-limiting enzyme in the alternative complement pathway. A phase 1b/2 study (MAHALO) investigating the safety, tolerability, and evidence of activity of lampalizumab as a possible treatment for GA, was recently completed and published results are anticipated. A phase 2 extension study is currently ongoing.

Antioxidants: Nutritional Supplements

The AREDS trial has reported that daily high doses of antioxidants, including β-carotene, vitamins C and E, and zinc reduced progression to advanced AMD by 25%.[9] However, the 25% benefit was reported only for the progression to neovascular (wet) AMD; there was no benefit in the progression to central GA. In addition, the reported 25% benefit for progression to wet AMD required an average of 6.3 years. Furthermore, the AREDS antioxidant–mineral formulation was reported as having no significant effect on the progression of GA in a more recent study.[22]

A multicenter, randomized study, AREDS2 assessed the addition of lutein, zeaxanthin, and/or long-chain ω-3 fatty acids, docosahexaenoic acid, and eicosapentaenoic acid to the original AREDS formulation on progression to advanced AMD. The study completed in early 2013 and showed that the addition of lutein or zeaxanthine did not significantly reduce risk of progression to advanced AMD (hazard ratio, 0.90; $P = 0.12$).[50]

OT-551. A phase 2 study investigated the safety and preliminary efficacy of OT-551, a disubstituted hydroxylamine with antioxidant properties, for the treatment of GA in 10 participants with bilateral GA. The study concluded that OT-551, in the current concentration and mode of delivery, may have limited or no benefit as a treatment for GA.

ω-3 Fatty Acids. Several studies are ongoing investigating the effects of ω-3 fatty acids, the ratio of ω-3 to ω-6 fatty acids, and lutein and zeaxanthin (AREDS2 study) in patients with AMD (Table 1, available online at www.aaojournal.org).

Visual Cycle Inhibitors

Another strategy for treating GA is the interruption of the normal visual cycle by decreasing the accumulation of toxic metabolites, such as A2E and lipofuscin. Abnormal accumulation of lipofuscin within the RPE occurs with age and early in the onset of AMD.

Fenretinide. Fenretinide (SirionTherapeutics, Tampa, FL) is an oral synthetic retinoid derivative that prevents the transport of retinol to the RPE, effectively downregulating photo receptor metabolism. In an animal study of Stargardt's disease, fenretidine was shown to decrease the formation of A2E and other fluorophores. A recent phase 2 study assessed fenretidine (100 and 300 mg orally administered daily versus placebo) for slowing lesion growth in 246 patients with GA. Data from this study showed a trend for reduced annual lesion growth rates (mean reduction, 0.33 mm^2) in patients in the 300 mg fenretindine group who achieved serum retinol levels of ≤1 μmol/L. Only 51% of patients receiving 300 mg and completing the 2-year study achieved this level of serum retinol reduction, resulting in a nonsignificant change in lesion growth rate versus the placebo group.[50]

ACU-4429. ACU-4429 (Acucela, Inc, Bothell, WA) is a small molecule that inhibits the conversion of all-trans-retinyl ester to 11-cis-retinol and prevents accumulation of A2E.[51] Phase 1 studies are complete, showing that the drug was well-tolerated up to 75 mg with expected dose-dependent suppression of scotopic electroretinography

responses. A phase 2 safety study in patients with GA is now complete; no results have been posted. A phase 2/3 study (n = 440) with a primary endpoint of change from baseline in total area of GA lesions is currently recruiting.

ALK-001 (Alkeus Pharmaceuticals, Boston, MA) is a modified vitamin A molecule, deuterated at the C20 position and thus able to prevent the dimerization of vitamin A molecules to form A2E. This will in turn slow the formation of lipofuscin and RPE apoptosis. This compound was initially designed to treat Stargardt's disease and has been shown to reduce A2E accumulation in a mouse model of Stargardt's disease. It may also benefit GA by reducing toxic A2E, all-trans retinal, and lipofuscin accumulation. This compound is currently in the preclinical stage.

Amyloid

RN6G. This is a new treatment strategy for AMD originally developed for the treatment of Alzheimer's disease; the rationale in AMD is related to the presence of amyloid β in drusen.[48] RN6G (PF-4382923; Pfizer, Inc, New York, NY) is a humanized monoclonal antibody intended to prevent accumulation of amyloid β-40 and β-42 and preserve photoreceptors and the RPE. A phase 1 study has been completed and 2 phase 2 trials are currently recruiting in patients with GA.

GSK933776. GSK933776 (GlaxoSmithKline, Research Triangle Park, NC) is a humanized monoclonal antibody intended to modulate amyloid β levels in patients with GA secondary to AMD. A phase 2 study is currently recruiting patients.

Choroidal Perfusion Enhancers

Trimetazidine. Trimetazidine is currently used for treatment of angina and is under investigation for slowing the conversion of intermediate dry to wet AMD. A recent European study in 1086 patients with drusen and/or RPE abnormalities in the study eye and CNV in the fellow eye assessed the effects of oral trimetazidine on CNV or GA. In this study, trimetazidine failed to prevent CNV and there were no significant differences in the progression of GA between drug and placebo.[53]

MC-1101. MC-1101 (MacuCLEAR, Inc, Plano, TX) is a topical agent with anti-inflammatory and antioxidative properties shown to increase choroidal blood flow; its intended action is to prevent rupture of Bruch's membrane. A phase 1, proof-of-concept, placebo-controlled study has been completed in subjects who self-administered MC-1101 using an ophthalmic topical delivery system (Mystic Pharmaceuticals, Austin, TX). Increased blood volume and velocity was found in eyes treated with MC-1101 2 hours after dosing. In patients with AMD, modest increases in blood flow were found 30, 60, and 120 minutes postdosing. A phase 2/3 study is currently recruiting patients with mild-to-moderate nonexudative AMD.

Neuroprotection

UF-021. UF-021 (isopropyl unoprostone; Ocuseva; Sucampo Pharmaceuticals, Japan) is a prostaglandin analog that was investigated in Japan in a phase 2 clinical study in 112 patients with mid- to late-stage retinitis pigmentosa. Patients received placebo, or 1 or 2 drops of UF-021 twice daily for 24 weeks. The primary endpoint of the study was a change from baseline in retinal sensitivity in the central 2 degrees as measured by microperimeter-1. The results showed that the high-dose group met the primary endpoint ($P = 0.018$). A US trial for dry AMD is in the planning stage.

Neuroprotectants have been shown to protect photoreceptors in in vitro models of retinal degeneration and animal models of glaucoma and retinitis pigmentosa. The mechanism by which neurotrophic factors, such as ciliary neurotrophic factor (CNTF) and basic fibroblast growth factor, protect photoreceptors is not fully understood, and it should be noted that the relevance of these animal models in AMD is not clear. The RPE and retina both produce fibroblast growth factor and the retina produces CNTF.

Ciliary Neurotrophic Factor. CNTF belongs to the IL-6 family and has potent neuroprotective capabilities. It has been shown to inhibit photoreceptor cell apoptosis in animal models of retinal degeneration and is being assessed as a treatment for dry AMD. A sustained-release platform with encapsulated human RPE cells engineered to release CNTF for 1 year or longer has been developed and was tested in a phase 2 study in patients with GA (CNTF/NT501; Neurotech, Lincoln, RI). There was an apparent stabilization of VA at month 12 (93% of high-dose group losing <15 letters vs 75% of sham group), but the difference was not significant. An analysis of data from patients with a baseline BCVA of ≥20/63 revealed that 100% of patients in the high-dose group lost <15 letters versus 55% of sham/low-dose patients ($P = 0.033$) and there was a significant increase in retinal thickness. However, no benefit in the progression of lesion expansion was found.[53,54]

Tandospirone. Tandospirone (AL-8309B; Alcon Research Ltd) is a selective serotonin 1A agonist that protects the retina from light damage; it is currently under development as a topical ophthalmic solution for patients with GA. A phase 3 trial, the Geographic Atrophy Treatment Evaluation (GATE), assessed the effect of topical tandospirone (1% and 1.75%) on the rate of progression of GA. The study was discontinued in 2012 owing to lack of efficacy.

Brimonidine Tartrate Intravitreal Implant. Brimonidine stimulates the production of neurotrophic factors and can protect photoreceptor cells in animal models of retinal degeneration. Brimonidine has been formulated as an intravitreal implant using Allegan's Novadur posterior segment drug delivery system (Allergan, Irvine, CA), which delivers the drug to the retina over a 3-month period. A phase 2 study assessed the safety of the implant in a 1-month dose-escalation (stage 1) and the efficacy and safety of the implant (stage 2), with progression of the area of GA at month 12 being the primary endpoint.

Stem Cell Therapy

MA09-hRPE. Advanced Cell Technology (Santa Monica, CA) has tested subretinal transplantation of human embryonic stem-cell–derived retinal pigmented epithelial (MA09-hRPE) cells, and the potential safety of this stem cell

approach was shown in a patient with GA and a patient with Stargardt's disease.[55] The company is currently recruiting patients with Stargardt's disease for clinical trials of stem cell transplantation. In addition, the US Food and Drug Administration has granted approval to test this technology in patients with GA and phase 1/2 studies are currently ongoing.

HuCNS-SC. Human neural stem cells are used in this study via sub-retinal transplantation in patients with retinal degenerative disease, such as AMD. A phase 1/2 study is currently ongoing (StemCells Inc, Newark, CA).

Clinical Implications

An appropriate short-term clinical endpoint for demonstrating efficacy of any pharmacologic intervention in GA remains to be identified. With neovascular (wet) AMD, VA loss is relatively rapid and a reduction in hyperpermeability and extracellular fluid may be observed soon after treatment with subsequent improvements in VA. In contrast, disease progression and vision loss in GA are gradual and relatively slow. Initially, GA may result in visual function deficits in reading, driving at night, dark adaptation, and contrast sensitivity; moreover, GA creates profound, irreversible visual field deficits (scotomas). However, decline in VA may be relatively minor if the fovea is spared. In general, VA may not be significantly compromised until progression to central GA.

Changes in macular anatomy are slow to manifest; therefore, VA may take years to show a clinically significant treatment benefit. Because of these concerns surrounding VA as an endpoint, alternative endpoints are being developed. These include eliminating the drusen burden, slowing the enlargement of GA lesion area, or slowing or eliminating the progression of intermediate dry to wet AMD. The laser-to-drusen trials used laser photocoagulation to assess the effect of drusen elimination on CNV development and VA outcomes. A systematic review of 9 trials with 2215 patients concluded that photocoagulation could result in drusen elimination, but there was no evidence that this reduced the risk of developing CNV, GA, or VA loss.[56] However, these trials selected drusen based on 2-dimensional size alone, rather than other properties such as volume on SD-OCT.

The progression of GA lesion area seems to be a clinically meaningful primary efficacy endpoint because GA is characterized by loss of photoreceptors and the RPE; loss of these structures is considered a surrogate primary efficacy endpoint for loss of visual function. Precision detection of GA can be achieved with a number of different imaging techniques, including color fundus photography, fluorescein angiography, FAF, near-infrared reflectance, and SD-OCT (for a detailed review of these modalities, see[28,57]). Moreover, previous studies using a confocal scanning laser ophthalmoscopy have identified several phenotypes of GA with variable abnormal patterns of FAF in the perilesional retina that are predictive of the progression rates of the GA areas; these perilesional FAF patterns may facilitate identification and enrollment of patients at risk for rapid progression for clinical trials.

References

1. Age-Related Eye Disease Study Research Group. Potential public health impact of Age-Related Eye Disease Study results: AREDS report no. 11. Arch Ophthalmol 2003;121:1621–4.
2. Gehrs KM, Anderson DH, Johnson LV, Hageman GS. Age-related macular degeneration—emerging pathogenetic and therapeutic concepts. Ann Med 2006;38:450–71.
3. Ferris FL III, Wilkinson CP, Bird A, et al; Beckman Initiative for Macular Research Classification Committee. Clinical classification of age-related macular degeneration. Ophthalmology 2013;120:844–51.
4. Klein R, Meuer SM, Knudtson MD, Klein BE. The epidemiology of progression of pure geographic atrophy: the Beaver Dam Eye Study. Am J Ophthalmol 2008;146:692–9.
5. Ramkumar HL, Zhang J, Chan CC. Retinal ultrastructure of murine models of dry age-related macular degeneration (AMD). Prog Retin Eye Res 2010;29:169–90.
6. Bhutto I, Lutty G. Understanding age-related macular degeneration (AMD): relationships between the photoreceptor/retinal pigment epithelium/Bruch's membrane/choriocapillaris complex. Mol Aspects Med 2012;33:295–317.
7. Klein R, Klein BE, Knudtson MD, et al. Prevalence of age-related macular degeneration in 4 racial/ethnic groups in the Multi-ethnic Study of Atherosclerosis. Ophthalmology 2006;113:373–80.
8. Klein JC, Thurby DA, Shahid H, et al; Genetic Factors in AMD Study. Smoking and age related macular degeneration: the number of pack years of cigarette smoking is a major determinant of risk for both geographic atrophy and choroidal neovascularisation. Br J Ophthalmol 2006;90:75–80.
9. Age-Related Eye Disease Study Research Group. A randomized, placebo-controlled, clinical trial of high-dose supplementation with vitamins C and E, beta carotene, and zinc for age-related macular degeneration and vision loss: AREDS report no. 8. Arch Ophthalmol 2001;119:1417–36.
10. Age-Related Eye Disease Study 2 (AREDS2) Research Group. Lutein + zeaxanthin and omega-3 fatty acids for age-related macular degeneration. JAMA 2013;309:2005–15.
11. Seddon JM, Ajani UA, Mitchell BD. Familial aggregation of age-related maculopathy. Am J Ophthalmol 1997;123:199–206.
12. Sobrin L, Ripke S, Yu Y, et al. Heritability and genome-wide association study to assess genetic differences between advanced age-related macular degeneration subtypes. Ophthalmology 2012;119:1874–85.
13. AMD Gene Consortium. Seven new loci associated with age-related macular degeneration. Nat Genet 2013;45:433–9.
14. Raychaudhuri S, Iartchouk O, Chin K, et al. A rare penetrant mutation in *CFH* confers high risk of age-related macular degeneration. Nat Genet 2011;43:1232–6.
15. Heinrich M, Martinez-Barricarte R, Francis NJ, et al. Common polymorphisms in C3, factor B, and factor H collaborate to determine systemic complement activity and disease risk. Proc Natl Acad Sci U S A 2011;108:8761–6.
16. Seddon JM, Yu Y, Miller EC, et al. Rare variants in *CFI*, *C3* and *C9* are associated with high risk of advanced age-related macular degeneration. Nat Genet 2013;45:1366–70.
17. Friedrich U, Myers CA, Fritsche LG, et al. Risk- and non-risk-associated variants at the 10q26 AMD locus influence *ARMS2* mRNA expression but exclude pathogenic effects due to protein deficiency. Hum Mol Genet 2011;20:1387–99.
18. Neale BM, Fagerness J, Reynolds R, et al. Genome-wide association study of advanced age-related macular degeneration identifies a role of the hepatic lipase gene (*LIPC*). Proc Natl Acad Sci U S A 2010;107:7395–400.

19. Chen W, Stambolian D, Edwards AO, et al; Complications of Age-Related Macular Degeneration Prevention Trial (CAPT) Research Group. Genetic variants near *TIMP3* and high-density lipoprotein-associated loci influence susceptibility to age-related macular degeneration. Proc Natl Acad Sci U S A 2010;107:7401–6.
20. Klein ML, Ferris FL III, Armstrong J, et al; AREDS Research Group. Retinal precursors and the development of geographic atrophy in age-related macular degeneration. Ophthalmology 2008;115:1026–31.
21. Brinkmann CK, Adrion C, Mansmann U, et al. Clinical characteristics, progression and risk factors of geographic atrophy [in German]. Ophthalmologe 2010;107:999–1006.
22. AREDS Research Group. Change in area of geographic atrophy in the Age-Related Eye Disease Study: AREDS report number 26. Arch Ophthalmol 2009;127:1168–74.
23. Csaky KG, Richman EA, Ferris FL III. Report from the NEI/FDA Ophthalmic Clinical Trial Design and Endpoints Symposium. Invest Ophthalmol Vis Sci 2008;49:479–89.
24. Fleckenstein M, Adrion C, Schmitz-Valckenberg S, et al; FAM Study Group. Concordance of disease progression in bilateral geographic atrophy due to AMD. Invest Ophthalmol Vis Sci 2010;51:637–42.
25. Ambati J, Ambati BK, Yoo SH, et al. Age-related macular degeneration: etiology, pathogenesis, and therapeutic strategies. Surv Ophthalmol 2003;48:257–93.
26. Schmitz-Valckenberg S, Brinkmann CK, Alten F, et al. Semi-automated image processing method for identification and quantification of geographic atrophy in age-related macular degeneration. Invest Ophthalmol Vis Sci 2011;52:7640–6.
27. Curcio CA, Johnson M, Huang JD, Rudolf M. Apolipoprotein B-containing lipoproteins in retinal aging and age-related macular degeneration. J Lipid Res 2010;51:451–67.
28. Gehlbach P, Li T, Hatef E. Statins for age-related macular degeneration. Cochrane Database Syst Rev 2012;3:CD006927.
29. **Grossniklaus HE, Ling JX, Wallace TM, et al. Macrophage and retinal pigment epithelium expression of angiogenic cytokines in choroidal neovascularization. Mol Vis [serial online] 2002;8:119–26. Available at: http://www.molvis.org/molvis/v8/a16/. Accessed October 29, 2013.**
30. Cherepanoff S, McMenamin P, Gillies MC, et al. Bruch's membrane and choroidal macrophages in early and advanced age-related macular degeneration. Br J Ophthalmol 2010;94:918–25.
31. **Ebrahimi KB, Handa JT. Lipids, lipoproteins, and age-related macular degeneration. J Lipids [serial online] 2011;2011:802059. Available at: http://www.hindawi.com/journals/jl/2011/802059/. Accessed October 29, 2013.**
32. Loyet KM, DeForge LE, Katschke KJ Jr, et al. Activation of the alternative complement pathway in vitreous is controlled by genetics in age-related macular degeneration. Invest Ophthalmol Vis Sci 2012;53:6628–37.
33. Tarallo V, Hirano Y, Gelfand BD, et al. DICER1 loss and Alu RNA induce age-related macular degeneration via the NLRP3 inflammasome and MyD88. Cell 2012;149:847–59.
34. Kaneko H, Dridi S, Tarallo V, et al. DICER1 deficit induces Alu RNA toxicity in age-related macular degeneration. Nature 2012;471:325–30.
35. Doyle SL, Campbell M, Ozaki E, et al. NLRP3 has a protective role in age-related macular degeneration through the induction of IL-18 by drusen components. Nat Med 2012;18:791–8.
36. Tseng WA, Thein T, Kinnunen K, et al. NLRP3 inflammasome activation in retinal pigment epithelial cells by lysosomal destabilization: implications for age-related macular degeneration. Invest Ophthalmol Vis Sci 2013;54:110–20.
37. Miller YI, Choi SH, Wiesner P, et al. Oxidation-specific epitopes are danger-associated molecular patterns recognized by pattern recognition receptors of innate immunity. Circ Res 2011;108:235–48.
38. Weismann D, Hartvigsen K, Lauer N, et al. Complement factor H binds malondialdehyde epitopes and protects from oxidative stress. Nature 2011;478:76–81.
39. Stahl A, Krohne TU, Sapieha P, et al. Lipid metabolites in the pathogenesis and treatment of neovascular eye disease. Br J Ophthalmol 2011;95:1486–501.
40. Zhou J, Jang YP, Kim SR, Sparrow JR. Complement activation by photooxidation products of A2E, a lipofuscin constituent of the retinal pigment epithelium. Proc Natl Acad Sci U S A 2006;103:16182–7.
41. Suter M, Reme C, Grimm C, et al. Age-related macular degeneration. The lipofuscin component N-retinyl-N-retinylidene ethanolamine detaches proapoptotic proteins from mitochondria and induces apoptosis in mammalian retinal pigment epithelial cells. J Biol Chem 2000;275:39625–30.
42. Palczewska G, Maeda T, Imanishi Y, et al. Noninvasive multiphoton fluorescence microscopy resolves retinol and retinal condensation products in mouse eyes. Nat Med 2010;16:1444–9.
43. Ablonczy Z, Higbee D, Anderson DM, et al. Lack of correlation between the spatial distribution of A2E and lipofuscin fluorescence in the human retinal pigment epithelium. Invest Ophthalmol Vis Sci 2013;54:5535–42.
44. Rudolf M, Vogt SD, Curcio CA, et al. Histologic basis of variations in retinal pigment epithelium autofluorescence in eyes with geographic atrophy. Ophthalmology 2013;120:821–8.
45. Johnson LV, Leitner WP, Rivest AJ, et al. The Alzheimer's A beta-peptide is deposited at sites of complement activation in pathologic deposits associated with aging and age-related macular degeneration. Proc Natl Acad Sci U S A 2002;99:11830–5.
46. Ding JD, Johnson LV, Herrmann R, et al. Anti-amyloid therapy protects against retinal pigmented epithelium damage and vision loss in a model of age-related macular degeneration. Proc Natl Acad Sci U S A 2011;108:E279–87.
47. Landa G, Rosen RB, Patel A, et al. Qualitative spectral OCT/SLO analysis of drusen change in dry age-related macular degeneration patients treated with copaxone. J Ocul Pharmacol Ther 2011;27:77–82.
48. Wong WT, Dresner S, Forooghian F, et al. Treatment of geographic atrophy with subconjunctival sirolimus: results of a phase I/II clinical trial. Invest Ophthalmol Vis Sci 2013;54:2941–50.
49. Yehoshua Z, Rosenfeld PJ, Albini TA. Current clinical trials in dry AMD and the definition of appropriate clinical outcome measures. Semin Ophthalmol 2011;26:167–80.
50. Mata NL, Lichter JB, Vogel R, et al. Investigation of oral fenretinide for treatment of geographic atrophy in age-related macular degeneration. Retina 2013;33:498–507.
51. Kubota R, Boman NL, David R, et al. Safety and effect on rod function of ACU-4429, a novel small-molecule visual cycle modulator. Retina 2012;32:183–8.
52. Cohen SY, Bourgeois H, Corbe C, et al. Randomized clinical trial France DMLA2: effect of trimetazidine on exudative and nonexudative age-related macular degeneration. Retina 2012;32:834–43.
53. Zhang K, Hopkins JJ, Heier JS, et al. Ciliary neurotrophic factor delivered by encapsulated cell intraocular implants for treatment of geographic atrophy in age-related macular degeneration. Proc Natl Acad Sci U S A 2011;108:6241–5.

54. Emerich DF, Thanos CG. NT-501: an ophthalmic implant of polymer-encapsulated ciliary neurotrophic factor-producing cells. Curr Opin Mol Ther 2008;10:506–15.
55. Schwartz SD, Hubschman JP, Heilwell G, et al. Embryonic stem cell trials for macular degeneration: a preliminary report. Lancet 2012;379:713–20.
56. Parodi MB, Virgili G, Evans JR. Laser treatment of drusen to prevent progression to advanced age-related macular degeneration. Cochrane Database Syst Rev 2009;(3):CD006537.
57. Gobel AP, Fleckenstein M, Schmitz-Valckenberg S, et al. Imaging geographic atrophy in age-related macular degeneration. Ophthalmologica 2011;226:182–90.

Footnotes and Financial Disclosures

Originally received: June 25, 2013.
Final revision: November 8, 2013.
Accepted: November 11, 2013.
Available online: January 15, 2014. Manuscript no. 2013-1021.

[1] Department of Ophthalmology, University of Bonn, Bonn, Germany.
[2] Genentech, Inc, South San Francisco, California.

Financial Disclosures:

The authors have made the following disclosures:

Genentech, Inc, South San Francisco, CA provided support for this review.

Frank G. Holz: Consultant—Acucela, Alcon, Allergan, Bayer, Genentech, Heidelberg Engineering, Novartis, Optos, and Roche

Erich C. Strauss: Employee—Genentech, Inc.

Steffen Schmitz-Valckenberg: Consultant—Novartis; Research Funding—Alcon, Carl Zeiss Meditec, Genentech, Heidelberg Engineering, Novartis, and Optos.

Menno van Lookeren Campagne: Employee—Genentech, Inc.

Support for third-party writing and formatting assistance for this manuscript was provided by Linda Merkel, PhD, CMPP, and was funded by Genentech, Inc., South San Francisco, California.

Correspondence:
Prof Dr Frank G. Holz, MD, FEBO, Department of Ophthalmology, University of Bonn, Ernst-Abbe-Str. 2, D-53127 Bonn, Germany. E-mail: Frank.Holz@ukb.uni-bonn.de.

Change in Drusen Volume as a Novel Clinical Trial Endpoint for the Study of Complement Inhibition in Age-related Macular Degeneration

Carlos Alexandre de Amorim Garcia Filho, MD; Zohar Yehoshua, MD, MHA; Giovanni Gregori, PhD; Renata Portella Nunes, MD; Fernando M. Penha, MD, PhD; Andrew A. Moshfeghi, MD, MBA; Kang Zhang, MD, PhD; William Feuer, MS; Philip J. Rosenfeld, MD, PhD

BACKGROUND AND OBJECTIVE: To evaluate the change in drusen volume following treatment with eculizumab, a systemic inhibitor of complement component 5.

PATIENTS AND METHODS: Single-center, prospective, randomized, double-masked clinical trial. Patients were randomized 2:1 to receive intravenous eculizumab or placebo over 26 weeks. Main outcome measure: decrease in drusen volume of at least 50% at 26-week follow-up.

RESULTS: Mean drusen cube root volumes were 0.49 mm and 0.47 mm ($P = .64$) at baseline and 0.51 mm and 0.42 mm ($P = .17$) at 26 weeks in the eculizumab and placebo groups, respectively. In the placebo group, one eye had a decrease in drusen volume of at least 50% and two eyes developed neovascularization through 26 weeks.

CONCLUSION: Systemic complement inhibition with eculizumab did not significantly reduce drusen volume. Drusen growth was dependent on the number of complement at-risk alleles. Future trials should consider the use of a composite clinical trial endpoint in which efficacy is defined by the treatment's ability to prevent drusen growth, neovascularization, and the formation of geographic atrophy over 1 year.

[*Ophthalmic Surg Lasers Imaging Retina.* **2014;45:18-31.**]

INTRODUCTION

The presence of large drusen is a characteristic feature of intermediate dry age-related macular degeneration (AMD).[1] The increase in the size of drusen is considered a risk factor for the progression to late AMD, which includes geographic atrophy (GA) and macular neovascularization.[1-3] Historically, drusen were imaged and quantified using color fundus imaging, but drusen morphology can now be reproducibly measured and their natural history followed using spectral-domain optical coherence tomography (SD-OCT) imaging.[4-7] The natural history of drusen morphology was followed for 2 years, and three different growth patterns were identified.[5] While most eyes showed an increase in the volume and area of drusen, other eyes showed stable drusen morphology, while a minority of eyes showed a decrease in drusen volume. In eyes showing a decrease in drusen volume, the drusen progressed to either GA or macular neovascularization or the drusen volume dramatically decreased without any obvious sequellae. While the reduction in drusen volume without the formation of GA or neovascularization and with the preservation of central visual acuity is a rare event, it would be a desired outcome for any therapy designed to treat dry AMD.

The laser-to-drusen trials were the first studies designed to reduce the drusen burden and positively

From the Department of Ophthalmology, Bascom Palmer Eye Institute, University of Miami Miller School of Medicine, Miami, Florida (CAAGF, ZY, GG, RPN, FMP, AAM, WF, PJR); Department of Ophthalmology, Federal University of São Paulo, UNIFESP, São Paulo, SP, Brazil (CAAGF, RPN, FMP); and Institute for Genomic Medicine and Shiley Eye Center, University of California San Diego, San Diego, California (KZ).

Originally submitted November 3, 2013. Accepted for publication December 4, 2013.

Presented in part at the Angiogenesis, Exudation, and Degeneration meeting, February 9, 2013, Miami, Florida.

Supported by Alexion Pharmaceuticals, the Macula Vision Research Foundation, Carl Zeiss Meditec, an unrestricted grant from Research to Prevent Blindness, NEI core center grant P30 EY014801 to the University of Miami, Department of Defense (DOD- Grant#W81XWH-09-1-0675), the Jerome A. Yavitz Charitable Foundation, the Emma Clyde Hodge Memorial Foundation, the Florman Family Foundation, and the Gemcon Family Foundation.

Dr. Rosenfeld has received research support from Acucela, Advanced Cell Technology, Alexion Pharmaceuticals, and GlaxoSmithKline and he is a consultant for Acucela, Alcon, Bayer, Boehringer Ingelheim, Chengdu Kanghong Biotech, Merck, Oraya, Roche, and Sanofi/Genzyme. Drs. Garcia Filho, Rosenfeld, Gregori, Penha, and Yehoshua received research support from Carl Zeiss Meditec. Dr. Gregori and the University of Miami co-own a patent that is licensed to Carl Zeiss Meditec. Dr. Zhang is a consultant for Acucela and received research support from Genentech. Dr. Penha is a consultant to Alcon, Thrombogenics, and Bayer. Dr. Moshfeghi is a consultant to ThromboGenics, Allergan, Alcon, Bausch & Lomb, Valeant, Genentech/Roche, Bayer, and Regeneron and has an equity interest in OptiSTENT.

The authors are grateful to Maria Esquiabro (Department of Ophthalmology, Bascom Palmer Eye Institute) for her exceptional clinical coordination of the study and Sandra O'Mellan (Department of Ophthalmology, Bascom Palmer Eye Institute) for her technical expertise in imaging subjects using the Cirrus SD-OCT instrument.

Address correspondence to Philip J. Rosenfeld MD, PhD, Bascom Palmer Eye Institute, 900 NW 17th street, Miami, FL 33136; 305-326-6148; fax: 305-326-6538; email: prosenfeld@med.miami.edu.

doi: 10.3928/23258160-20131217-01

TABLE 1

Drusen Volume Measurements at Baseline in the Central 3 and 5 mm

	Study Eyes			Study and Fellow Eyes		
Drusen Measurements	**Placebo n = 10, mm (SD)**	**Active Treatment n = 20, mm (SD)**	***P* Value***	**Placebo n = 14, mm (SD)**	**Active Treatment n = 28, mm (SD)**	***P* Value***
Central 3 mm						
Mean drusen volume, mm^3 0.12 (0.08)	0.12 (0.08)	0.15 (0.17)	.64	0.12 (0.10)	0.18 (0.20)	.29
Cube root volume, mm	0.47 (0.10)	0.49 (0.14)		0.46 (0.12)	0.51(0.16)	
Central 5 mm						
Mean drusen volume, mm^3	0.18 (0.19)	0.17 (0.17)	.99	0.17 (0.18)	0.21 (0.21)	.47
Cube root volume (mm)	0.52 (0.15)	0.52 (0.14)		0.50 (0.16)	0.54 (0.16)	

SD = standard deviation.
**Two-sided, two-sample t-test*

influence disease progression.[8-13] These trials confirmed the anecdotal observations that laser photocoagulation to the macula caused the disappearance of drusen. Color fundus imaging confirmed these observations. However, there was no evidence that this overall loss of drusen resulted in any benefit in terms of preventing visual acuity loss or the development of choroidal neovascularization (CNV) and GA.[14] Moreover, these studies relied on the en-face appearance of drusen on examination and color imaging, so the investigators could only assess the area and not the volume measurements of drusen. As a result, they based their enrollment on drusen area, which may have resulted in a diverse population of drusen at different stages of growth or regression, and many of the drusen may have already started to regress into GA. Moreover, using color fundus imaging, the investigators would not have been able to follow the incremental changes in drusen volume, outer retinal anatomy, and integrity of the retinal pigment epithelium (RPE), which are essential in assessing future visual function. However, at the time these studies were conducted, there was no reliable natural history data and no method for reproducibly measuring drusen morphology, so these trials relied on large numbers of patients to adequately power their studies to overcome all these uncertainties.[15] In contrast, the use of SD-OCT imaging to assess drusen volume in the central macula has provided a unique, reliable, and reproducible method for measuring the morphology of drusen over time. This SD-OCT imaging strategy identifies a specific subset of drusen that elevate the RPE.[16] As a result, the change in volume for these drusen can now be used as a novel clinical trial endpoint when studying therapies for dry AMD.[5,17]

While the pathogenesis of AMD is multifactorial, resulting from a combination of genetic and environmental risk factors, there is convincing evidence that the complement system plays an important role in causing AMD.[18] Even before the genetic studies showed an association between AMD and complement genes, evidence of complement activation in AMD was provided by the presence of complement components 3 (C3) and 5 (C5), complement factor H, and the membrane attack complex in drusen.[19-22] Genetic studies have implicated these same gene products as well as other genetic loci in the complement pathway as having a protective or risk-enhancing role for the development of AMD.[23-26] In addition, the role of complement in AMD is suggested by the appearance of macular drusen in eyes of patients with complement-mediated renal disease[27] and by the data from animal studies showing that complement activation has a role in CNV.[28-30]

Currently, there is no proven therapy that stops the progression of dry AMD, but the inhibition of complement could be a viable treatment strategy given the evidence that complement activation has a role in AMD and the encouraging unpublished results from a study investigating complement inhibition for the treatment of GA.[31] Currently, the only inhibitor of terminal complement activation approved by the U.S. Food and Drug Administration is eculizumab (Soliris; Alexion Pharmaceuticals, Cheshire, CT), a humanized monoclonal antibody derived from the murine anti-human C5 antibody m5G1. Eculizumab is approved for the treatment of paroxysmal nocturnal hemoglobinuria and atypical-hemolytic uremic syndrome. Eculizumab is given intravenously and specifically binds the terminal complement protein

TABLE 2

Changes in Drusen Volumes From Baseline to 26 and 52 Weeks

	Study Eyes			Study and Fellow Eyes		
	Placebo (n = 9)	Active Treatment (n = 18)	*P* Value[1]	Placebo (n = 12)	Active Treatment (n = 25)	*P* Value[1]
26 Weeks of Follow-up						
Cube root volume (mm) change in central 3 mm (SD)	–0.05 (0.15)	0.02 (0.01)	.17*	–0.03 (0.13)	0.03 (0.01)	.18*
Cube root volume (mm) change in central 5 mm (SD)	–0.04 (0.11)	0.03 (0.05)	.14*	-0.02 (0.10)	0.03 (0.01)	.16*
52 Weeks of Follow-up						
Cube root volume (mm) change in central 3 mm (SD)	–0.04 (0.15)	0.02 (0.05)	.26*	–0.02 (0.13)	0.02 (0.05)	.25*
Cube root volume (mm) change in central 5 mm (SD)	–0.03 (0.12)	0.02 (0.05)	.14*	–0.01 (0.11)	0.03 (0.05)	.26*

SD = standard deviation.

[1] *Two-sided, two-sample t-test*
* *Unpooled variance test*

C5, thereby inhibiting its cleavage to C5a and C5b during complement activation and preventing the formation of the membrane attack complex.

The COMPLETE (Complement inhibition with eculizumab for the treatment of non-exudative age-related macular degeneration) study was designed to evaluate the safety and efficacy of systemic eculizumab for the treatment of drusen in dry AMD. The change in drusen volume was chosen as a surrogate endpoint because it could be studied over a shorter period of time compared with other dry AMD efficacy endpoints such as the progression to advanced AMD or vision loss, which require years of follow-up. Moreover, this is the first prospective, randomized clinical trial to use complement inhibition for the treatment and assessment of drusen in dry AMD and the first study to use the volumetric assessment of drusen as a clinical trial endpoint.

PATIENTS AND METHODS

Study Design

The COMPLETE study is a 12-month investigator-sponsored, single-center, prospective, randomized, double-masked study designed to evaluate the safety and efficacy of intravenous eculizumab for the treatment of patients with drusen secondary to AMD. All subjects and study personnel other than the clinical coordinator were masked to treatment assignment. The study was performed with FDA approval (IND #104471). Before the initiation of the study, additional approval was obtained from the institutional review board at the University of Miami Miller School of Medicine. Informed consent was obtained from all patients before determination of full eligibility, and the study was performed in accordance with the Health Insurance Portability and Accountability Act. The COMPLETE study is registered at www.clinicaltrials.gov (NCT00935883).

From November 2009 to May 2011, 30 patients were enrolled. Eligibility criteria included age of 50 years or more, the presence in the study eye of high-risk drusen, and best corrected visual acuity (BCVA) of 20/63 or better (ETDRS letter score of at least 59). High-risk drusen were defined by the presence of at least one druse with a diameter of at least 250 μm observed on fundus biomicroscopy or color fundus photography and a total volume of drusen of at least 0.03 mm^3 as measured by SD-OCT within a 3 mm diameter circle centered on the fovea. Exclusion criteria included visual acuity worse than 20/63, presence of any GA, or any history of macular neovascularization in the study eye. If both eyes were eligible for the study, then one eye was chosen as the study eye at the discretion of the investigator. All patients enrolled in the study received a meningococcal vaccine at least 15 days prior to the initiation of treatment as described in the package insert approved by the FDA (http://soliris.net/sites/default/files/assets/soliris_pi.pdf).[32]

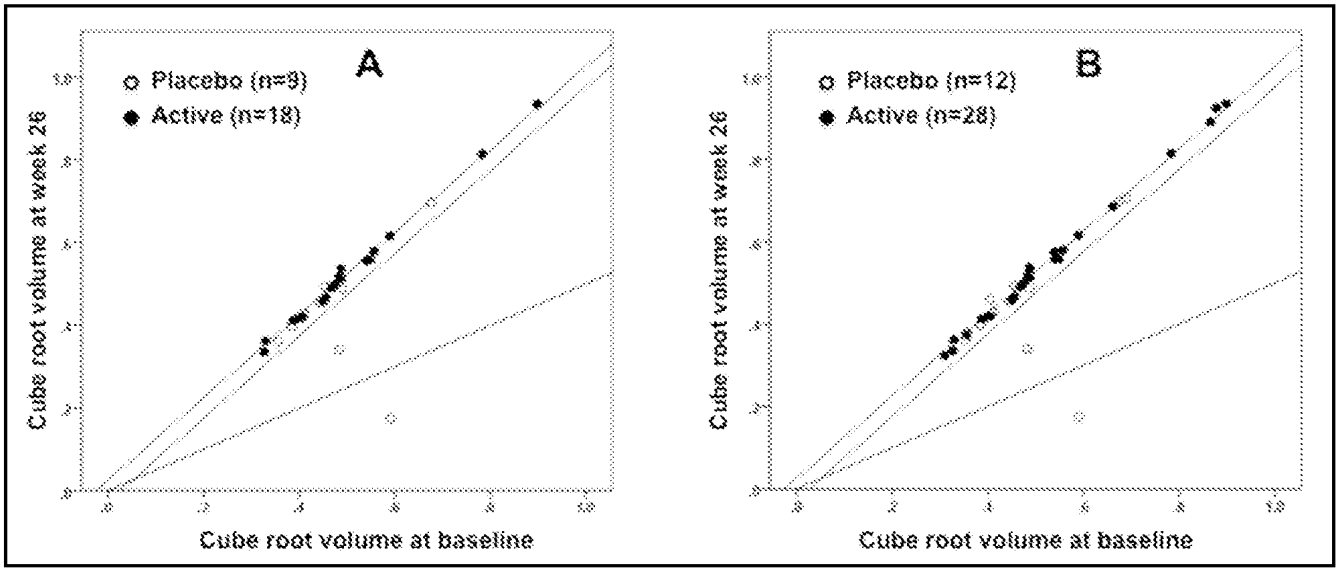

Figure 1. Drusen volume changes over 26 weeks. These scatter plots depict the baseline cube root drusen volume within a 3 mm circle centered on the fovea along the x-axis and the cube root drusen volume at 26 weeks along the y-axis. The dotted lines represent the 95% test-retest confidence intervals for the variability associated with measurements. The solid diagonal line represents the cut-off for a 50% decrease in the baseline cube-root volume. (A) Study eyes. (B) Study eyes plus eligible fellow eyes.

Treatment Protocol

Patients were randomized 2:1 to receive active treatment with eculizumab or placebo in a double-masked fashion. Randomization schedules were stratified with the use of a permuted-block strategy to insure balance. During the treatment period, patients received eculizumab for a period of 24 weeks with the primary endpoint at 26 weeks. The treatment period was divided into an induction period and a maintenance period. The first 10 patients in the eculizumab group received a low dose of eculizumab (600 mg via intravenous infusion weekly for 4 weeks followed by 900 mg every 2 weeks until week 24), while the next 10 patients received a high dose (900 mg eculizumab via intravenous infusion weekly for 4 weeks followed by 1,200 mg every 2 weeks until week 24). After 26 weeks, patients were monitored without treatment every 3 months for an additional 6 months.

The presence of any study-related adverse event that was considered to be severe in intensity by the investigators led to the discontinuation of treatment in the study, but masking was maintained. Patients were encouraged to continue with the study visits but no treatment was administered.

Ophthalmological Examination and Imaging Procedures

Ophthalmological examination included BCVA measured using the ETDRS chart at 4 meters, low luminance visual acuity testing at 4 meters using a 2.0-log unit neutral density filter (Kodak Wratten filter; Kodak, Rochester, NY),[33] slit lamp biomicroscopy, IOP measurement, and fundus examination. All imaging studies were performed at baseline, 12 weeks, 26 weeks, 38 weeks, and 52 weeks of follow-up. These studies included color and autofluorescence imaging with a fundus camera–based flash system (TRC-50DX; Topcon Medical Systems, Oakland, NJ; AF Excitation λ: 535-585 nm, Detection λ: 605-715 nm), autofluorescence and fluorescein angiographic imaging with a confocal SLO system (Spectralis; Heidelberg Engineering, Heidelberg, Germany; AF excitation λ: 488 nm; detection λ: > 500 nm), and SD-OCT imaging with both the Cirrus (Carl Zeiss Meditec, Dublin, CA) and Spectralis instruments.

SD-OCT drusen volume maps were obtained using the Cirrus instrument and the macular 200 × 200 raster scan pattern and a proprietary algorithm, which is now available in version 6.0 of the Cirrus operating system.[4] This algorithm calculated the difference between the elevation of the RPE caused by drusen and a virtual RPE floor free of deformations, which resulted in reproducible measurements of drusen area and volume. Only drusen that elevated the RPE would be measured using this strategy. For this study, the drusen volume was measured within a 3 mm and 5 mm diameter circle centered on the fovea. The position of the fovea was determined manually by scanning through the OCT data sets and finding the spot where the geometry of the inner retinal layers best matched the known anatomic configuration in the fovea. Drusen measurements were performed in the

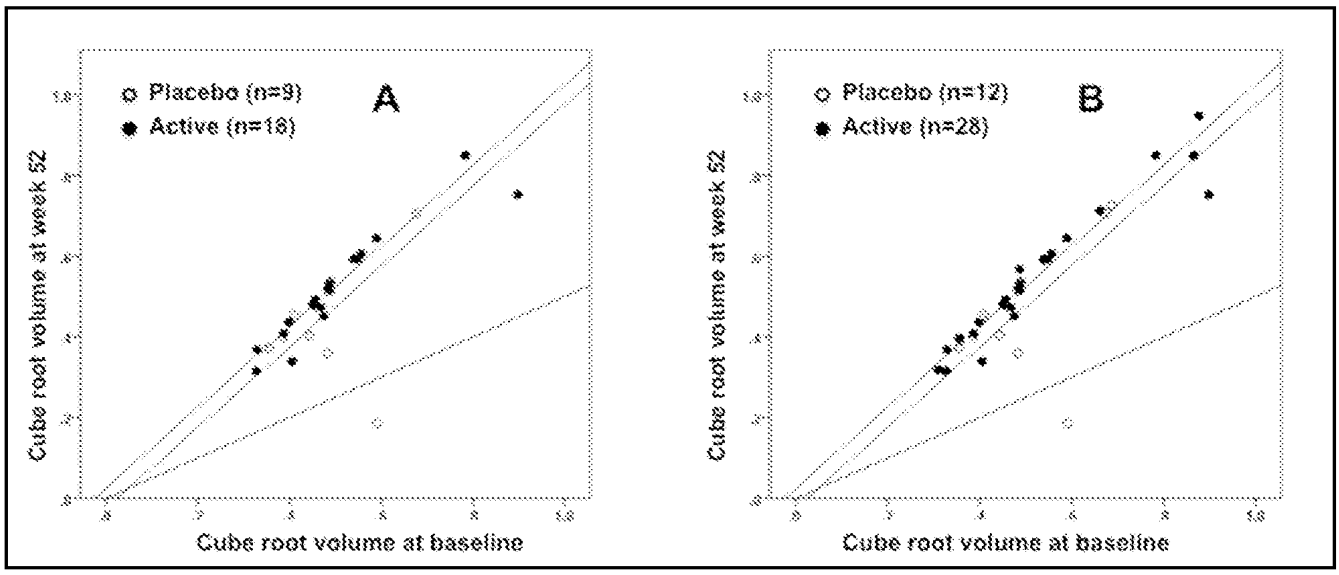

Figure 2. Drusen volume changes over 52 weeks. These scatter plots depict the baseline cube root drusen volume within a 3 mm circle centered on the fovea along the x-axis and the cube root drusen volume at 52 weeks along the y-axis. The dotted lines represent the 95% test-retest confidence intervals for the variability associated with measurements. The solid diagonal line represents the cut-off for a 50% decrease in the baseline cube-root volume. (A) Study eyes. (B) Study eyes plus eligible fellow eyes.

same areas contained within these circles at baseline and at follow-up visits. A single experienced operator obtained the images, and they were actively monitored for quality and the presence of artifacts that could influence the drusen volume measurements. The same scan pattern was used to generate the OCT fundus image (OFI) and the sub-RPE slab OFIs.[34,35] These images were used to assess the development of GA during the follow-up visits. Autofluorescence and fluorescein angiography images were used as well to assess the formation of GA. Fluorescein angiography and SD-OCT imaging were used to assess the formation of macular neovascularization.

Choroidal imaging was performed with the Spectralis instrument using the enhanced depth imaging (EDI) protocol. Two independent graders manually measured choroidal thickness at the foveal center, and a consensus image was used for quantitation.

Outcome Measures

The primary outcome was to determine whether the treatment with eculizumab could decrease the volume of drusen by 50% within a 3 mm circle centered on the fovea over a 6-month treatment period. The primary outcome included both the low-dose and high-dose groups. Fellow eyes that met inclusion criteria were included in the analysis of secondary outcomes. Secondary outcomes also included the change in drusen volume in the central 5 mm, the change in drusen area within the 3 mm and 5 mm diameter circles, the change in BCVA from baseline, a comparison of the low-dose and the high-dose groups, and the conversion rate from dry to wet AMD in study and fellow eyes over 12 months, which included the 6-month treatment period and the 6-month observation period.

To eliminate the influence of drusen size at baseline on the measurement of drusen growth and to eliminate the influence of drusen size on the 95% tolerance limits of the variability associated with the test-retest measurements, we performed an appropriate transformation of the data before statistical analyses were performed.[4] These transformations included a square root transformation for drusen area measurements and a cube root transformation for drusen volume measurements.

Safety was assessed through the summary of ocular and nonocular adverse events, serious adverse events, ocular assessments, deaths, laboratory test results, and vital signs. Safety analyses included subjects who received at least one eculizumab infusion. Adverse events leading to discontinuation from the study were listed.

Statistical Analysis

The principal treatment efficacy outcome was the success rate at 6 months of follow-up. Success was defined as a decrease in the drusen cube root volume of at least 50% compared with the baseline cube root volume without evidence of progression to GA or

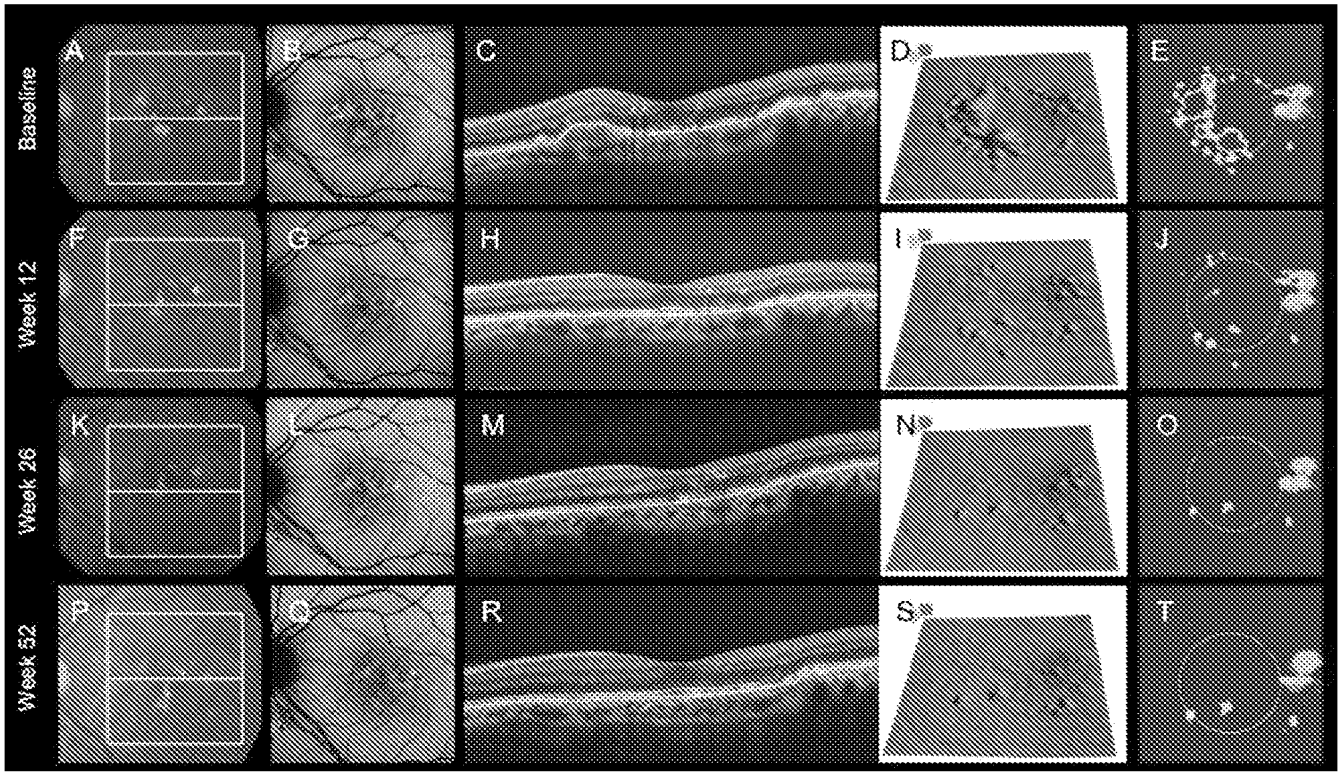

Figure 3. Decrease in drusen volume over 52 weeks. This left eye of a 61-year-old man treated with placebo demonstrated a decrease in drusen volume over 52 weeks. (A, F, K, P) Color fundus images with white box representing the spectral-domain OCT (SD-OCT) scan area (200 × 200) and a line centered on the fovea representing the location of the SD-OCT B-scan, at baseline, 12 weeks, 26 weeks, and 52 weeks. (B, G, L, Q) Heidelberg autofluorescence images at baseline, 12 weeks, 26 weeks, and 52 weeks. (C, H, M, R) SD-OCT B-scan centered on the fovea at baseline, 12 weeks, 26 weeks, and 52 weeks. (D, I, N, S) Retinal pigment epithelium segmentation maps at baseline, 12 weeks, 26 weeks, and 52 weeks. (E, J, O, T) Drusen volume maps with a 3 mm circle centered on the fovea. The drusen volume in the central 3 mm was calculated to be 0.2 mm^3 at baseline (E), 0.009 mm^3 at 12 weeks (J), 0.005 mm^3 at 26 weeks (O), and 0.006 mm^3 at 52 weeks (T).

neovascular disease.[5] Success rates were compared between study eyes randomized to eculizumab and those randomized to placebo with the Fisher exact test. Volume and area reductions were compared with the two-sample *t*-test. Average change in drusen volume and area over time constituted a secondary outcome variable and were compared between groups with the two-sample *t*-test. Analysis of variance was used to examine the effect of genotype on the change in lesion size.

The rationale for sample size determination is presented in a previously published natural history study.[5] Assuming a 5% rate of success in placebo-treated patients, this randomized trial was designed with 80% power, at an alpha error level of 0.05, to detect a 65% or greater success rate in patients randomized to eculizumab.

Pharmacokinetic and Complement Factors Analysis

During the study, blood samples for pharmacokinetic and complement factor screening were drawn and analyzed in a masked fashion at baseline and at every planned visit at weeks 1, 2, 3, 4, 6, 8, 10, 12, 14, 16, 18, 20, 22, 24, 26, 28, 38, and 52. Alexion Pharmaceuticals laboratory measured soluble C5b-9 and performed a hemolytic assay for C5 activity. Levels of factor H and C3 were also measured.

Genetic Analysis

Genetic testing for seven single-nucleotide polymorphisms (SNPs) was performed in all patients as previously described,[36] and the prevalence of the following [alleles] was assessed: CFH-rs1061170 [C], C3-rs2230199 [G], CFH-rs2274700 [C], HTRA1-rs10490924 [T], CFB-rs641153-R32Q [G] C2_rs9332739-E318D [G]. Blood samples from each patient were sent to the University of California San Diego for the testing. Genomic DNA was extracted from peripheral blood leucocytes according to established protocols. All SNPs were genotyped using the SNaPshot method according to the manufacturer's recommendations.[36]

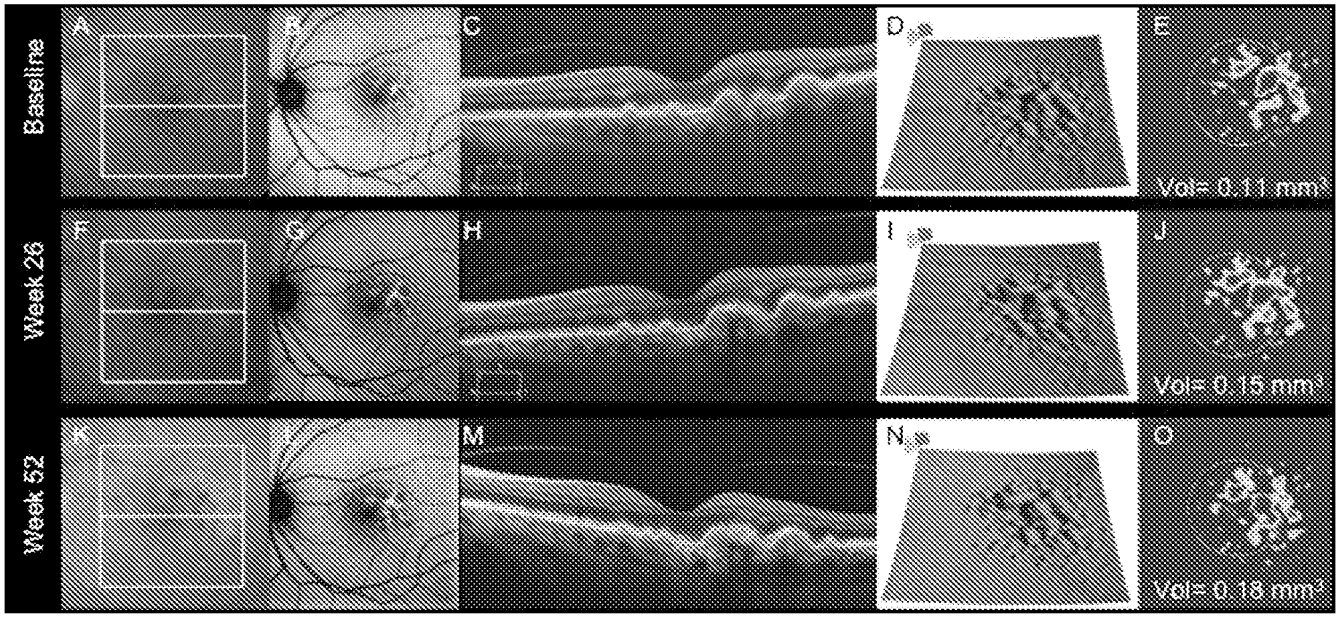

Figure 4. Increase in drusen volume over 52 weeks. This left eye of a 72-year-old man treated with placebo demonstrated an increase in drusen volume over 52 weeks. (A, F, K) Color fundus images with white box representing the spectral-domain OCT (SD-OCT) scan area (200 × 200) and a line centered on the fovea representing the location of the SD-OCT B-scan at baseline, 26 weeks, and 52 weeks. (B, G, L) Heidelberg autofluorescence images at baseline, 26 weeks, and 52 weeks. (C, H, M) SD-OCT B-scan centered on the fovea at baseline, 26 weeks, and 52 weeks. (D, I, N) Retinal pigment epithelium segmentation maps at baseline, 26 weeks, and 52 weeks. (E, J, O) Drusen volume maps with a 3 mm circle centered on the fovea. The drusen volume in the central 3 mm was calculated to be 0.11 mm^3 at baseline (E), 0.15 mm^3 at 26 weeks (J), and 0.18 mm^3 at 52 weeks (O).

RESULTS

Baseline Characteristics

Thirty eyes of 30 patients were enrolled in the study and randomized 2:1 to active eculizumab treatment and placebo. Patients in the eculizumab group were randomized to receive the low-dose or high-dose treatment regimen. The first 10 patients on eculizumab received the low-dose regimen and the next 10 patients received the high-dose regimen. Twelve fellow eyes met inclusion criteria and were analyzed as a secondary endpoint.

The mean ages (standard deviation) of patients in the placebo and active treatment groups were 70.7 (7.8) and 70.7 (6.8), respectively. Mean ages in the low-dose and high-dose regimen groups were also similar: 72.4 (6.5) and 69.0 (7.0), respectively. Mean ETDRS visual acuity was 78.0 (10.0) letters in the placebo group and 80.9 (5.9) in the active treatment group ($P = .33$). Low-dose and high-dose groups had similar ETDRS visual acuity letter scores of 81.1 (3.8) and 80.7 (7.7) letters, respectively ($P = .88$).

The drusen volumes at baseline are shown in Table 1 (page 19). At baseline, the mean cube root drusen volume (SD) in the central 3 mm was 0.49 mm (0.14) and 0.47 mm (0.10) in the eculizumab and placebo groups, respectively ($P = .64$). Volumes on the untransformed scale were 0.15 (0.17) mm^3 and 0.12 (0.08) mm^3 in the eculizumab and placebo groups. Mean square root drusen area at baseline in the central 3 mm was 1.40 (0.33) mm and 1.37 (0.24) mm for the eculizumab and placebo groups, respectively ($P = .71$). Areas on the untransformed scale were 2.07 (1.00) mm^2 and 1.93 (0.71) mm^2 in the eculizumab and placebo groups. The baseline measurements of placebo and eculizumab groups were similar by all volume and area measurements.

Patient Retention, Treatment Compliance, and Safety

Twenty-eight patients completed 52 weeks of follow-up. Two of the patients in the high-dose group refused further participation after 3 weeks of follow-up because of personal conflicts with the treatment schedule and exited the study. No adverse events were identified in these patients. One placebo patient failed to complete a full course of infusions because of chest discomfort during one of the infusions, which required a hospitalization. However, she remained masked, treatment was halted, and she continued to be monitored in the study without further infusion. After unmasking at the end of the study, she was found to have received placebo. Systemic therapy with eculizumab was well tolerated through 6 months, and no drug-related adverse events were identified in the patients included in the study.

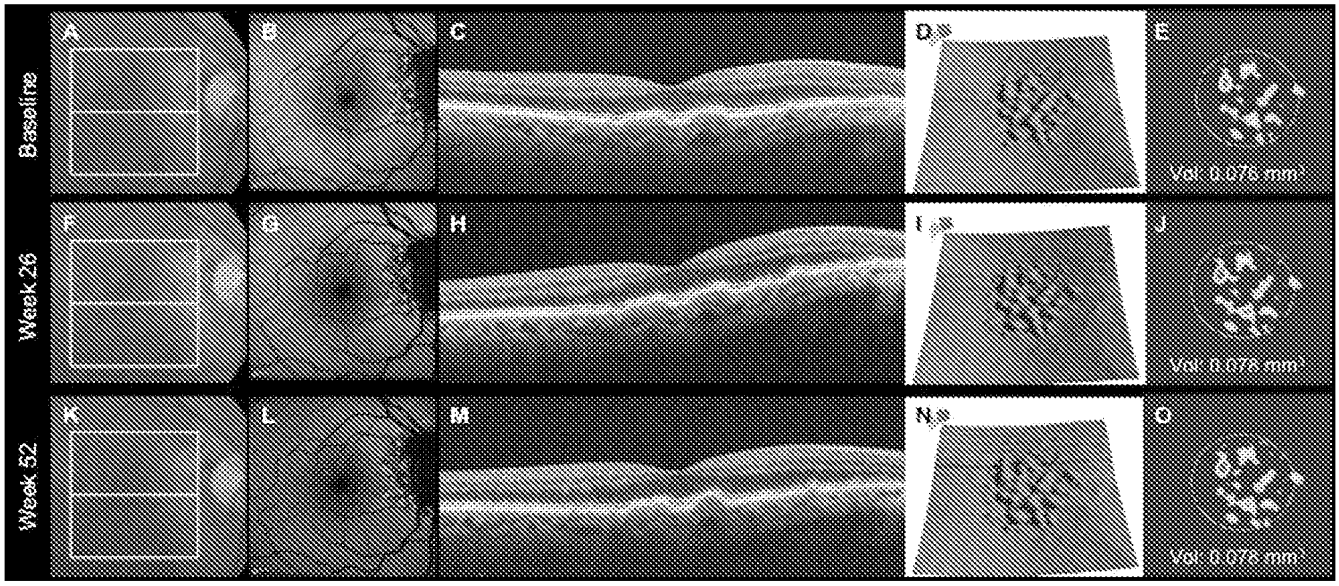

Figure 5. Stable drusen volume over 52 weeks. This right eye of a 79-year-old man treated with low dose of eculizumab demonstrated a stable drusen volume over 52 weeks. (A, F, K) Color fundus images with white box representing the spectral-domain OCT (SD-OCT) scan area (200 × 200) and a line centered on the fovea representing the location of the SD-OCT B-scan at baseline, 26 weeks, and 52 weeks. (B, G, L) Heidelberg autofluorescence images at baseline, 26 weeks, and 52 weeks. (C, H, M) SD-OCT B-scan centered on the fovea at baseline, 26 weeks, and 52 weeks. (D, I, N) Retinal pigment epithelium segmentation maps at baseline, 26 weeks, and 52 weeks. (E, J, O). Drusen volume maps with a 3 mm circle centered on the fovea. The drusen volume in the central 3 mm was calculated to be 0.076 mm^3 at baseline (E), 0.078 mm^3 at 26 weeks (J), and 0.078 mm^3 at 52 weeks (O).

Primary Outcome

Figure 1 (page 21) shows the change in drusen volumes in the study eyes from baseline to 26 weeks. At 6 months of follow-up, none of the 18 eculizumab-treated study eyes demonstrated a 50% reduction in drusen volume, whereas one eye (10%) in the placebo group showed a 50% reduction in drusen volume (P = .36, Fisher exact test; Figure 3, page 23). One additional placebo-treated eye experienced a decrease in drusen volume that was less than 50% of the baseline volume. In the eculizumab group, no study eyes decreased in volume beyond the 95% tolerance interval for test-retest variability limits shown by the dotted lines in Figure 1. The remainder of the eyes either showed an increase in drusen volume beyond the test-retest variability limits (Figure 4, page 7) or remained stable (Figure 5). The 95% confidence interval around the difference between the treatment and placebo groups with respect to the proportions with a successful outcome ranged from –0.55 to 0.21, which effectively ruled out a treatment-related positive outcome of a 50% drusen reduction in 22% or more of the eyes treated with eculizumab.

Secondary Outcomes

There was no difference in drusen growth between the placebo- and eculizumab-treated study eyes (Table 2, page 20). At 26 weeks of follow-up, the placebo eyes (n = 9, excluding the eye that progressed to neovascular disease) averaged a –0.05 mm (SD = .15) change in cube root drusen volume within the central 3 mm, whereas the eculizumab-treated group (n = 18) averaged a 0.02 (SD = .01) increase in cube root drusen volume (P = 0.17, unpooled variance t-test). The 95% confidence interval for the difference in the mean change in drusen volume between the eculizumab and placebo groups ranged from –0.04 to +0.19. Thus, a reduction in drusen volume growth due to eculizumab was not detected (Table 2). Between weeks 26 and 52 (Table 2; Figure 2, page 22), no additional eyes experienced a 50% reduction in drusen volume.

A subset of 12 fellow eyes met the study inclusion criteria. One eye was excluded from the final analysis because the patient exited the study. Figures 1 and 2 (pages 21 and 22, respectively) show the changes in drusen volumes from baseline to 26 weeks and from baseline to 52 weeks for both the study and the fellow eyes. There were no differences between the eculizumab- and placebo-treated groups when the fellow eyes were included in the analyses (Tables 1 and 2, pages 2 and 3, respectively). In addition, there were no detectable differences when comparing the effects of low-dose with high-dose eculizumab regimens on the change in drusen volume over 26 weeks (P = .63) or 52 weeks (P = .59).

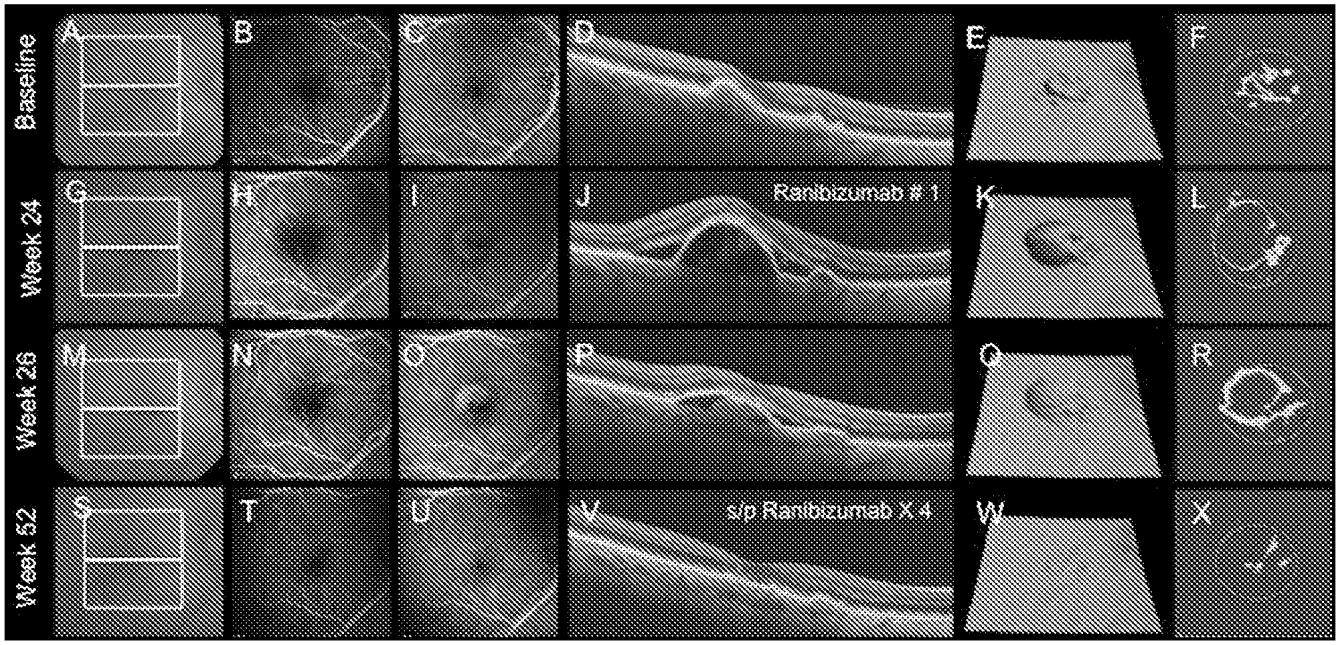

Figure 6. Conversion of dry to wet AMD over 26 weeks. This right eye of a 75-year-old woman treated with placebo demonstrated a conversion from dry to wet AMD. (A, G, M, S) Color fundus images with white box representing the spectral-domain OCT (SD-OCT) scan area (200 × 200) and a line centered on the fovea representing the location of the SD-OCT B-scan at baseline, 24 weeks, 26 weeks, and 52 weeks. (B, C, H, I, N, O, T, U) Early- and late-phase fluorescein angiographic images at baseline, 24 weeks, 26 weeks, and 52 weeks. (D, J, P, V), Foveal SD-OCT B-scans at baseline, 24 weeks, 26 weeks, and 52 weeks. (E, K, Q, W) Retinal pigment epithelium segmentation maps at baseline, 24 weeks, 26 weeks, and 52 weeks. (F, L, R, X) Drusen volume maps with a 3 mm circle centered on the fovea at baseline, 24 weeks, 26 weeks, and 52 weeks. (G, H, I, J, K, L) Choroidal neovascularization was first visualized at the week 24 visit. Visual acuity was 20/40 (69 ETDRS letters). Note the leakage on the fluorescein angiography (H, I), the presence of subretinal fluid (J), and a retinal pigment epithelial detachment (PED) (J, K, L). The patient received an injection of ranibizumab, and after 15 days (week 26 visit), the fluid and PED olume had decreased. After 52 weeks of follow-up, the patient had received four injections of ranibizumab and visual acuity was 20/32 (75 ETDRS letters).

By 26 weeks of follow-up, a single placebo study eye progressed to neovascular disease with the development of a vascularized retinal pigment epithelial detachment (PED) and the appearance of intraretinal fluid (Figure 6). A single non-study but eligible fellow eye, also in the placebo group, progressed to neovascularization at 20 weeks of follow-up. No additional eyes developed neovascularization between weeks 26 and 52. None of the eyes developed GA over 52 weeks.

The BCVA of both study and fellow eyes remained stable over 26 weeks of follow-up with small increases in the number of ETDRS letters read in both groups: +2.4 (3.9) in the active eculizumab group and +4.0 (7.0) in the placebo group (P = .36). The maximum number of letters lost by any eye meeting inclusion criteria was five letters (one eculizumab eye). There was a deficit in the low luminance visual acuity compared to standard visual acuity test at baseline of 14.4 (5.1) letters and 15.5 (5.4) letters in the eculizumab and placebo groups, respectively (P = .60). After 26 week of follow-up, the deficit increased to 16.5 (4.8) and 16.3 (5.8) letters in the eculizumab and placebo groups, respectively (P = .92). The difference between baseline and 26 weeks of follow-up was not statistically significant (P = .37).

No correlation was found between choroidal thickness and the area or volume of drusen at baseline either with or without adjusting for age and axial length (all P > .12), and no correlation was found between choroidal thickness and the progression of drusen area or volume over 26 and 52 weeks of follow-up (all P > .53).

Genetic Analysis

The distribution of patients according to the number of at-risk alleles they carry is shown in Table 3 (page 27). This table also shows the association between these genotypes and the volume of drusen at baseline and the change in volume of drusen over 26 and 52 weeks. The drusen volume at baseline in the central 3 mm measured by SD-OCT was not associated with

TABLE 3

Correlation Between Genotype and Change in Drusen Volume Through 52 Weeks

Single-Nucleotide Polymorphism [At-Risk Allele]	Number of At-Risk Alleles (Number of Patients With Genotype)	Cube Root of Drusen Volume at Baseline (SD)	*P* Value[1]	Change in Cube Root of Drusen Volume at 26 Weeks (SD)	*P* Value[1]	Change in Cube Root of Drusen Volume at 52 Weeks (SD)	*P* Value[1]
CFH-rs1061170 [C]	- - (2)	0.5 (0.12)	.069	- 0.417 (n=1)*	.001	-0.405 (n=1)*	< .001
	+ - (17)	0.54 (0.16)		+0.012 (0.04)		0.008 (0.061)	
	+ + (11)	0.42 (0.07)		+0.025 (0.01)		0.026 (0.024)	
CFH-rs2274700 [C]	- - (0)		.56		.03		.13
	+ - (8)	0.52 (0.14)		-0.06 (0.17)		-0.048 (0.170)	
	+ + (22)	0.48 (0.14)		+0.023 (0.01)		-0.001 (0.095)	
HTRA1-rs10490924 [T]	- - (8)	0.51 (0.13)	.65	- 0.063 (0.16)	.09	-0.043 (0.173)	.35
	+ - (13)	0.51 (0.14)		+0.02 (0.01)		0.004 (0.055)	
	+ + (9)	0.45 (0.15)		+0.028 (0.01)		0.027 (0.024)	
C3-rs2230199 [G]	- - (20)	0.51 (0.14)	.51	- 0.002 (0.1)	.92	-0.005 (0.111)	.94
	+ - (8)	0.49 (0.15)		+0.003 (0.06)		0.005 (0.062)	
	+ + (2)	0.38 (0)		+0.025 (0.01)		0.017 (0.004)	
CFBrs641153 [G]	- - (0)		.84		.59		.87
	+ - (4)	0.51 (0.05)		- 0.022 (0.082)		-0.008 (0.082)	
	+ + (26)	0.49 (0.15)		+0.005 (0.093)		0.001 (0.098)	

SD = standard deviation.

[1]*One-way analysis of variance.*

**One patient converted to wet AMD and was not included in the drusen change over 26 weeks. All patients carried both at-risk alleles for SNP C2_rs9332739-E318D (data not shown).*

the number of at-risk alleles in each patient ($P = .87$) or whether a particular locus was homozygous or heterozygous (all $P > .05$). However, the growth of drusen volume over 26 and 52 weeks was associated with the number of at-risk alleles for the SNP CFH-rs1061170 carried by a patient, and this association was statistically significant ($P < .001$). This SNP identifies the H1 at-risk haplotype. For the SNP CFH-rs2274700, there was a statistically significant difference in the growth of drusen volume at 26 weeks if the patients carried one or both copies of the at-risk allele ($P = .03$). However, the statistical significance observed at 26 weeks was lost at 52 weeks. This SNP identifies both the H1 and the H3 CFH haplotypes. No other at-risk allele tested showed a correlation between the allelic burden and the growth of drusen volume through 52 weeks (all $P > .05$). A secondary analysis was performed to determine whether the genotype had any influence on the treatment outcome. There was no correlation between any of the SNPs and the potential treatment effect of eculizumab (all $P > .05$).

Pharmacokinetics

During the study, blood samples were collected to assay for eculizumab and C5 activity. Among patients receiving eculizumab, all samples collected between the onset of treatment and week 26 showed measurable levels of drug. Eculizumab levels rose rapidly during treatment weeks 1 to 4, with the low-dose cohort averaging 91 to 285 mg/mL and the high-dose cohort averaging 84 to 239 µg/mL. Differences between levels in the low- and high-dose groups were not statistically significant (all $P > .2$). Between weeks 6 and 26, eculizumab levels continued to increase by only 1.5 µg/mL/week in actively treated patients. On average, C5 activity decreased to less than 8% of normal levels by 1 week after treatment and less than 0.5% by week 26. Among the patients

TABLE 4

Sample Size Estimates for Each Treatment Group Based on the Predicted Percentage of Failures at 1 Year

	Number of Subjects Needed for Each Treatment Group Based on the Predicted Percentage of Failures in Actively Treated Group at 1 Year*			
Power	**30% Failure Rate**	**15% Failure Rate**	**5% Failure Rate**	**1% Failure Rate**
80%	48	21	13	11
90%	62	26	16	14

**Based on an estimated failure rate of 60% in the placebo group and 1:1 randomization. Failure was defined as growth of drusen volume and formation of any neovascularization or geographic atrophy at 1 year.*

receiving placebo injections, levels of eculizumab were undetectable.

DISCUSSION

The COMPLETE study is the first randomized, phase 2 clinical trial performed to evaluate the clinical efficacy and safety of complement inhibition for the treatment of drusen in dry AMD. A number of strategies for modulating the complement system are currently being used in dry AMD patients, and these approaches include the inhibition of complement proteins such as C3, C5, and factor D.[37] In this study, eculizumab, an anti-complement drug that blocks the activation of C5, was intravenously administered in a population of patients with drusen secondary to AMD.

The effects of eculizumab on drusen volume and area were assessed and compared against placebo. As described above, the square root transformation of drusen area measurements and the cube root transformation of drusen volume measurements were performed to eliminate the influence of drusen size on their 95% test-retest reproducibility limits and on their overall growth rates.[4] Overall, there was no statistically significant effect of eculizumab on drusen volume and area. The majority of patients in the active treatment and placebo groups maintained a stable drusen volume over 52 weeks with some dynamic changes around the test-retest 95% confidence intervals shown as the dotted lines in Figures 1 and 2 (pages 21 and 22 respectively). Figure 1 shows the scatter plots of the baseline and follow-up cube root drusen volumes at 26 weeks for the placebo and eculizumab patients. Two eyes included in the placebo group had a significant decrease in the drusen volume over 26 weeks, and these two eyes can be observed below the test-retest dotted line. Only one eye lost at least 50% of its baseline volume, and this eye is shown below the solid diagonal line. Neither eye progressed to GA or CNV. Figure 3 (page 23) shows the color fundus image, autofluorescence image, OCT B-scans, and drusen volume maps of an eye in the placebo group that experienced a significant reduction in drusen volume over 26 weeks. In this example, some drusen that would be classified as hard or calcific drusen in the color image appeared to resolve during the follow-up period. One study eye in the placebo group progressed to CNV during follow-up (Figure 6, page 26). This patient presented with an increase in drusen volume over the first 20 weeks of follow-up before developing subretinal fluid and a vascularized RPE detachment at week 24. In addition, one fellow eye of a patient included in the placebo group presented with neovascularization at week 20. Overall, there were no differences in the drusen volumes between treatment groups through 52 weeks.

In this study, we were not able to identify any effect of systemic eculizumab treatment on drusen volume measured with SD-OCT. These results raise questions of whether complement inhibition is a viable treatment strategy, whether our study was too small and too short to detect a treatment effect, whether C5 is the appropriate target to prevent complement-mediated disease progression, whether systemic therapy is appropriate for the treatment of dry AMD, whether an adequate dose of eculizumab was used, whether intravitreal injections would have been a better route for drug delivery, or whether complement inhibition may only be effective in a genetic subgroup of AMD patients who carry the at-risk alleles of complement genes. While eculizumab inhibits C5 and prevents terminal complement activation, it is entirely possible that more proximally activated complement proteins such as C3a and C3b need to be suppressed to affect drusen volume and eculizumab is unable to suppress these anaphylotoxins. While the doses used in this study were based on the effective doses of eculizumab used to treat paroxysmal

nocturnal hemoglobinuria and atypical hemolytic uremic syndrome, and these doses completely inhibit systemic complement C5 in these diseases,[38,39] it is possible that an even higher dose is needed to penetrate the back of the eye to reduce drusen volume. Of course, this assumes that C5 activation in the retina has a role in the growth of drusen. However, if C5 inhibition is needed in the choroid to induce drusen regression, then the doses used in this study should have been adequate to show a treatment effect. While it's possible that complement activation may not have a role in the reduction of drusen volume, our genetic data suggest that complement activation clearly has a role in drusen growth.

Although the number of patients in this study is small for a genetic association study, it is striking that there was a highly statistically significant correlation between the growth of drusen volume and the number of at-risk CFH alleles carried by the patients. Of the seven SNPs evaluated in this study (Table 3, page 27), only the SNP associated with the high-risk H1 haplotype, the CFH allele (CFH-rs1061170), showed an association with the growth of drusen volume at 26 and 52 weeks ($P < .001$). This highly significant association suggests that complement may play an important role in the growth of drusen volume, and it is unlikely due to alpha error inflation as a result of multiple statistical comparisons.[40,41] Perhaps a more appropriate endpoint might have been the inhibition of drusen growth rather than the reduction of drusen volume. However, our study was not powered to study the inhibition of drusen growth. It is also interesting that two placebo eyes converted from dry to wet AMD. While it is possible that complement inhibition might be an effective treatment to prevent the conversion of dry to wet AMD, no conclusion is possible due to the small size of our study. However, such a prevention strategy could be used as a clinical trial endpoint in the study of complement inhibition for dry AMD. Previously, this prevention endpoint was used unsuccessfully to study anecortave acetate for the treatment of dry AMD (www.clinicaltrial.gov; NCT00333216).

Our data suggest that a novel composite clinical trial endpoint should be used when designing future phase 2 clinical trials to test potential therapies for nonexudative AMD (Table 4). This composite endpoint uses the three likely outcomes when following the normal progression of drusen, and the power calculations in Table 4 are derived from the natural history study previously published by Yehoshua et al[5] and confirmed in the current study. We found that when eyes with a baseline drusen volume of 0.03 mm^3 or greater in the absence of any GA are followed up for 1 year, the proportion of eyes at follow-up with decreasing, stable, and increasing drusen volumes are 20%, 26%, 54%, respectively. If we then assume, based on our previous research, a cumulative incidence of CNV at 1 year of 4.5% and a cumulative incidence of GA at 1 year of 5.0%, then we can design a composite clinical trial endpoint in which the goal of treatment is to prevent normal disease progression. If normal disease progression occurs, then this would be considered a failure, and failure would be defined as the growth of drusen volume beyond test-retest limits, the appearance of any neovascularization, or the appearance of GA at 1 year. If we assume an expected failure rate of 60% in the placebo group, then Table 4 shows the number of subjects in each group required to perform a study with 80% or 90% power to detect a decrease in the defined failure rate.

The current study had an 80% power to detect a 50% decrease in the drusen volume in 65% of subjects receiving drug compared with 5% of subjects receiving placebo. After 6 months, we not only failed to detect this predetermined treatment effect, but based on our outcomes, we are confident that we could have detected a treatment effect that decreased the drusen volume in as few as 30% of the subjects receiving drug. If we now apply this novel composite clinical trial endpoint that focuses on drusen growth rather than a decrease in drusen volume to the outcomes from the current study, then eculizumab once again failed to show a positive treatment effect. However, we never would have expected to see a positive treatment effect using the composite clinical trial endpoint given the small number of patients and the short follow-up in this current study. In fact, the current study design would have only been suitable if we had hypothesized a reduction in the composite failure rate of 90% or more following treatment with eculizumab, which would have been an overly optimistic prediction. Table 4 shows the actual number of subjects that would be needed to design a study with 80% power to detect a 50% decrease in the failure rate from 60% to 30% at 1 year using this composite endpoint. The study would require 48 subjects in both the placebo and the eculizumab arms. While this number is greater than the number of patients enrolled in our current study, it still represents fewer subjects than the number enrolled in previous and ongoing phase 2 clinical trials designed to test novel therapies for nonexudative AMD.

The use of composite endpoints has been controversial especially when used to increase the statistical power of a trial by combining several outcomes that occur individually at a low incidence.[42,43] This was not the motivation behind our suggested compos-

ite endpoint. Rather, the principal outcome of interest and the one with the highest incidence in historical controls is the growth of drusen volume. The analytical issue then becomes how to handle progression to either neovascularization or GA. One option is to label them as adverse events and include them in a safety evaluation. This would involve censoring the enrolled eyes of patients at the time of progression in the final analysis of efficacy. Because these are the worst possible outcomes for patients, we feel their proper role in the efficacy analysis is to be considered failures; however, trials employing this composite outcome should examine the component outcomes separately as well.

In summary, systemic complement inhibition with eculizumab was well tolerated through 6 months, and no drug-related adverse events were identified, but complement inhibition with eculizumab did not reduce the volume of drusen in patients with dry AMD. While patients in the placebo group did have a higher incidence of neovascularization, suggesting an effect of complement inhibition in preventing the conversion of dry to wet AMD, the study was too small to draw any definitive conclusions about eculizumab in preventing this conversion. The study showed an association between the number of at-risk CFH alleles and drusen growth, suggesting that complement activation has a role in the formation of drusen, but the study was not powered adequately to look for a decrease in drusen growth. Whether C5 inhibition is the appropriate target or intravitreal injections might be a better way to deliver the drug remains to be determined. Although it failed to meet the primary outcome measure, the study demonstrated the utility of using SD-OCT to measure drusen volume as a clinical trial endpoint. The results from this first trial investigating the effects of C5 inhibition on drusen volume are sufficiently intriguing to suggest that future investigations of complement inhibition for dry AMD should be pursued using a composite clinical trial endpoint, which would include the prevention of drusen growth and the prevention of neovascularization and GA.

REFERENCES

1. Ferris FL, 3rd, Wilkinson CP, Bird A, et al. Clinical Classification of Age-related Macular Degeneration. *Ophthalmology.* 2013;120(4):844-851.
2. Ferris FL, Davis MD, Clemons TE, et al. A simplified severity scale for age-related macular degeneration: AREDS Report No. 18. *Arch Ophthalmol.* 2005;123(11):1570-1574.
3. Davis MD, Gangnon RE, Lee LY, et al. The Age-Related Eye Disease Study severity scale for age-related macular degeneration: AREDS Report No. 17. *Arch Ophthalmol.* 2005;123(11):1484-1498.
4. Gregori G, Wang F, Rosenfeld PJ, et al. Spectral domain optical coherence tomography imaging of drusen in nonexudative age-related macular degeneration. *Ophthalmology.*;118(7):1373-1379.
5. Yehoshua Z, Wang F, Rosenfeld PJ, Penha FM, Feuer WJ, Gregori G. Natural history of drusen morphology in age-related macular degeneration using spectral domain optical coherence tomography. *Ophthalmology.* 2011;118(12):2434-2441.
6. Rothman KJ, Funch DP, Dreyer NA. Bromocriptine and puerperal seizures. *Epidemiology.* 1990;1(3):232-238.
7. Poole C, Rothman KJ. Epidemiologic science and public health policy. *J Clin Epidemiol.* 1990;43(11):1270-1271.
8. Olk RJ, Friberg TR, Stickney KL, et al. Therapeutic benefits of infrared (810-nm) diode laser macular grid photocoagulation in prophylactic treatment of nonexudative age-related macular degeneration: two-year results of a randomized pilot study. *Ophthalmology.* 1999;106(11):2082-2090.
9. Figueroa MS, Regueras A, Bertrand J. Laser photocoagulation to treat macular soft drusen in age-related macular degeneration. *Retina.* 1994;14(5):391-396.
10. Frennesson CI. Prophylactic laser treatment in early age-related maculopathy: an 8-year follow-up in a randomized pilot study shows a reduced incidence of exudative complications. *Acta Ophthalmol Scand.* 2003;81(5):449-454.
11. Friberg TR, Musch DC, Lim JI, et al. Prophylactic treatment of age-related macular degeneration report number 1: 810-nanometer laser to eyes with drusen. Unilaterally eligible patients. *Ophthalmology.* 2006;113(4):e622 e621.
12. Friberg TR, Brennen PM, Freeman WR, Musch DC, Group PS. Prophylactic treatment of age-related macular degeneration report number 2: 810-nanometer laser to eyes with drusen: bilaterally eligible patients. *Ophthalmic Surg Lasers Imaging.* 2009;40(6):530-538.
13. Rodanant N, Friberg TR, Cheng L, et al. Predictors of drusen reduction after subthreshold infrared (810 nm) diode laser macular grid photocoagulation for nonexudative age-related macular degeneration. *Am J Ophthalmol.* 2002;134(4):577-585.
14. Parodi MB, Virgili G, Evans JR. Laser treatment of drusen to prevent progression to advanced age-related macular degeneration. *Cochrane Database Syst Rev.* 2009(3):CD006537.
15. Davis MD, Gangnon RE, Lee LY, et al. The Age-Related Eye Disease Study severity scale for age-related macular degeneration: AREDS Report No. 17. *Arch Ophthalmol.* 2005;123(11):1484-1498.
16. Yehoshua Z, Gregori G, Sadda SR, et al. Comparison of drusen area detected by spectral domain optical coherence tomography and color fundus imaging. *Invest Ophthalmol Vis Sci.* 2013;54(4):2429-2434.
17. Maguire MG. Drusen volume as a study endpoint. *Ophthalmology.* 2012;119(7):1501-1502; author reply 1502.
18. Khandhadia S, Cipriani V, Yates JR, Lotery AJ. Age-related macular degeneration and the complement system. *Immunobiology.*;217(2):127-146.
19. Mullins RF, Oh KT, Heffron E, Hageman GS, Stone EM. Late development of vitelliform lesions and flecks in a patient with best disease: clinicopathologic correlation. *Arch Ophthalmol.* 2005;123(11):1588-1594.
20. Hageman GS, Anderson DH, Johnson LV, et al. A common haplotype in the complement regulatory gene factor H (HF1/CFH) predisposes individuals to age-related macular degeneration. *Proc Natl Acad Sci USA.* 17 2005;102(20):7227-7232.
21. Johnson LV, Leitner WP, Staples MK, Anderson DH. Complement activation and inflammatory processes in Drusen formation and age related macular degeneration. *Exp Eye Res.* 2001;73(6):887-896.
22. Nozaki M, Raisler BJ, Sakurai E, et al. Drusen complement components C3a and C5a promote choroidal neovascularization. *Proc Natl Acad Sci USA.* 2006;103(7):2328-2333.
23. Fagerness JA, Maller JB, Neale BM, Reynolds RC, Daly MJ, Seddon JM. Variation near complement factor I is associated with risk of advanced AMD. *Eur J Hum Genet.* 2009;17(1):100-104.
24. Maller JB, Fagerness JA, Reynolds RC, Neale BM, Daly MJ, Seddon JM. Variation in complement factor 3 is associated with risk of age-related macular degeneration. *Nat Genet.* 2007;39(10):1200-1201.
25. Gold B, Merriam JE, Zernant J, et al. Variation in factor B (BF) and complement component 2 (C2) genes is associated with age-related macular degeneration. *Nat Genet.* 2006;38(4):458-462.

26. Yates JR, Sepp T, Matharu BK, et al. Complement C3 variant and the risk of age-related macular degeneration. *N Engl J Med.* 2007;357(6):553-561.
27. Bomback AS, Smith RJ, Barile GR, et al. Eculizumab for dense deposit disease and C3 glomerulonephritis. *Clin J Am Soc Nephrol.* 2012;7(5):748-756.
28. Rohrer B, Long Q, Coughlin B, et al. A targeted inhibitor of the complement alternative pathway reduces RPE injury and angiogenesis in models of age-related macular degeneration. *Adv Exp Med Biol.* 2010;703:137-149.
29. Bora PS, Sohn JH, Cruz JM, et al. Role of complement and complement membrane attack complex in laser-induced choroidal neovascularization. *J Immunol.* 2005;174(1):491-497.
30. Bora NS, Kaliappan S, Jha P, et al. Complement activation via alternative pathway is critical in the development of laser-induced choroidal neovascularization: role of factor B and factor H. *J Immunol.* 2006;177(3):1872-1878.
31. Lanes SF, Rothman KJ. Tampon absorbency, composition and oxygen content and risk of toxic shock syndrome. *J Clin Epidemiol.* 1990;43(12):1379-1385.
32. Rothman KJ. Statistics in nonrandomized studies. *Epidemiology.* 1990;1(6):417-418.
33. Sunness JS, Rubin GS, Broman A, Applegate CA, Bressler NM, Hawkins BS. Low luminance visual dysfunction as a predictor of subsequent visual acuity loss from geographic atrophy in age-related macular degeneration. *Ophthalmology.* 2008;115(9):1480-1488, 1488 e1481-1482.
34. Yehoshua Z, Rosenfeld PJ, Gregori G, et al. Progression of geographic atrophy in age-related macular degeneration imaged with spectral domain optical coherence tomography. *Ophthalmology.* 2011;118(4):679-686.
35. Yehoshua Z, Garcia Filho CA, Penha FM, et al. Comparison of Geographic Atrophy Measurements from the OCT Fundus Image and the Sub-RPE Slab Image. *Ophthalmic Surg Lasers Imaging Retina.* 2013;44(2):127-132.
36. Chen Y, Zeng J, Zhao C, et al. Assessing susceptibility to age-related macular degeneration with genetic markers and environmental factors. *Arch Ophthalmol.* 2011;129(3):344-351.
37. Yehoshua Z, Rosenfeld PJ, Albini TA. Current Clinical Trials in Dry AMD and the Definition of Appropriate Clinical Outcome Measures. *Semin Ophthalmol.* 2011;26(3):167-180.
38. Hill A, Hillmen P, Richards SJ, et al. Sustained response and long-term safety of eculizumab in paroxysmal nocturnal hemoglobinuria. *Blood.* 2005;106(7):2559-2565.
39. Hillmen P, Young NS, Schubert J, et al. The complement inhibitor eculizumab in paroxysmal nocturnal hemoglobinuria. *N Engl J Med.* 2006;355(12):1233-1243.
40. Rothman KJ. No adjustments are needed for multiple comparisons. *Epidemiology.* 1990;1(1):43-46.
41. Katz MH. Multivariable analysis: a practical guide for clinicians. 2nd ed. Cambridge: Cambridge University Press; 2006.
42. Ferreira-Gonzalez I, Busse JW, Heels-Ansdell D, et al. Problems with use of composite end points in cardiovascular trials: systematic review of randomised controlled trials. *BMJ.* 2007;334(7597):786.
43. Tomlinson G, Detsky AS. Composite end points in randomized trials: there is no free lunch. *JAMA.* 2010;303(3):267-268.

Published in final edited form as:
Ophthalmology. 2014 March ; 121(3): 693–701. doi:10.1016/j.ophtha.2013.09.044.

Systemic Complement Inhibition with Eculizumab for Geographic Atrophy in Age-Related Macular Degeneration:

The COMPLETE Study

Zohar Yehoshua, MD, MHA[1], **Carlos Alexandre de Amorim Garcia Filho, MD**[1,2], **Renata Portella Nunes, MD**[1], **Giovanni Gregori, PhD**[1], **Fernando M. Penha, MD, PhD**[1,2], **Andrew A. Moshfeghi, MD, MBA**[1], **Kang Zhang, MD, PhD**[3], **SriniVas Sadda, MD**[4], **William Feuer, MS**[1], and **Philip J. Rosenfeld, MD, PhD**[1]

[1] Department of Ophthalmology, Bascom Palmer Eye Institute, University of Miami Miller School of Medicine, Miami, Florida.

[2] Department of Ophthalmology, Federal University of São Paulo, UNIFESP, São Paulo, Brazil.

[3] Institute for Genomic Medicine and Shiley Eye Center, University of California, San Diego, La Jolla, California.

[4] Doheny Eye Institute, Keck School of Medicine, University of Southern California, Los Angeles, California.

Abstract

Purpose—To evaluate the effect of eculizumab, a systemic inhibitor of complement component (C5), on the growth of geographic atrophy (GA) in patients with age-related macular degeneration (AMD).

Design—Prospective, double-masked, randomized clinical trial.

Participants—Patients with GA measuring from 1.25 to 18 mm^2 based on spectral-domain optical coherence tomography imaging.

Methods—Patients were randomized 2:1 to receive intravenous eculizumab or placebo over 6 months. In the eculizumab treatment arm, the first 10 patients received a low-dose regimen of 600 mg weekly for 4 weeks followed by 900 mg every 2 weeks until week 24, and the next 10 patients

Correspondence: Philip J. Rosenfeld, MD, PhD, Bascom Palmer Eye Institute, University of Miami Miller School of Medicine, 900 NW 17th Street, Miami, FL 33136. prosenfeld@med.miami.edu..

Supplemental material is available at www.aaojournal.org.

Financial Disclosure(s): The author(s) have made the following disclosure(s): Zohar Yehoshua: Financial support–Carl Zeiss Meditec, Inc.
Carlos Alexandre de Amorim Garcia Filho: Financial support e Carl Zeiss Meditec, Inc.
Giovanni Gregori: Financial support–Carl Zeiss Meditec, Inc.;
Patents–Carl Zeiss Meditec, Inc. (with the University of Miami) Fernando M. Penha: Financial support–Carl Zeiss Meditec, Inc.
Andrew A. Moshfeghi: Consultant–Allergan, Alcon, Genentech/Roche, Valeant, Bayer, and Regeneron
Kang Zhang: Consultant–Acucela; Financial supporteGenentech SriniVas Sadda: Consultant–Heidelberg Engineering; Financial supporteCarl Zeiss Meditec, Inc.
Philip J. Rosenfeld: Consultant–Acucela, Alcon, Bayer, Boehringer Ingelheim, Chengdu Kanghong Biotech, Merck, Oraya, Roche, and Sanofi/ Genzyme; Financial support–Alexion Pharmaceuticals, Acucela, Advanced Cell Technology, GlaxoSmithKline, and Carl Zeiss Meditec, Inc.

received a high-dose regimen of 900 mg weekly for 4 weeks followed by 1200 mg every 2 weeks until week 24. The placebo group was infused with saline. Patients were observed off treatment for an additional 26 weeks. Both normal-luminance and lowluminance visual acuities were measured throughout the study, and the low-luminance deficits were calculated as the difference between the letter scores.

Main Outcome Measures—Change in area of GA at 26 weeks.

Results—Thirty eyes of 30 patients were enrolled. Eighteen fellow eyes also met inclusion criteria and were analyzed as a secondary endpoint. For the 30 study eyes, mean square root of GA area measurements ± standard deviation at baseline were 2.55±0.94 and 2.02±0.74 mm in the eculizumab and placebo groups,respectively ($P = 0.13$). At 26 weeks, GA enlarged by a mean of 0.19±0.12 and 0.18±0.15 mm in the eculizumab and placebo groups, respectively ($P = 0.96$). At 52 weeks of follow-up, GA enlarged by a mean of 0.37±0.22 mm in the eculizumab-treated eyes and by a mean of 0.37±0.21 mm in the placebo group ($P = 0.93$, 2 sample t test). None of the eyes converted to wet AMD. No drug-related adverse events were identified.

Conclusions—Systemic complement inhibition with eculizumab was well tolerated through 6 months but did not decrease the growth rate of GA significantly. However, there was a statistically significant correlation between the lowluminance deficit at baseline and the progression of GA over 6 months.Ophthalmology 2014;121:693-701 © 2014 by the American Academy of Ophthalmology.

The pathogenesis of age-related macular degeneration (AMD) is multifactorial, resulting from a combination of genetic and environmental risk factors.[1] Over the past decade, there has been growing evidence implicating a role for the complement system in AMD.[2] Histopathologic studies have identified various complement components in drusen, in Bruch's membrane, and in the inner choroid.[3,4] Moreover, deposits similar in appearance to drusen in AMD have been found in eyes of patients with complement-mediated renal diseases.[5] Genetic association studies using different populations have shown that genetic polymorphisms associated with AMD have been localized within or close to genes that encode complement proteins.[6] In 2005, 4 groups identified a genetic polymorphism in complement factor H (*CFH*), which has been associated strongly with an increased risk of developing AMD.[7–10] In addition, polymorphisms within other complement genes, such as complement component 3 (*C3*) genes[11] and the complement factor B (*CFB*)/complement component 2 (*C2*) locus,[12] have been associated with an increased risk of AMD. The most common risk-conferring *CFH* genetic variant for AMD is the Y402H polymorphism, resulting in a tyrosine-to-histidine substitution at amino acid position 402 within the CFH protein. Protective alleles associated with the complement pathway also have been reported. Two of the 5 CFH-related genes (*CFHR1–5*) that lie within the regulators of complement activation locus on chromosome 1q32, known as *CFHR1* and *CFHR3*, are considered to be protective against AMD.[13]

Currently, there is no proven therapy that stops the progression of dry AMD. The cessation of smoking along with vitamin and nutritional supplements combined with a healthy diet are considered the only options for slowing disease progression.[14,15] Several treatment strategies that modulate the complement system in AMD are being investigated. These

treatments inhibit complement activation by targeting various effectors molecules, such as C3, C5, and factor D.[15–17] The only inhibitor of terminal complement activation approved by the US Food and Drug Administration is eculizumab (Soliris; Alexion Pharmaceuticals, Cheshire, CT), a humanized monoclonal antibody derived from the murine anti-human C5 antibody. Eculizumab is approved for the systemic treatment of paroxysmal nocturnal hemoglobinuria and atypical hemolytic uremic syndrome. Both paroxysmal nocturnal hemoglobin-uria[18] and atypical hemolytic uremic syndrome[19] result from complement dysregulation, and eculizumab successfully controls these diseases by inhibiting C5 and preventing terminal complement activation and formation of membrane attack complex (C5b-9).[20]

To investigate the role of systemic complement activation in AMD, we performed the Complement Inhibition with Eculizumab for the Treatment of Nonexudative Age-Related Macular Degeneration (COMPLETE) study, which was designed to evaluate the safety and efficacy of systemic eculizumab for the treatment of geographic atrophy (GA) in AMD.

Methods

Study Design

The COMPLETE study is an investigator-sponsored, randomized, double-masked, single-center study designed to evaluate the safety and efficacy of intravenous eculizumab for the treatment of patients with GA secondary to AMD. The study was performed with the approval of the Food and Drug Administration (investigational new drug application no. 104471). Before the initiation of the study, additional approval was obtained from the institutional review board at the University of Miami Miller School of Medicine. Informed consent was obtained from all patients before determination of full eligibility, and the study was performed in accordance with the Health Insurance Portability and Accountability Act. The COMPLETE study is registered at www.clinicaltrials.gov, and the clinical trial accession number is NCT00935883 (accessed September 18, 2013).

From November 2009 through March 2011, a total of 30 patients were enrolled. Eligibility criteria included age 50 years or older, total GA area of 1.25 to 18 mm^2, and visual acuity of 20/63 or better (Early Treatment Diabetic Retinopathy Study [ETDRS] letter score of at least 59). Exclusion criteria were visual acuity worse than 20/63, a total GA area of more than 18 mm^2 (7 disc areas), GA contiguous with any peripapillary atrophy, and any history of choroidal neovascularization in the study eye. If both eyes were eligible for the study, then 1 eye was chosen as the study eye at the discretion of the investigator. All patients enrolled in the study received a meningococcal vaccine at least 15 days before the initiation of treatment.

Treatment Protocol

Patients were randomized 2:1 to receive active treatment with eculizumab or placebo in a double-masked fashion. Randomization schedules were stratified with the use of a permuted-block strategy to insure balance. During the treatment period, patients received eculizumab for a period of 24 weeks with the primary endpoint at 26 weeks. The treatment

period was divided into an induction period and a maintenance period. The first 10 patients in the eculizumab group received the low dose of eculizumab (600 mg via intravenous infusion for 4 weeks followed by 900 mg every 2 weeks until week 24), whereas the next 10 patients received the high dose (900 mg eculizumab via intravenous infusion for 4 weeks followed by 1200 mg every 2 weeks until week 24). After 26 weeks, patients were followed up without treatment every 3 months for an additional 6 months.

Ophthalmologic Examination and Imaging Procedures

Ophthalmologic examination included best-corrected visual acuity measured using the ETDRS chart at 4 meters, low-luminance visual acuity testing at 4 meters using a 2.0-log unit neutral density filter (Wratten filter; Kodak, Rochester, NY),[21] slit-lamp bio-microscopy, intraocular pressure measurement, and fundus examination. All imaging studies were performed at baseline, 12 weeks, 26 weeks, and 52 weeks of follow-up. These studies included color and autofluorescence (AF) imaging with a fundus camera-based flash system (TRC-50DX; Topcon Medical Systems, Oakland, NJ; AF excitation λ, 535e585 nm; detection λ, 605–715 nm), AF and fluorescein angiographic imaging with a confocal scanning laser ophthalmoscopy system (Spectralis; Heidelberg Engineering, Heidelberg, Germany; AF excitation λ, 488 nm; detection λ, >500 nm), and spectral-domain (SD) optical coherence tomography (OCT) imaging with both the Cirrus (Carl Zeiss Meditec, Inc., Dublin, CA) and Spectralis (Heidelberg Engineering) instruments.

The Cirrus SD OCT system was used to acquire 200 200 cubes centered at the fovea. From these datasets, one can generate en face OCT fundus images (OFIs) and en face OCT partial fundus images derived from a slab beneath the retinal pigment epithelium (sub-RPE slab).[22] The OFIs represent virtual fundus images resulting from the en face summation of the reflected light from each A-scan.

The areas of GA observed in the OFI and the sub-RPE slab image were outlined manually by 2 independent graders (C.A.A.G.F., Z.Y.) at the Bascom Palmer Eye Institute using a CintiQ WACOM digitizing tablet (WACOM Corp., Vancouver, WA) and image analysis software (Adobe Photoshop CS2; Adobe Systems, Inc., San Jose, CA) as previously described.[23] A consensus image was used for measurements. In the cases in which the 2 graders could not reach an agreement on the outlines of the GA, a third senior grader (P.J.R.) outlined the lesion and his measurement was used for the analysis. The Topcon flash AF images were registered to the OFI using custom-built retinal image registration software based on the blood vessel ridges.[24] These registered flash-AF images, the confocal scanning laser ophthalmoscopy AF images, and the fluorescein angiography images were outlined manually by 2 certified graders at the Doheny Eye Institute Reading Center, and one consensus measurement was used for the analysis. The area measurements of GA underwent a square root transformation. This approach eliminated the influence of lesion size on test–retest variability and growth rates.[23] The growth of GA was defined as the difference of the square root of the area measurements at the suitable time points.

Choroidal imaging was performed with the Spectralis instrument (Heidelberg Engineering) and the enhanced depth imaging protocol. Two independent graders (Z.Y. and C.A.A.G.F.)

manually measured choroidal thickness at the foveal center, and a consensus image was used for quantitation.

Outcome Measures

The primary outcome of the study was to evaluate the effect of inhibiting C5 on the growth of GA in patients randomized to receive eculizumab treatment (including low-dose and high-dose regimens) versus placebo. The primary outcome was to be determined from the measurements of GA area obtained using SD OCT sub-RPE slab images. Growth rates were expressed as differences in the square root area measurements (in millimeters). Fellow eyes that met inclusion criteria were used for secondary outcome analysis. Secondary outcomes included the change in area of GA in study eyes measured with autofluorescence and fluorescein angiographic imaging; the change in area of GA in fellow eyes measured with SD OCT, AF, and fluorescein angiographic imaging; the change from baseline in normal-luminance and lowluminance ETDRS visual acuity in both study and fellow eyes; and conversion rate from dry AMD to wet AMD in both study and fellow eyes. Changes in renal function, C-reactive protein (CRP) levels, and complement protein levels were assessed as well.

Safety was assessed through the summary of ocular and nonocular adverse events, serious adverse events, ocular assessments, deaths, laboratory test results, and vital signs. Safety analyses included subjects who received at least 1 eculizumab infusion. Adverse events leading to discontinuation from the study were documented. After being enrolled, all subjects were vaccinated against *Neisseria meningitides*, and the first infusion was performed at least 2 weeks after the vaccination.

Statistical Analysis

Previous studies have demonstrated that taking the square root of area measurements before calculation of enlargement rates of GA removed the dependence of growth on baseline area and resulted in a homogeneous test–retest variance across the range of lesion sizes. Enlargement rates were compared between actively treated and placebo groups with the 2-sample *t* test. An ancillary analysis conducted with analysis of variance compared enlargement rates between eyes treated with placebo, a low-dose regimen, and a high-dose regimen. The primary study analysis included only 1 eye per patient; however, a secondary analysis included fellow eyes that would have been eligible for the study.

Sample Size Determination

The study was designed with 80% power to detect a 75% reduction in mean enlargement rate at 26 weeks based on previously published natural history data.[23]

Pharmacokinetic and Complement Factors Analysis

During the study, blood samples for pharmacokinetic and complement factor screening were drawn and analyzed in a masked fashion at baseline and at every planned visit at weeks 1, 2, 3, 4, 6, 8, 10, 12, 14, 16, 18, 20, 22, 24, 26, 28, 38, and 52. Alexion Pharmaceuticals laboratory measured soluble C5b-9 and performed a hemolytic assay for C5 activity. Levels of factor H and C3 also were measured.

Renal Function and C-Reactive Protein Levels

Renal function, as assessed by serum creatinine levels and glomerular filtration rate, and CRP levels were evaluated at baseline and at weeks 26 and 52. Glomerular filtration rate and CRP were evaluated at baseline and at weeks 26 and 52.

Genetic Analysis

Genetic testing for 7 single nucleotide polymorphisms was performed in all patients as previously described,[25] and the prevalence of the following [alleles] was assessed: C5, rs17611 [G]; CFH, rs1061170 [C]; C3, rs2230199 [G]; CFH, rs2274700 [C]; HTRA1, rs10490924 [T]; CFB, rs641153-R32Q [G]; and C2, rs9332739-E318D [G].

Results

Baseline Characteristics

A total of 30 patients were enrolled in the study and were randomized 2:1 to receive eculizumab or placebo. The first 10 patients who received eculizumab received the low-dose regimen, and the next 10 patients received the high-dose regimen. Eighteen fellow eyes met inclusion criteria and were analyzed as a secondary endpoint. The mean age ± standard deviation was 79±7 years in the eculizumab group and 81±6 years in the placebo groups. The mean age of patients in the low-dose regimen was 79±7 years and 80±7 years for those receiving the high-dose regimen. For the 30 study eyes, the mean area at baseline in the eculizumab group was 7.3±4.8 mm^2 and that in the placebo group was 4.6±3.6 mm^2 (P = 0.12). On the square root scale, which was used to determine the growth of GA, the mean standard ± deviation area measurements were 2.55±0.94 and 2.02±0.74 mm the placebo groups, in eculizumab and respectively (P = 0.13). Low- and high-dose eculizumab groups had similar square root area measurements at baseline (P = 0.44). Mean visual acuity at baseline was 71.3±7.8 EDTRS letters in the eculizumab group and 78.6±5.2 letters in the placebo group (P = 0.012). The mean visual acuity in the high-dose group was 67.8±7.4 EDTRS letters, 7 letters fewer than in the low-dose group, which was 74.8±6.7 EDTRS letters (P 0.040).

Primary Outcome: Enlargement Rate of Geographic Atrophy at 26 Weeks

All the patients completed 26 weeks of follow-up. Table 1 and Figure 1 show the growth at week 26 for the eculizumab and placebo groups. There was no difference between any of the groups. At 26 weeks, the mean changes in GA were 0.19±0.12 and 0.18±0.15 mm in the eculizumab and placebo groups, respectively (P = 0.96). This outcome ruled out a treatment-related reduction in the enlargement rate of 55% or more based on the 95% confidence interval of the difference in growth rates between active and placebo groups, which ranged from –0.10 to +0.10 mm. When we stratified the growth of GA according to the dose of eculizumab, there was no difference in growth rate, either (Table 1). The mean GA enlargement rates were not significantly different (P = 0.40), with the low-dose group having a change of 0.16±0.07 mm and the high-dose group having a change of 0.21±0.15 mm over 26 weeks (Table 1). As expected, there was no correlation between baseline lesion

size and enlargement rates using the square root area scale, either within treatment groups or with treatment groups combined (all |r| < 0.4; all P>0.29).

Secondary Outcomes

Fellow Eyes at 26 Weeks. Eighteen fellow eyes met inclusion criteria to enter the study and were analyzed as a secondary end point (Fig 1; Table 1). Evaluation of the enlargement rate for 48 eyes (30 study eyes plus 18 fellow eyes) showed no difference (P = 0.70) between the eculizumab-treated group (mean, 0.17; standard deviation, 0.10) and the placebo group (mean, 0.16; standard deviation, 0.10) or between the low-dose eculizumab group (mean, 0.16; standard deviation, 0.06) and the high-dose eculizumab group (mean, 0.17; standard deviation, 0.13; P = 0.82).

52-Week Follow-up. Although the primary outcome was considered to be the enlargement rate at the 26-week visit, the patients were followed up through 52 weeks to determine if there was any delayed treatment effect. At 52 weeks, there was no difference between the enlargement rates of the study eyes in the eculizumab and placebo groups (P = 0.93). The annual enlargement rate was 0.37±0.21 and 0.37±0.22 in the eculizumab and placebo groups, respectively. Similarly, mmthere was no difference between the low- and high-dose eculizumab groups (P 0.55). Evaluation of the enlargement rate for all 48 eyes (30 study eyes and 18 fellow eyes) showed no difference at 52 weeks between the eculizumab and placebo groups (P = 0.83).

Comparison of enlargement in study eyes during the first 26 weeks with that during the following 26 weeks (weeks 26 to 52) did not find a change in enlargement rate between these periods (P = 0.92, repeated measures analysis of variance) nor an interaction between period and treatment group (P = 0.97, repeated measures analysis of variance). Changes in the size of GA from weeks 26 to 52 were 0.19±0.11 mm in the eculizumab group and 0.18±0.14 mm in the placebo group. Figure 2 and Figure 3 (available online at www.aaojournal.org) show examples of GA lesions that grew over the 52 weeks of follow-up. None of the eyes demonstrated macular neovascularization during the 52 weeks of follow-up.

Visual Acuity. Table 2 (available online at www.aaojournal.org) displays changes in ETDRS visual acuity in placebo and control groups at 26 and 52 weeks of follow-up. In the study eyes, the average change in ETDRS acuity in the placebo group at week 26 was –2.6±7.2 compared with +2.5±4.1 in the eculizumab group (P = 0.019). The significance of this difference was largely the result of a single placebo eye that lost 22 letters of visual acuity when this eye's GA affected the fovea. At 52 weeks, the average change in ETDRS visual acuity in the placebo group was 2.9±7.0 compared with 0.7±7.2 in the eculizumab group (P = 0.43).

Low-Luminance Acuity Deficit. At 26 and 52 weeks, the enlargement of GA was not associated with either the baseline normal luminance ETDRS visual acuity letter score or the baseline low-luminance ETDRS visual acuity letter score (all |r| < 0.18; all P>0.23), as presented in Figure 4. However, the baseline low-luminance visual acuity deficit, which is defined as the difference between the normal luminance letter score and the low-luminance

visual acuity letter score, was shown to correlate with the enlargement rate of GA over 52 weeks. A statistically significant association existed between the lowluminance visual acuity deficit at baseline and the enlargement rate of GA at 26 and 52 weeks (Pearson correlation for 26 weeks: r = 0.38, $P = 0.008$; Pearson correlation for 52 weeks: $r = 0.4$, $P = 0.004$).

Choroidal Thickness. No correlation was found between choroidal thickness and the baseline square root area of GA or the growth of GA at 26 and 52 weeks, with or without including fellow eyes in the analysis (all $P>0.25$) as presented in Figure 5 (available at www.aaojournal.org). After adjustment for age and axial length, there was modest correlation between choroidal thickness and square root baseline area (study eyes, $r = –0.37$, $P = 0.056$; study eyes and fellow eyes, $r = –0.34$, $P = 0.022$). After adjusting for age and axial length, baseline choroidal thickness was not correlated with growth of square root area at 26 weeks ($P>0.10$) or 52 weeks (study eyes, $P = 0.12$; study eyes and fellow eyes, $P = 0.085$).

Genetic Analysis

There were no differences in baseline areas of GA and the number of copies of the at-risk alleles studied (Table 3, available at www.aaojournal.org). All patients carried at least 1 at-risk allele. For the CFB rs641153 and C2 rs9332739 single nucleotide polymorphisms, all but 1 participant had 2 copies of the at-risk alleles. Moreover, there was no evidence of an effect of the number of at-risk alleles at a particular locus on the enlargement rate of GA and there was no evidence of an interaction between the total number of alleles on the enlargement rate of GA.

Pharmacokinetics

During the study, blood samples were collected to assay for eculizumab (enzyme-linked immunosorbent assay in micrograms per milliliter) and C5 activity. Among patients receiving eculizumab, all samples collected between onset of treatment and week 26 showed measurable levels of drug. Eculizumab levels rose rapidly during treatment weeks 1 to 4, with the low-dose cohort averaging 65 to 189 μg/ml and the high-dose cohort averaging 122 to 259 μg/ml. Between weeks 6 and 26, eculizumab levels continued to increase minimally by 2 μg/ml weekly in actively treated patients. On average, C5 activity decreased to less than 9% of normal levels by week 1 after treatment and to less than 1% by week 2. Among the patients receiving placebo injections, circulating levels of eculizumab were undetectable and C5 activity was normal.

Renal Function and C-Reactive Protein Levels

Renal function, as assessed by serum creatinine levels and glomerular filtration rate, and CRP levels were evaluated at baseline and through week 26. When all randomized treatment groups were compared, there were no differences in renal function and CRP levels at baseline and at week 26 (all $P>0.1$). Baseline renal function (Pearson's $r = 0.11$ [$P = 0.58$], Spearman's $\rho = 0.02$ [$P = 0.90$]) and CRP levels (Pearson's $r = –0.05$ [$P = 0.80$], Spearman's $\rho = 0.12$ [$P = 0.54$]) did not correlate with disease progression.

Safety Outcome

Systemic complement inhibition with eculizumab was well tolerated through 52 weeks, and no drug-related adverse events were identified in the patients included in the study.

Discussion

The COMPLETE study was the first prospective, randomized, placebo-controlled investigation of complement inhibition for the treatment of AMD. This phase 2 clinical trial was performed to evaluate the clinical efficacy and safety of C5 inhibition using a systemically administered Food and Drug Administration–approved drug known as eculizumab. The study had an 80% power to detect a 75% reduction in the mean growth rate of GA over 26 weeks, and after 26 weeks we can say definitively that the treatment failed to meet this endpoint. Based on the 95% confidence interval of the difference in growth rates between active and placebo groups, we effectively can rule out a treatment effect of 55% or more for the slowing of the GA enlargement rate. Moreover, there was no apparent treatment effect when comparing the low-dose eculizumab regimen and high-dose regimen. However, we did detect a statistically significant correlation between the low-luminance deficit at baseline and the progression of GA over 6 months. Previously, Sunness et al[21] reported that low-luminance visual acuity deficits were correlated with the loss of visual acuity over 2 years. If we assume that the growth of GA eventually results in the loss of visual acuity over 2 years, then our results support their findings and demonstrate that this lowluminance visual acuity deficit correlates with the short-term expansion of GA. Moreover, our results suggest that the low-luminance deficit, a simple test of visual function, can detect central photoreceptor dysfunction even before the edge of GA extends through the foveal center and that this dysfunction correlates with the growth rate of GA. In clinical trials, this may serve as a useful way of identifying and stratifying eyes into groups at baseline that are more likely to progress. It is entirely possible that an experimental drug may have a different onset of action in eyes in which the GA is more likely to progress rapidly compared with the effect the drug might have in eyes that are progressing more slowly. Unfortunately, the COMPLETE study was powered inadequately to perform the type of subgroup analysis to detect such a differential treatment effect if one existed. However, we suggest that low-luminance deficit testing should be used in all future clinical trials of dry AMD.

Although our study may have been too small to detect a treatment effect that reduced the growth rate of GA to 55% or less of the normal growth rate, it is also possible that the drug had no effect on the growth rate because complement activation has no role in the growth of GA. We showed that there was no association between the number of at-risk genetic alleles and the growth of GA, and this result is consistent with recent publications showing no association between the progression rates of GA and these same at-risk alleles.[26,27] Although the genetics of AMD suggest a role for complement in the pathogenesis of AMD, it is entirely possible that complement plays a role in the earlier stages of the disease, rather than in the progression of GA, which is classified as an advanced form of AMD.[28]

Other possible explanations for the lack of a treatment effect could be that the dose of eculizumab was too low or the drug should have been delivered as a direct intravitreal

injection to achieve an adequate level of drug in the retina or the RPE. If complement inhibition was needed in the choroid to stop the growth of GA, then the dose of eculizumab should have been adequate; however, if the complement inhibition was needed in the eye, then the amount of drug delivered systemically was probably inadequate to penetrate the RPE. The rationale for using a systemic drug was based on the belief that complement activation in the choroid played an important role in the progression of dry AMD. Moreover, eculizumab already has been approved for systemic delivery, so systemic delivery of eculizumab was possible without additional safety studies. In contrast, the use of intravitreal eculizumab would have required extensive animal testing and a human, phase 1, dose-escalation safety study. Moreover, systemic delivery had certain advantages over frequent monthly injections of a drug into the eye. Because AMD is a bilateral disease, systemic therapy would be able to deliver the drug to both eyes with a single infusion. Based on previous studies of patients with paroxysmal nocturnal hemoglobinuria and atypical hemolytic uremic syndrome, we also knew that these dosing regimens of eculizumab achieved drug concentrations of more than 35 μg/ml in the peripheral blood, and at this concentration, systemic complement C5 is completely inhibited.[18,29,30] This was confirmed by the pharmacokinetic studies of our patients who received the drug. In particular, C5 activity decreased to less than 1% of the pretreatment average by week 2, demonstrating that therapeutic blood levels were reached and inhibition of C5 activity was achieved. Of note, the drug has systemic risks, most notably meningococcal meningitis, which can be prevented with the use of the meningococcal vaccine. However, now that this systemic approach has failed to show a dramatic treatment effect in our study, it is entirely possible that an intravitreal dosing strategy with eculizumab might have resulted in a different outcome.

Another possible explanation for why systemic C5 inhibition failed to show a treatment effect could be that C5 was the wrong complement target. C5 inhibition prevents only terminal complement activation, and by preserving more proximal complement function, such as production of C3a anaphylotoxin and C3b, complement-mediated damage could have continued. After all, polymorphisms in C3 have been associated with AMD, whereas there is no clear association between genetic variants in the *C5* gene and AMD.[11,31,32]

Two additional shortcomings of the study include the small sample size and its short duration. The sample size shortcoming would be even more of an issue if eculizumab was effective only in the smaller genetic subgroup of patients, such as the patients carrying the at-risk alleles in the CFH locus. In addition, it is possible that there may be a lag in the onset of a treatment effect, so studies would need to be run for at least 2 years to appreciate a treatment effect. However, this exploratory study was designed as a pilot investigation to determine if systemic therapy showed any suggestion of a treatment benefit. Based on the linearity of the growth rates and the lack of any suggestion of a treatment effect, it is unlikely that further systemic investigations with this drug will be undertaken to determine whether a smaller treatment effect could be observed because of the cost and the intensity of the treatment regimen.

It is possible that a different endpoint might have shown a treatment effect. Such an endpoint could be the ability of a treatment to decrease the conversion rates from dry to wet

AMD or the effect of the drug on the GA margins. These kinds of endpoint would require many more patients and a longer study duration. We chose lesion growth rate as the outcome variable for this trial because our goal was to use a Food and Drug Administration–approved endpoint to serve as a surrogate for the preservation of visual acuity, and the Food and Drug Administration agreed with our choice. Lesion area is a straightforward measurement that can be obtained with commercially available OCT software and can be performed easily with current imaging techniques. If we had demonstrated an effect of eculizumab on GA growth, that would have justified a large phase 3 study with acuity preservation as an outcome variable. In such a study, the imbalance in acuity we saw between our small randomized groups could have confounded interpretation; however, in the current study, with lesion growth as the outcome, it is immaterial. In addition to SD OCT measurements, we also assessed lesion area growth with Heidelberg and Topcon AF imaging and fluorescein angiography. These other methods did not suggest a different conclusion; however, presenting these data is outside the scope of this article and is the subject of one currently in preparation.

In summary, C5 inhibition with systemic eculizumab did not slow the growth rate of GA in the COMPLETE study. However, we did detect a statistically significant correlation between the low-luminance visual acuity deficit at baseline and the progression of GA over 6 months. Ongoing clinical trials using other intravitreal drugs that target C5 and factor D will determine whether complement inhibition for the treatment of GA is a viable treatment strategy in AMD.

Supplementary Material

Refer to Web version on PubMed Central for supplementary material.

Acknowledgments

Supported by Alexion Pharmaceuticals; the Macula Vision Research Foundation; Carl Zeiss Meditec, Inc., Dublin, California; an unrestricted grant from Research to Prevent Blindness, Inc., New York, New York; the National Eye Institute, National Institutes of Health, Bethesda, Maryland (core center grant no.: P30 EY014801 to the University of Miami); the Department of Defense, Washington, DC (grant no.: W81XWH-09-1-0675); the Jerome A. Yavitz Charitable Foundation; the Emma Clyde Hodge Memorial Foundation; the Florman Family Foundation, Inc.; and the Gemcon Family Foundation.

References

1. Lim LS, Mitchell P, Seddon JM, et al. Age-related macular degeneration. Lancet. 2012; 379:1728–38. [PubMed: 22559899]
2. Khandhadia S, Cipriani V, Yates JR, Lotery AJ. Age-related macular degeneration and the complement system. Immunobiology. 2012; 217:127–46. [PubMed: 21868123]
3. Anderson DH, Mullins RF, Hageman GS, Johnson LV. A role for local inflammation in the formation of drusen in the aging eye. Am J Ophthalmol. 2002; 134:411–31. [PubMed: 12208254]
4. van der Schaft TL, Mooy CM, de Bruijn WC, de Jong PT. Early stages of age-related macular degeneration: an immunofluorescence and electron microscopy study. Br J Ophthalmol. 1993; 77:657–61. [PubMed: 8218037]
5. Mullins RF, Aptsiauri N, Hageman GS. Structure and composition of drusen associated with glomerulonephritis: implications for the role of complement activation in drusen biogenesis. Eye (Lond). 2001; 15:390–5. [PubMed: 11450763]

6. Gehrs KM, Jackson JR, Brown EN, et al. Complement, age-related macular degeneration and a vision of the future. Arch Ophthalmol. 2010; 128:349–58. [PubMed: 20212207]
7. Edwards AO, Ritter R III, Abel KJ, et al. Complement factor H polymorphism and age-related macular degeneration. Science. 2005; 308:421–4. [PubMed: 15761121]
8. Hageman GS, Anderson DH, Johnson LV, et al. A common haplotype in the complement regulatory gene factor H (HF1/CFH) predisposes individuals to age-related macular degeneration. Proc Natl Acad Sci U S A. 2005; 102:7227–32. [PubMed: 15870199]
9. Haines JL, Hauser MA, Schmidt S, et al. Complement factor H variant increases the risk of age-related macular degeneration. Science. 2005; 308:419–21. [PubMed: 15761120]
10. Klein RJ, Zeiss C, Chew EY, et al. Complement factor H polymorphism in age-related macular degeneration. Science. 2005; 308:385–9. [PubMed: 15761122]
11. Yates JR, Sepp T, Matharu BK, et al. Genetic Factors in AMD Study Group. Complement C3 variant and the risk of age-related macular degeneration. N Engl J Med. 2007; 357:553–61. [PubMed: 17634448]
12. Gold B, Merriam JE, Zernant J, et al. AMD Genetics Clinical Study Group. Variation in factor B (BF) and complement component 2 (C2) genes is associated with age-related macular degeneration. Nat Genet. 2006; 38:458–62. [PubMed: 16518403]
13. Hageman GS, Hancox LS, Taiber AJ, et al. AMD Clinical Study Group. Extended haplotypes in the complement factor H (CFH) and CFH-related (CFHR) family of genes protect against age-related macular degeneration: characterization, ethnic distribution and evolutionary implications. Ann Med. 2006; 38:592–604. [PubMed: 17438673]
14. Age-Related Eye Disease Study 2 Research Group. Chew EY, SanGiovanni JP, Ferris FL III, et al. Lutein/zeaxanthin for the treatment of age-related cataract: AREDS2 randomized trial report no. 4. JAMA Ophthalmol. 2013; 131:843–50. [PubMed: 23645227]
15. Yehoshua Z, Rosenfeld PJ, Albini TA. Current clinical trials in dry AMD and the definition of appropriate clinical outcome measures. Semin Ophthalmol. 2011; 26:167–80. [PubMed: 21609230]
16. Zarbin MA, Rosenfeld PJ. Pathway-based therapies for age-related macular degeneration: an integrated survey of emerging treatment alternatives. Retina. 2010; 30:1350–67. [PubMed: 20924259]
17. Ross SC, Densen P. Complement deficiency states and infection: epidemiology, pathogenesis and consequences of neis-serial and other infections in an immune deficiency. Medicine (Baltimore). 1984; 63:243–73. [PubMed: 6433145]
18. Hillmen P, Young NS, Schubert J, et al. The complement inhibitor eculizumab in paroxysmal nocturnal hemoglobinuria. N Engl J Med. 2006; 355:1233–43. [PubMed: 16990386]
19. Maga TK, Nishimura CJ, Weaver AE, et al. Mutations in alternative pathway complement proteins in American patients with atypical hemolytic uremic syndrome. Hum Mutat. 2010; 31:E1445–60. [PubMed: 20513133]
20. Thomas TC, Rollins SA, Rother RP, et al. Inhibition of complement activity by humanized anti-C5 antibody and single-chain Fv. Mol Immunol. 1996; 33:1389–401. [PubMed: 9171898]
21. Sunness JS, Rubin GS, Broman A, et al. Low luminance visual dysfunction as a predictor of subsequent visual acuity loss from geographic atrophy in age-related macular degeneration. Ophthalmology. 2008; 115:1480–8. [PubMed: 18486216]
22. Yehoshua Z, Garcia Filho CA, Penha FM, et al. Comparison of geographic atrophy measurements from the OCT fundus image and the sub-RPE slab image. Ophthalmic Surg Lasers Imaging Retina. 2013; 44:127–32. [PubMed: 23510038]
23. Yehoshua Z, Rosenfeld PJ, Gregori G, et al. Progression of geographic atrophy in age-related macular degeneration imaged with spectral domain optical coherence tomography. Ophthalmology. 2011; 118:679–86. [PubMed: 21035861]
24. Li Y, Gregori G, Knighton RW, et al. Registration of OCT fundus images with color fundus photographs based on blood vessel ridges. Opt Express [serial online]. 2011; 19:7–16. Available at: http://www.opticsinfobase.org/oe/abstract.cfm?uri=oe-19-1-261.

25. Chen Y, Zeng J, Zhao C, et al. Assessing susceptibility to age-related macular degeneration with genetic markers and environmental factors. Arch Ophthalmol. 2011; 129:344–51. [PubMed: 21402993]
26. Klein ML, Ferris FL III, Francis PJ, et al. Progression of geographic atrophy and genotype in age-related macular degeneration. Ophthalmology. 2010; 117:1554–9. [PubMed: 20381870]
27. Scholl HP, Fleckenstein M, Fritsche LG, et al. CFH, C3 and ARMS2 are significant risk loci for susceptibility but not for disease progression of geographic atrophy due to AMD. PLoS One [serial online]. 2009; 4:e7418. Available at: http://www.plosone.org/article/info%3Adoi%2F10.1371%2Fjournal.pone.0007418.
28. Ferris FL III, Wilkinson CP, Bird A, et al. Beckman Initiative for Macular Research Classification Committee. Clinical classification of age-related macular degeneration. Ophthalmology. 2013; 120:844–51. [PubMed: 23332590]
29. Hill A. Eculizumab for the treatment of paroxysmal nocturnal hemoglobinuria. Clin Adv Hematol Oncol. 2005; 3:849–50. [PubMed: 16491626]
30. Hill A, Hillmen P, Richards SJ, et al. Sustained response and long-term safety of eculizumab in paroxysmal nocturnal hemoglobinuria. Blood. 2005; 106:2559–65. [PubMed: 15985537]
31. Baas DC, Ho L, Ennis S, et al. The complement component 5 gene and age-related macular degeneration. Ophthalmology. 2010; 117:500–11. [PubMed: 20022638]
32. Thakkinstian A, McKay GJ, McEvoy M, et al. Systematic review and meta-analysis of the association between complement component 3 and age-related macular degeneration: a HuGE review and meta-analysis. Am J Epidemiol. 2011; 173:1365–79. [PubMed: 21576320]

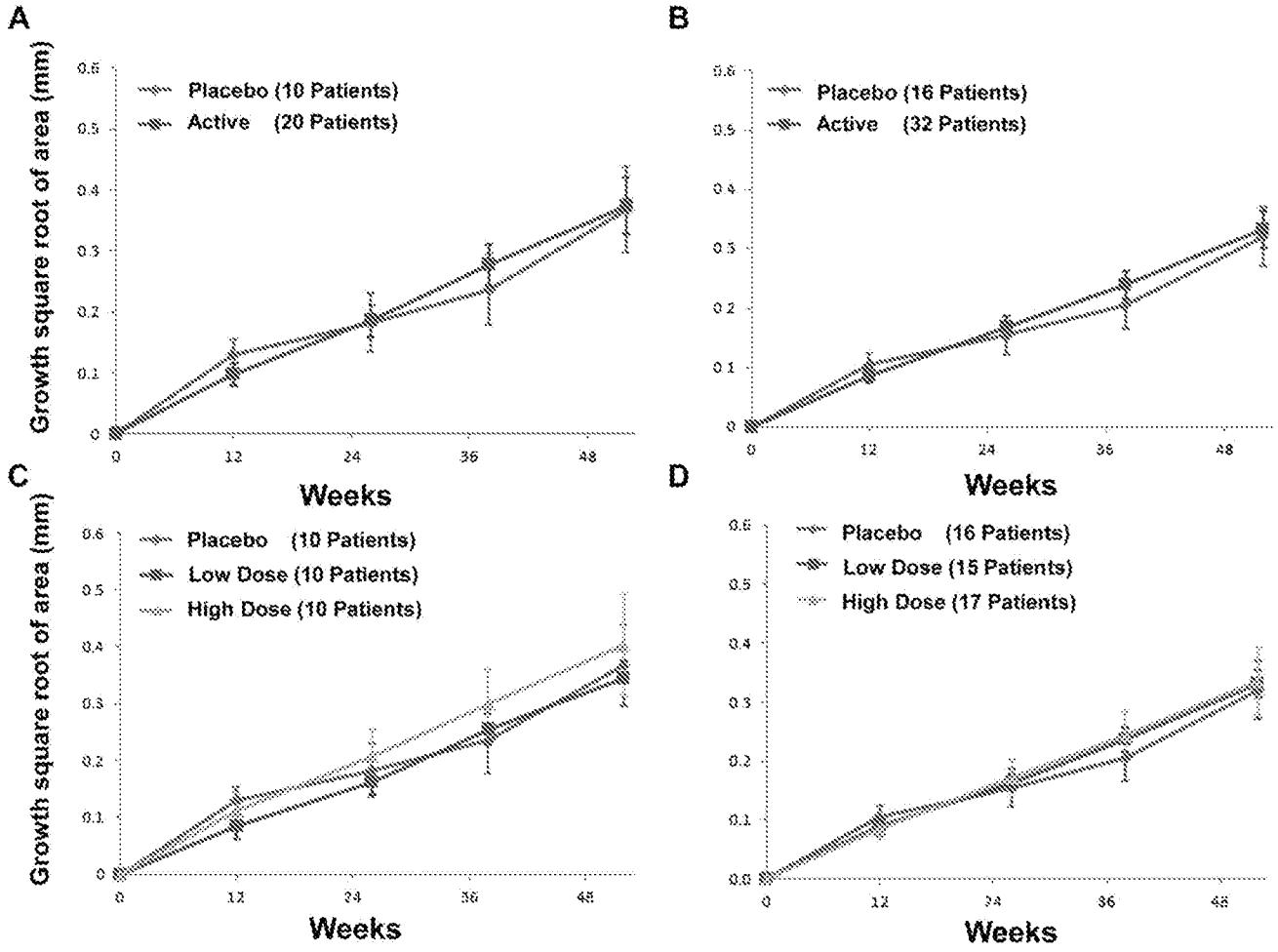

Figure 1.

Graphs showing the growth of geographic atrophy over 52 weeks in patients receiving the eculizumab versus placebo. Outcomes (**A** and **C**) for the study eyes and (**B** and **D**) the pooled study eyes and fellow eyes, outcomes for (A and B) the placebo and all the active treatment arms, outcomes for (**C** and **D**) the low-dose and high-dose treatment arms, as well as the placebo arms, for study eyes and fellow eyes that met inclusion criteria.

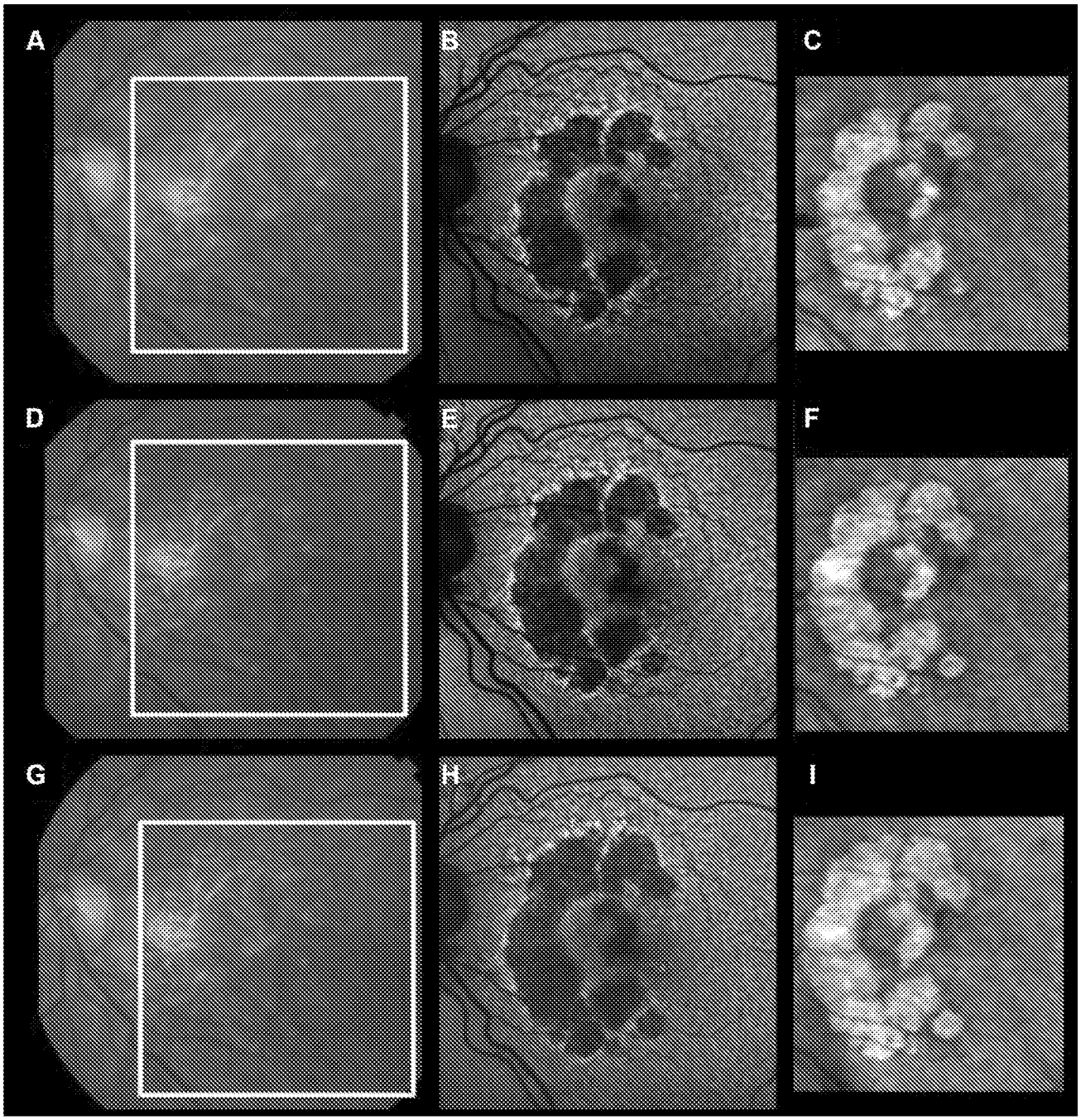

Figure 2.

Images from the left eye of a 73-year-old woman included in the low-dose group with growth in the area of geographic atrophy over 52 weeks. (**A**,**D**,**G**) Color fundus images obtained at baseline, 26 weeks, and 52 weeks, respectively. (**B**,**E**,**H**) Fundus autofluorescence images (Heidelberg Spectralis) obtained at baseline, 26 weeks, and 52 weeks, respectively. (**C**,**F**,**I**) Sub-retinal pigment epithelium slab en face image generated from spectral-domain optical coherence tomography datasets (Zeiss Cirrus) at baseline, 26

weeks, and 52 weeks, respectively. Area measurements were (**C**) 8.26 mm^2 at baseline, (**F**) 9.47 mm^2 at 26 weeks, and (**I**) 10.88 mm^2 at 52 weeks.

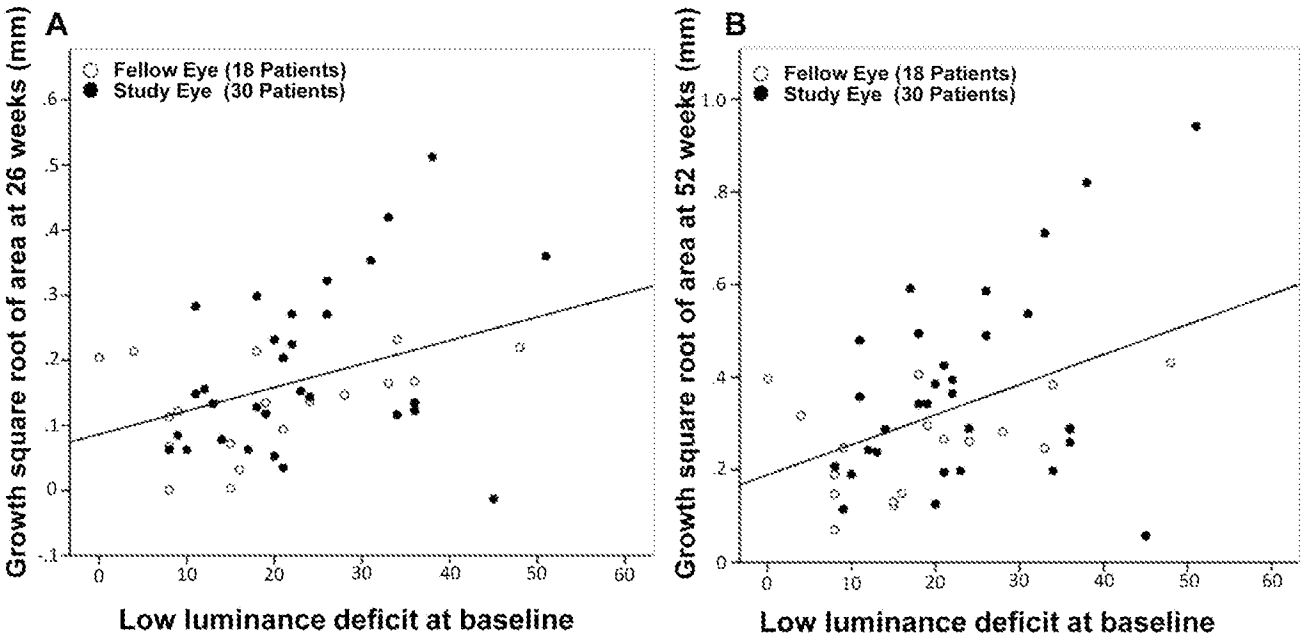

Figure 4.

Graph showing the relationship between low-luminance visual acuity deficit at baseline and growth of the square root of the area of geographic atrophy over (**A**) 26 weeks and (**B**) 52 weeks. Both study eyes (30 eyes) and fellow eyes (18 eyes) that met inclusion criteria are shown. For 26 weeks, r 0.38 and P ¼ 0.008; for 52 weeks, r = 0.41 and *P* = 0.004.

Table 1

Mean (Standard Deviation) Geographic Atrophy Enlargement (in Millimeters) by Treatment Group and Length of Follow-up

	Study Eyes						Study and Fellow Eyes					
				Only Eyes Randomized to Active Treatment						*Only Eyes Randomized to Active Treatment*		
Follow-up (wks)	***Placebo (n = 10)***	***Active (n = 20)***	***P Value****	***Low Dose (n = 10)***	***High Dose (n = 10)***	***P Value****	***Placebo (n = 16)***	***Active (n = 32)***	***P Value****	***Low Dose (n = 15)***	***High Dose (n = 17)***	***P Value****
26	0.18 (0.15)	0.19 (0.12)	0.96	0.16 (0.07)	0.21 (0.15)	0.40	0.16 (0.13)	0.17 (0.10)	0.70	0.16 (0.06)	0.17 (0.13)	0.82
52	0.37 (0.22)	0.37 (0.21)	0.93	0.35 (0.10)	0.40 (0.28)	0.55	0.32 (0.20)	0.33 (0.18)	0.72	0.33 (0.09)	0.33 (0.23)	0.95

*Two-sample *t* test.

JAMA Ophthalmology | Original Investigation

Efficacy and Safety of Lampalizumab for Geographic Atrophy Due to Age-Related Macular Degeneration

Chroma and Spectri Phase 3 Randomized Clinical Trials

Frank G. Holz, MD; Srinivas R. Sadda, MD; Brandon Busbee, MD; Emily Y. Chew, MD; Paul Mitchell, MD, PhD; Adnan Tufail, MD, FRCOphth; Christopher Brittain, MBBS; Daniela Ferrara, MD, PhD; Sarah Gray, PhD; Lee Honigberg, PhD; Jillian Martin, MD; Barbara Tong, PhD; Jason S. Ehrlich, MD, PhD; Neil M. Bressler, MD; for the Chroma and Spectri Study Investigators

IMPORTANCE Geographic atrophy (GA) secondary to age-related macular degeneration is a leading cause of visual disability in older individuals. A phase 2 trial suggested that lampalizumab, a selective complement factor D inhibitor, reduced the rate of GA enlargement, warranting phase 3 trials.

OBJECTIVE To assess the safety and efficacy of lampalizumab vs sham procedure on enlargement of GA.

DESIGN, SETTING, AND PARTICIPANTS Two identically designed phase 3 double-masked, randomized, sham-controlled clinical trials, Chroma and Spectri, enrolled participants from August 28, 2014, to October 6, 2016, at 275 sites in 23 countries. Participants were aged 50 years or older, with bilateral GA and no prior or active choroidal neovascularization in either eye and GA lesions in the study eye measuring 2.54 to 17.78 mm^2 with diffuse or banded fundus autofluorescence patterns.

INTERVENTIONS Participants were randomized 2:1:2:1 to receive 10 mg of intravitreous lampalizumab every 4 weeks, sham procedure every 4 weeks, 10 mg of lampalizumab every 6 weeks, or sham procedure every 6 weeks, through 96 weeks.

MAIN OUTCOMES AND MEASURES Safety and efficacy assessed as mean change from baseline in GA lesion area at week 48 from centrally read fundus autofluorescence images of the lampalizumab arms vs pooled sham arms, in the intent-to-treat population and by complement factor I–profile genetic biomarker.

RESULTS A total of 906 participants (553 women and 353 men; mean [SD] age, 78.1 [8.1] years) were enrolled in Chroma and 975 participants (578 women and 397 men; mean [SD] age, 77.9 [8.1] years) were enrolled in Spectri; 1733 of the 1881 participants (92.1%) completed the studies through 48 weeks. The adjusted mean increases in GA lesion area from baseline at week 48 were 1.93 to 2.09 mm^2 across all groups in both studies. Differences in adjusted mean change in GA lesion area (lampalizumab minus sham) were −0.02 mm^2 (95% CI, −0.21 to 0.16 mm^2; $P = .80$) for lampalizumab every 4 weeks in Chroma, 0.16 mm^2 (95% CI, 0.00-0.31 mm^2; $P = .048$) for lampalizumab every 4 weeks in Spectri, 0.05 mm^2 (95% CI, −0.13 to 0.24 mm^2; $P = .59$) for lampalizumab every 6 weeks in Chroma, and 0.09 mm^2 (95% CI, −0.07 to 0.24 mm^2; $P = .27$) for lampalizumab every 6 weeks in Spectri. No benefit of lampalizumab was observed across prespecified subgroups, including by complement factor I–profile biomarker. Endophthalmitis occurred after 5 of 12 447 injections (0.04%) or in 5 of 1252 treated participants (0.4%) through week 48.

CONCLUSIONS AND RELEVANCE In Chroma and Spectri, the largest studies of GA conducted to date, lampalizumab did not reduce GA enlargement vs sham during 48 weeks of treatment. Results highlight the substantial and consistent enlargement of GA, at a mean of approximately 2 mm^2 per year.

TRIAL REGISTRATION ClinicalTrials.gov Identifier: NCT02247479 and NCT02247531

JAMA Ophthalmol. 2018;136(6):666-677. doi:10.1001/jamaophthalmol.2018.1544
Published online May 2, 2018.

Supplemental content

CME Quiz at jamanetwork.com/learning

Author Affiliations: Author affiliations are listed at the end of this article.

Group Information: The Chroma and Spectri Study Investigators are listed at the end of this article.

Corresponding Author: Neil M. Bressler, MD, Johns Hopkins University School of Medicine, Maumenee 752, Johns Hopkins Hospital, 600 N Wolfe St, Baltimore, MD 21287 (nmboffice@jhmi.edu).

Geographic atrophy (GA), an advanced form of age-related macular degeneration (AMD), is a leading cause of visual disability in elderly individuals,[1-3] with prevalence increasing substantially among those older than 75 years of age.[2,3] No approved treatment slows or halts the progression of GA, or reverses the associated loss of macular tissue. In contrast, neovascular AMD, the other form of advanced AMD, is often treated successfully with intravitreous anti-vascular endothelial growth factor (anti-VEGF) medications.[4-6] Similarly, the Age-Related Eye Disease Study[7] and the Age-Related Eye Disease Study 2[8] reported that dietary supplements reduce the risk of developing advanced neovascular AMD but have no apparent effect on GA.

Occurrence and enlargement of GA lesions can result in substantial visual disability.[9-11] Because lesions typically first appear outside the fovea,[11-13] testing of best-corrected visual acuity (BCVA) may inadequately assess functional impairment in individuals with preserved foveal function despite loss of pericentral macula.[14] Other measures, including low-luminance visual acuity, reading speed, fundus-controlled microperimetry, and patient-reported outcomes, might assess impairment of visual function in patients with GA,[15,16] but these measures were not extensively used in earlier GA trials.

Although the pathophysiology of GA is incompletely understood, dysregulation of the complement cascade, a component of the innate immune system,[17,18] has been implicated in AMD[19,20] and in GA specifically.[21] Overall, genetic factors are estimated to account for 71% to 80% of the risk of advanced AMD,[22,23] and common genetic variants near *CFH*, *CFI*, *C3*, and *C2/CFB*, which act in the alternative complement pathway, may account for 57% of known disease risk variants.[20]

Given this genetic link, complement factor D was selected as a therapeutic target because it is the rate-limiting enzyme of the alternative complement pathway and is present in comparatively low abundance.[24-26] Lampalizumab is an antigen-binding fragment of a humanized monoclonal antibody that is directed against, and inhibits, complement factor D.[27,28] In a phase 2 trial, monthly intravitreous lampalizumab, 10 mg (n = 42), reduced the mean enlargement of GA lesion area from baseline to 18 months by 20% (80% CI, 4%-37%; $P = .12$) vs sham (n = 40).[29] In an exploratory subgroup analysis of carriers of the complement factor I (CFI) risk allele, monthly lampalizumab reduced the enlargement of GA by 44% vs sham.[29] No benefit was observed with lampalizumab treatment every 8 weeks.

To test phase 2 observations, we conducted 2 identically designed phase 3 randomized clinical trials, Chroma and Spectri, to assess the efficacy and safety of 10 mg of lampalizumab administered by intravitreal injection every 4 or 6 weeks vs sham treatment. These studies also prospectively investigated the prognostic and predictive diagnostic hypothesis of the CFI profile genetic biomarker. The 48-week primary outcome of these trials is presented herein.

Key Points

Question Does lampalizumab, a selective complement factor D inhibitor, reduce enlargement of lesions from geographic atrophy secondary to age-related macular degeneration?

Findings In 2 phase 3 randomized clinical trials (906 Chroma participants and 975 Spectri participants), no meaningful differences in the primary end point of mean change from baseline in geographic atrophy lesion area at week 48 were identified among eyes receiving 10-mg lampalizumab intravitreal injections either every 4 weeks or every 6 weeks vs sham.

Meaning These phase 3 trials showed that lampalizumab was ineffective as a treatment of geographic atrophy secondary to age-related macular degeneration.

Methods

The Chroma (trial protocol and statistical analysis plan are available in Supplement 1) and Spectri (trial protocol and statistical analysis plan are available in Supplement 2) studies were identically designed, phase 3 double-masked, multicenter, randomized, sham injection–controlled clinical trials at 131 (Chroma) and 144 (Spectri) sites in 23 countries. The studies adhered to the tenets of the Declaration of Helsinki[30] and were conducted in accordance with the International Conference on Harmonisation E6 Guidelines for Good Clinical Practice[31] and with applicable local, state, and federal laws. All sites received institutional review board or ethics committee approval before study initiation (eAppendix 1 in Supplement 3). Participants provided written informed consent. An independent data monitoring committee provided ongoing oversight. Key aspects of the study design are described herein and in eAppendix 2 in Supplement 3.

Study Population

Eligible participants (eTable 1 in Supplement 3) were aged 50 years or older with bilateral GA secondary to AMD and no evidence of active or prior choroidal neovascularization (CNV) nor previous treatment for CNV in either eye. Key study eye inclusion criteria were a total GA lesion size from 2.54 to 17.78 mm^2 (1-7 disc areas) measured on blue-light fundus autofluorescence, as confirmed by the reading center; perilesional banded or diffuse autofluorescence patterns; and an Early Treatment Diabetic Retinopathy Study (ETDRS) BCVA letter score of 49 or more (Snellen equivalent, 20/100 or better). Geographic atrophy lesions could be multifocal or unifocal, but at least 1 lesion had to be 1.27 mm^2 or larger (≥0.5 disc areas). In study eyes with a BCVA letter score of 79 or more (Snellen equivalent, 20/25 or better), at least 1 lesion was required within 250 μm of the foveal center. One eye was selected as the study eye. If both eyes were eligible, the eye with the poorer visual function as determined by the investigator and the patient was selected, followed by the eye with the

larger GA lesion. Participants were also evaluated at screening for CFI-profile genetic biomarker status (eTable 2 in Supplement 3).

Randomization

Participants were randomly assigned 2:1:2:1 to receive 10 mg of lampalizumab every 4 weeks, sham procedure every 4 weeks, 10 mg of lampalizumab every 6 weeks, and sham procedure every 6 weeks, via an interactive voice and web response system. In the sham groups, the eye was prepped in a manner similar to lampalizumab groups to preserve masking, including subconjunctival anesthesia. However, instead of an actual intravitreal injection, only the hub of a syringe was placed against the planned injection site. For randomization, a permuted block design was used, and participants were stratified by CFI-profile biomarker status, baseline BCVA ETDRS chart Snellen equivalent (20/50 or better vs worse than 20/50), sex, and eligibility for microperimetry. Participant numbers were capped by CFI-profile biomarker status to achieve a 3:2 ratio for CFI-positive to CFI-negative participants. Sham arms were pooled for analysis, resulting in a 1:1:1 ratio for lampalizumab every 4 weeks, lampalizumab every 6 weeks, and sham.

Study Treatment and Assessments

Treatment was administered to the study eye at randomization (day 1) and every 4 or 6 weeks (±5 days) thereafter through 44 weeks for groups receiving treatment every 4 weeks or 42 weeks for groups receiving treatment every 6 weeks, before week 48 primary efficacy assessments, continuing through 90 or 92 weeks per study design. Safety and ocular assessments, including BCVA, were performed at day 8 and at each subsequent visit on the same day as treatment. Verbatim descriptions of adverse events (AEs) were coded using *Medical Dictionary for Regulatory Activities*, version 20.0.[32] Fundus images of both eyes at screening and specified visits were evaluated at the Doheny Image Reading Center (Los Angeles, California). Autofluorescence pattern eligibility was determined by the GRADE Reading Center (Bonn, Germany). Additional visual function assessments were performed as scheduled.

Outcomes

The primary efficacy outcome was mean change in GA lesion area from baseline to week 48 measured by fundus autofluorescence, graded at the reading center. Secondary efficacy outcomes assessing visual function were exploratory at week 48, with formal statistical testing planned at week 96. Safety outcomes were assessed through a summary of ocular and nonocular AEs, deaths, results of serial electrocardiograms (selected participants), incidence of antidrug antibodies, and ocular assessments.

Statistical Analysis

For each study, a sample size of 188 CFI-positive participants per lampalizumab treatment arm and 94 CFI-positive participants per sham arm provided greater than 95% power to detect a difference in change in GA lesion area assuming a population difference of 1.45 mm^2 (approximately 40% reduction relative to sham control) and an SD of 2.51 in the CFI-positive population. A sample size of 124 CFI-negative participants per lampalizumab treatment arm and 62 CFI-negative participants per sham arm provided 80% power to detect a difference assuming a population difference of 0.66 mm^2 (approximately 40% reduction relative to control) and an SD of 1.68 in the CFI-negative population (eTable 3 in Supplement 3). Calculations were based on 2-sided t tests at the $\alpha = .0495$ level with the assumption of a 15% dropout rate by week 48.

The primary efficacy analysis for comparison between each lampalizumab arm and the pooled sham arms was performed on the intent-to-treat population (all randomized participants) using a mixed effects model repeated-measures model based on available data to week 48, with no imputation for missing data. Change-from-baseline analysis excluded participants without a baseline measurement or at least 1 post-baseline measurement. The primary analysis adjusted for baseline GA lesion area, subfoveal vs nonsubfoveal location, and multifocal vs nonmultifocal configuration; CFI-profile biomarker status; BCVA (better than vs worse than 20/50 Snellen equivalent); and sex. Preplanned subgroup analyses by CFI-profile biomarker were performed similarly, except with the model fit separately for each biomarker group and without biomarker status as a covariate. Hypothesis testing was performed at a 2-sided $\alpha = .0496$ level to account for a 0.0001 nominal penalty for each of 4 planned independent data monitoring committee unmasked data reviews occurring before the primary analysis.

To assess robustness of the primary efficacy results, additional analyses included the growth slope of the GA lesion area over 48 weeks, the change from baseline in the square root of the GA lesion area at week 48, and the percentage change from baseline in the GA lesion area at week 48. Exploratory analyses by prespecified clinical subgroup were performed using mixed effects model repeated-measures analysis similar to the primary efficacy analysis, excluding baseline covariates not relevant for the particular subgroup. Safety analyses were performed on the population that received 1 or more doses of lampalizumab or sham, grouped according to actual treatment received regardless of assignment. Analyses were performed using SAS, version 9.4 (SAS Institute), separately by study and based on pooled data from Chroma and Spectri, which included an additional covariate adjustment for study, as appropriate.

Results

Between August 28, 2014, and October 6, 2016, 906 Chroma participants and 975 Spectri participants were randomized to receive sham every 4 weeks (153 Chroma participants; 161 Spectri participants), lampalizumab every 4 weeks (298 Chroma participants; 330 Spectri participants), sham every 6 weeks (152 Chroma participants; 160 Spectri participants), or lampalizumab every 6 weeks (303 Chroma participants; 324 Spectri participants) (**Figure 1**). The baseline demographic characteristics of the participants (**Table 1** and eTables 4 and 5 in

Figure 1. CONSORT Flow Diagram for Chroma and Spectri Randomized Clinical Trials

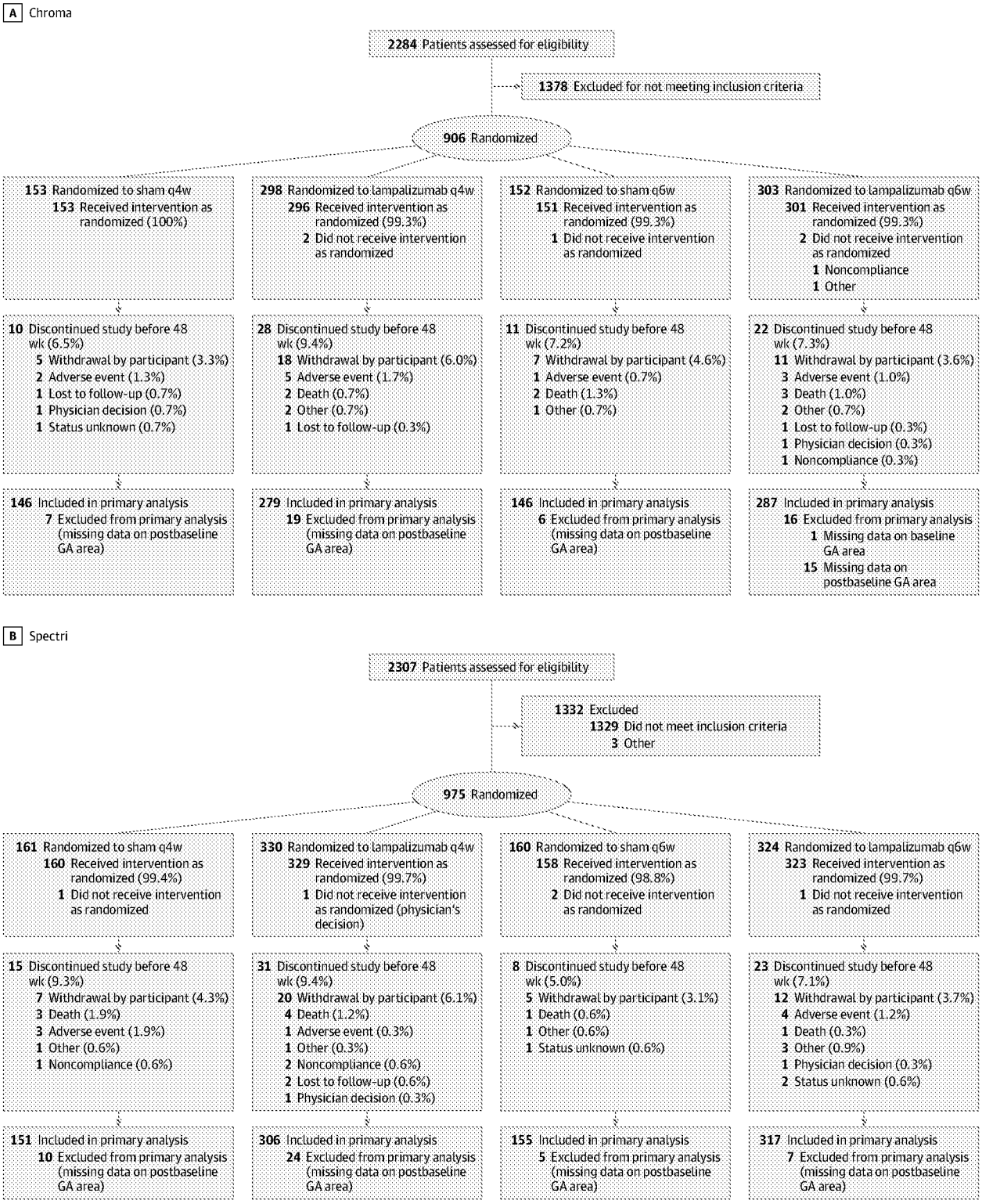

GA indicates geographic atrophy; q4w, every 4 weeks; and q6w, every 6 weeks.

Supplement 3) were well balanced across treatment groups (mean [SD] age of 78.0 [8.1] years, 1131 [60.1%] female, and 1827 [97.1%] white). The mean baseline GA lesion area was between 7.55 and 8.50 mm^2 across treatment groups. The mean

Table 1. Pooled Demographic and Baseline Characteristics of Chroma and Spectri Participants

Characteristic	Sham			Lampalizumab, 10 mg		
	q4w (n = 314)	q6w (n = 312)	Pooled (n = 626)	q4w (n = 628)	q6w (n = 627)	All (N = 1881)
Demographics						
Age, y						
Mean (SD)	78.1 (8.1)	78.0 (7.9)	78.0 (8.0)	77.4 (7.9)	78.5 (8.3)	78.0 (8.1)
Median (range)	78 (51-96)	78 (51-95)	78 (51-96)	78 (50-95)	80 (53-97)	79 (50-97)
Female sex, No. (%)	187 (59.6)	190 (60.9)	377 (60.2)	379 (60.4)	375 (59.8)	1131 (60.1)
White race, No. (%)[a]	306 (97.5)	302 (96.8)	608 (97.1)	608 (96.8)	611 (97.4)	1827 (97.1)
Tobacco use, No. (%)						
Never	153 (48.7)	136 (43.6)	289 (46.2)	293 (46.7)	290 (46.3)	872 (46.4)
Previous	147 (46.8)	155 (49.7)	302 (48.2)	295 (47.0)	295 (47.0)	892 (47.4)
Current	14 (4.5)	21 (6.7)	35 (5.6)	40 (6.4)	42 (6.7)	117 (6.2)
Study eye baseline characteristics						
GA area,[b] mm^2						
Mean (SD)	7.557 (3.884)	7.942 (4.025)	7.749 (3.956)	8.119 (3.904)	8.314 (4.249)	8.061 (4.044)
Median (range)	6.460 (1.58-17.56)	7.020 (2.61-30.56)	6.695 (1.58-30.56)	7.325 (2.54-17.74)	7.485 (2.29-22.19)	7.205 (1.58-30.56)
GA lesion contiguity, No. (%)[b]						
Multifocal	238 (75.8)	253 (81.1)	491 (78.4)	496 (79.0)	477 (76.2)	1464 (77.9)
Nonmultifocal	76 (24.2)	59 (18.9)	135 (21.6)	132 (21.0)	149 (23.8)	416 (22.1)
GA lesion location, No. (%)[b]						
Subfoveal	172 (54.8)	166 (53.2)	338 (54.0)	329 (52.4)	320 (51.1)	987 (52.5)
Nonsubfoveal	142 (45.2)	146 (46.8)	288 (46.0)	299 (47.6)	306 (48.9)	893 (47.5)
Hyperautofluorescence pattern, No. (%)						
Banded	12 (3.8)	11 (3.5)	23 (3.7)	22 (3.5)	35 (5.6)	80 (4.3)
Diffuse	301 (95.9)	301 (96.5)	602 (96.2)	605 (96.3)	591 (94.3)	1798 (95.6)
Not applicable	1 (0.3)	0	1 (0.2)	1 (0.2)	1 (0.2)	3 (0.2)
BCVA, mean (SD) letter score[c]	66.4 (10.0)	65.6 (9.6)	66.0 (9.8)	66.1 (9.8)	66.0 (9.9)	66.0 (9.9)
<64 (worse than 20/50)	115 (37.0)	118 (38.2)	233 (37.6)	253 (40.5)	247 (39.7)	733 (39.3)
≥64 (20/50 or better)	196 (63.0)	191 (61.8)	387 (62.4)	372 (59.5)	375 (60.3)	1134 (60.7)
LLVA, mean (SD) letter score[d]	36.6 (16.0)	36.2 (16.3)	36.4 (16.1)	36.5 (17.6)	36.0 (16.7)	36.3 (16.8)
Low-luminance deficit (BCVA − LLVA), mean (SD) letter score[e]	29.8 (16.1)	29.3 (15.9)	29.6 (16.0)	29.6 (16.3)	30.1 (15.7)	29.7 (16.0)

Abbreviations: BCVA, best-corrected visual acuity; GA, geographic atrophy; LLVA, low-luminance visual acuity; q4w, every 4 weeks; q6w, every 6 weeks.

[a] Of the total study population, race/ethnicity was identified as 0.5% (n = 9) American Indian or Alaskan Native, 0.3% Asian (n = 5), 0.05% (n = 1) black or African American, 0.1% (n = 2) Native Hawaiian or other Pacific Islander, 0.2% (n = 4) multiple, and 1.8% unknown (n = 33).

[b] For GA area, GA contiguity, and GA lesion location, there were 626 participants for the lampalizumab q6w arm.

[c] For BCVA, there were 311 participants for the sham q4w arm, 309 for the sham q6w arm, 625 for the lampalizumab q4w arm, and 622 for the lampalizumab q6w arm.

[d] For LLVA, there were 304 participants for the sham q4w arm, 305 for the sham q6w arm, 609 for the lampalizumab q4w arm, and 603 for the lampalizumab q6w arm.

[e] Low-luminance deficit = BCVA − LLVA; there were 303 participants for the sham q4w arm, 304 for the sham q6w arm, 609 for the lampalizumab q4w arm, and 603 for the lampalizumab q6w arm.

baseline BCVA letter score was between 65 and 66 (approximate Snellen equivalent, 20/50) in each group.

A total of 1733 of 1881 participants (92.1%) in Chroma and Spectri completed the first 48 weeks of the study, during which across treatment arms more than 76% of participants receiving treatment every 4 weeks received at least 12 injections (13 possible) and more than 85% of participants receiving treatment every 6 weeks received at least 8 injections (9 possible) (eAppendix 3 in Supplement 3).

After the Spectri primary analysis in September 2017, lampalizumab treatment was suspended for both studies at the sponsor's recommendation with the agreement of the chair of the independent data monitoring committee because the apparent lack of efficacy did not warrant continued intravitreal injections.

Efficacy of Lampalizumab Treatment

GA Enlargement

At week 48, the adjusted mean increase in GA lesion area from baseline was 1.93 to 2.09 mm^2 across all groups in both studies (**Table 2**, **Figure 2**A, and eFigure 1A-B in Supplement 3). The differences in the adjusted mean change of the GA lesion area (lampalizumab minus sham) were −0.02 mm^2 (95% CI, −0.21 to 0.16 mm^2; P = .80) for lampalizumab every 4 weeks in

Table 2. Change in GA Area From Baseline at Week 48 in Chroma and Spectri Pooled Intent-to-Treat Population[a]

Measure	Sham	Lampalizumab, 10 mg	
	Pooled (n = 598)	q4w (n = 596)	q6w (n = 603)
Change from baseline in GA area at 48 wk, mm^2			
Adjusted mean (SE)	1.984 (0.043)	2.055 (0.043)	2.054 (0.043)
Difference in means (vs sham pooled)		0.071	0.070
95% CI		-0.049 to 0.191	-0.050 to 0.190
Relative reduction, %		-3.6	-3.5
P value		.25	.25
Rate of change in GA area (growth slope) from baseline to 48 wk, $mm^2/365.25$ d[b]			
Adjusted mean slope (SE)	1.998 (0.045)	2.076 (0.045)	2.085 (0.045)
Difference in slopes (vs sham pooled)		0.078	0.086
95% CI		-0.048 to 0.204	-0.039 to 0.212
Relative reduction, %		-3.9	-4.3
P value		.22	.18
Change from baseline in square root of GA area at 48 wk, mm			
Adjusted mean (SE)	0.342 (0.007)	0.349 (0.007)	0.352 (0.007)
Difference in means (vs sham pooled)		0.006	0.010
95% CI		-0.013 to 0.026	-0.009 to 0.029
Relative reduction, %		-1.8	-2.9
P value		.53	.32
% Change from baseline in GA area at 48 wk			
Adjusted mean (SE)	30.032 (0.856)	29.546 (0.859)	30.815 (0.853)
Difference in means (vs sham pooled)		-0.486	0.783
95% CI		-2.864 to 1.891	-1.586 to 3.153
Relative reduction, %		1.6	-2.6
P value		.69	.52

Abbreviations: GA, geographic atrophy; q4w, every 4 weeks; q6w, every 6 weeks.

[a] Sample sizes shown in headers are the number of patients included in the mixed effects model repeated-measures analysis. All *P* values are 2-sided and calculated for the difference between means (lampalizumab minus sham).

[b] For growth slope mixed effects model repeated-measures analysis, there were 626 participants for the sham pooled arm, 628 for the lampalizumab q4w arm, and 626 for the lampalizumab q6w arm.

Chroma, 0.16 mm^2 (95% CI, 0.00-0.31 mm^2; $P = .048$ favoring sham) for lampalizumab every 4 weeks in Spectri, 0.05 mm^2 (95% CI, −0.13 to 0.24 mm^2; $P = .59$) for lampalizumab every 6 weeks in Chroma, and 0.09 mm^2 (95% CI, −0.07 to 0.24 mm^2; $P = .27$) for lampalizumab every 6 weeks in Spectri. Similarly, no benefit of lampalizumab over sham was observed in robustness assessments for the primary efficacy result (Table 2 and eTables 6 and 7 in Supplement 3). Furthermore, no benefit of lampalizumab over sham was observed for either CFI-profile biomarker subgroup (Figure 2 and eFigure 1 and eTable 8 in Supplement 3). Because baseline characteristics, follow-up, treatment adherence, and primary outcomes were similar in Chroma and Spectri, subsequent results report pooled data, with unpooled results in Supplement 3.

GA Enlargement by Clinical Subgroup

No consistent benefit of lampalizumab over sham was observed for any subgroup (eFigures 2-4 in Supplement 3).

Best-Corrected Visual Acuity

Best-corrected visual acuity declined from baseline to week 48 in all arms of both studies (eTable 9 and eFigure 5 in Supplement 3), with an adjusted mean BCVA letter score change of −4.9 (95% CI, −5.8 to −4.0) for sham treatment, −4.1 (95% CI, −5.0 to −3.2) for lampalizumab every 4 weeks, and −4.9 (95% CI, −5.8 to −3.9) for lampalizumab every 6 weeks.

Safety of Lampalizumab Treatment

No new ocular or nonocular safety signals beyond what would be anticipated with intravitreal injections were observed with lampalizumab through week 48 (eTables 10-19 in Supplement 3). The percentage of participants with ocular AEs and serious AEs (SAEs) were higher with lampalizumab compared with sham treatment, in alignment with expectations for intravitreal injections. Overall, 2.7% (17 of 619) of participants receiving the sham treatment, 6.2% (39 of 626) of participants receiving lampalizumab every 4 weeks, and 6.1% (38 of 626) of participants receiving lampalizumab every 6 weeks experienced 1 or more ocular SAEs.

Increases in intraocular pressure (IOP) were of interest because lampalizumab was injected as 0.1 mL, twice the volume of most intravitreal injections of anti-VEGF. Incidences of any IOP of 30 mm Hg or higher after injection, regardless of whether the events were considered SAEs, were reported in 0.3% (2 of 618) of participants receiving the sham treatment, 8.3% (52 of 625) of participants receiving lampalizumab every 4 weeks, and 5.6% (35 of 626) of participants receiving lampalizumab every 6 weeks. Increases in IOP considered to be SAEs were reported in 0.2% (1 of 619) of participants receiving the sham treatment, 3.2% (20 of 626) of the participants receiving lampalizumab every 4 weeks, and 2.6% (16 of 626) of participants receiving lampalizumab every 6 weeks. The mean preinjection IOP remained constant from baseline to

Figure 2. Adjusted Mean Change From Baseline in Geographic Atrophy (GA) Area Over Time From Baseline to 48 Weeks in Chroma and Spectri Pooled as Measured on Fundus Autofluorescence Imaging

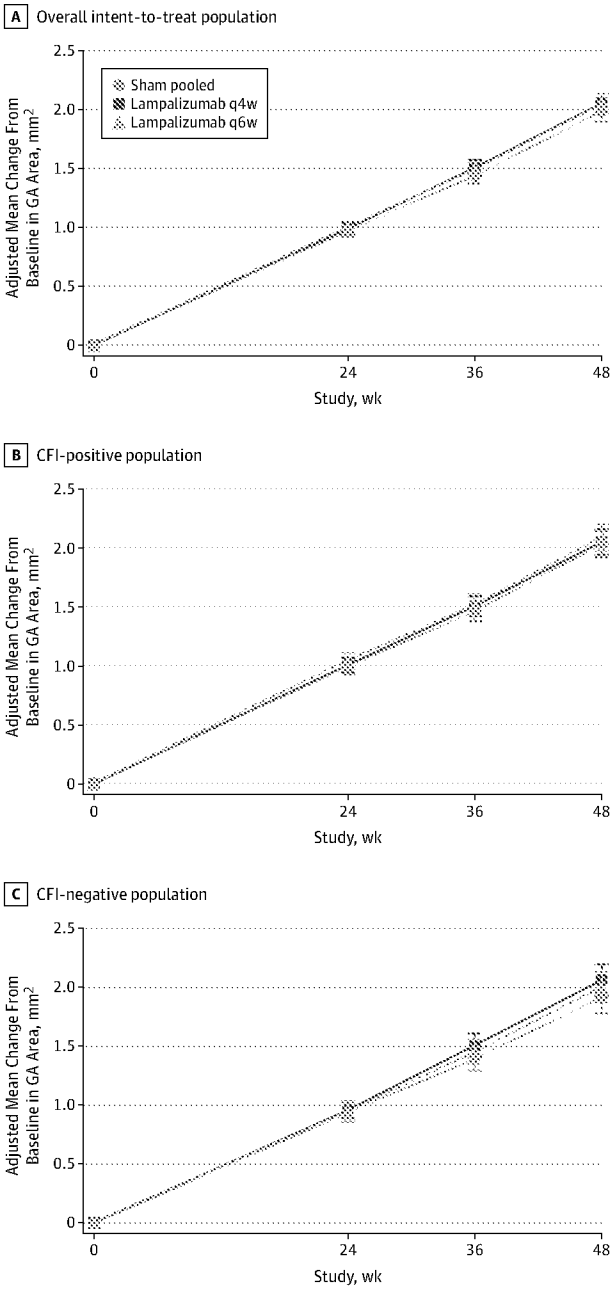

A, Overall intent-to-treat population. B, Complement factor I (CFI)–positive population. C, CFI-negative population. The mixed effects model repeated-measures analysis was adjusted for baseline GA area, baseline GA lesion location, baseline GA lesion contiguity, baseline best-corrected visual acuity category, sex, biomarker status (overall population only), and study. Error bars indicate 95% CIs. q4w Indicates every 4 weeks; q6w, every 6 weeks.

week 48 across all arms (eTable 18 and eFigure 6 in Supplement 3). Per investigator discretion, 3.1% (39 of 1252) of participants receiving lampalizumab also received paracentesis in the study eye owing to AEs of increased IOP or transient vision loss (5.6 procedures per 1000 injections).

Endophthalmitis occurred after 5 of 12 447 injections (0.4 events per 1000 injections [0.04%]) or in 5 of 1252 treated participants (0.4%) through week 48. Neovascular AMD was observed after randomization in 1.1% (7 of 619) of study eyes in the group receiving the sham treatment, 1.9% (12 of 626) of study eyes in the group receiving lampalizumab every 4 weeks, 1.9% (12 of 626) of study eyes in the group receiving lampalizumab every 6 weeks, 1.3% (8 of 619) of fellow eyes in the group receiving the sham treatment, 1.6% (10 of 626) of fellow eyes in the group receiving lampalizumab every 4 weeks, and 1.8% (11 of 626) of fellow eyes in the group receiving lampalizumab every 6 weeks, with no events of bilateral neovascular AMD (eTable 19 in Supplement 3).

Nonocular SAEs were reported in 16.6% (103 of 619) of participants in the group receiving the sham treatment, including 7 deaths; 19.2% (120 of 626) of participants in the group receiving lampalizumab every 4 weeks, including 7 deaths; and 13.9% (87 of 626) of participants in the group receiving lampalizumab every 6 weeks, including 5 deaths.

Discussion

To our knowledge, Chroma and Spectri were the largest, most comprehensive studies of GA conducted to date. In the primary analysis, lampalizumab did not reduce the enlargement of GA lesions from baseline at week 48 vs sham. Furthermore, no benefit of lampalizumab was suggested by the results of robustness assessments or subgroup analyses, including by CFI-profile biomarker. No new safety signals were observed with lampalizumab treatment, and incidences of endophthalmitis, increase in IOP, or other injection-related SAEs were low and consistent with those observed in studies of anti-VEGF.[5,6,33]

The Chroma and Spectri trials provide the largest cohorts to date of patients with bilateral GA and no CNV in either eye, with detailed documentation of anatomical and functional outcomes. The rates of progression of GA in Chroma and Spectri (approximately 2 mm^2 per year on average) were within the range of previous studies (approximately 0.53-2.6 mm^2 per year),[15] with differences across studies likely attributable to inclusion criteria reflected in the characteristics of each study cohort. In Chroma and Spectri, eligibility criteria included factors associated with faster GA progression, such as bilateral GA and banded or diffuse perilesional fundus autofluorescence patterns.[15] Consistent with prior studies,[15] Chroma and Spectri subgroup analyses demonstrated that larger baseline GA lesion area, multifocal configurations, and nonfoveal GA lesions are associated with faster rates of progression. This large data set, from 2 multicenter global trials conducted in 23 countries, is likely generalizable to the broader population of patients with GA who would meet the eligibility criteria of these trials and could serve as an important normative database for future studies and provide further insights into the natural history of GA.

The Chroma and Spectri cohorts experienced a notable decline in visual function, with a mean BCVA letter score loss of approximately 5 letters in 48 weeks. This finding underscores the potential burden of vision loss from GA.

The safety outcomes presented here can inform future trials through at least 1 year. Intravitreal injection volumes of 0.1 mL were associated with low rates of increased posttreatment IOP SAEs and no change in mean pretreatment IOP during 48 weeks, suggesting that this volume may be given safely within a trial setting. Also, Chroma and Spectri documented that new CNV in patients with bilateral GA occurred in less than 2% of study or fellow eyes. This finding is consistent with observational studies, which reported conversion rates of 2% at 2 years and 11% at 4 years in patients with bilateral GA and no baseline CNV,[34] and a conversion rate of 1.5% by 1 to 2 years in studies in which most patients had bilateral GA.[35] In contrast, for patients with CNV in 1 eye and GA in the other, much higher rates of CNV in the eye with GA have been reported (18% at 2 years[34] and 34%-49% at 4-5 years[34,36]), similar to conversion rates for eyes with large drusen or focal hyperpigmentations.[36,37] Thus, future GA trials must consider the effect of including participants with any history of CNV in either eye because its presence may confound the accurate measurement of the enlargement of GA lesions and affect visual function assessments.

The primary rationales for exploring complement inhibition in GA were the strong genetic linkage and the feasibility of clinical trials evaluating the enlargement of GA lesions. To date, 6 molecules that act as complement pathway inhibitors have entered clinical trials for GA, including APL-2 (target, C3), which met its primary end point in a phase 2 trial[38]; CLG-561 (target, properdin), currently in a phase 2 trial[39]; and avacincaptad pegol (target, C5),[40] currently in a phase 2b trial. Two other C5 inhibitors, one given systemically[41] and the other intravitreally,[42] were not effective in phase 2 trials. Taken together with the Chroma and Spectri results, it remains unclear whether the complement cascade is an appropriate intraocular therapeutic target for GA, at least through the alternative pathway via complement factor D or downstream in the cascade via C5. Geographic atrophy therapeutics investigating targets outside the complement cascade are also in development.

Although the CFI-profile biomarker was thought to be associated with faster progression of GA based on the Mahalo phase 2 trial of lampalizumab,[29] the much larger prospective analysis of Chroma and of Spectri does not support CFI-profile status as a genetic biomarker for progression of GA. This finding is consistent with other studies performed after the initiation of Chroma and Spectri, which also reported no association between CFI risk alleles and the rate of GA progression.[43-45] Although it is still not clear why such results were observed in Mahalo, in light of the results from Chroma and Spectri, one may hypothesize that they may have been related to a small sample size and may have occurred by chance.

Strengths and Limitations

There are several strengths and limitations of these studies that could affect the interpretation of the results. The randomization of a large cohort; duplication of results across 2 identically designed, multicenter, double-masked, randomized clinical trials; and good follow-up and adherence to the protocol make it less likely that confounding or bias affected these topline results. However, the results apply only to 48 weeks of treatment and may not apply to all cases of GA. Based on the inclusion and exclusion criteria of these trials, they may not apply to patients with smaller or larger lesions, unilateral GA, autofluorescence patterns other than banded or diffuse, eyes with current or prior CNV, GA from causes other than AMD, or earlier disease stages.

Conclusions

In 2 identically designed phase 3 trials, lampalizumab, a selective complement factor D inhibitor, did not reduce the enlargement of GA lesions vs sham. The results highlight both the potential burden of vision loss facing patients with bilateral GA and the substantial retinal tissue loss that occurs during 48 weeks. Further analysis of Chroma and Spectri, including genotype-phenotype correlations enabled by whole-genome sequencing, may yield additional insights into AMD pathophysiology and support future clinical trials.

ARTICLE INFORMATION

Accepted for Publication: March 25, 2018.

Published Online: May 2, 2018. doi:10.1001/jamaophthalmol.2018.1544

Open Access: This article is published under the JN-OA license and is free to read on the day of publication.

Author Affiliations: Department of Ophthalmology, University of Bonn, Bonn, Germany (Holz); Doheny Eye Institute, Los Angeles, California (Sadda); Department of Ophthalmology, University of California at Los Angeles (Sadda); Tennessee Retina, Nashville (Busbee); Division of Epidemiology and Clinical Applications, National Eye Institute, National Institutes of Health, Bethesda, Maryland (Chew); Department of Ophthalmology and Westmead Institute for Medical Research, University of Sydney, Sydney, Australia (Mitchell); Moorfields Eye Hospital, London, United Kingdom (Tufail); Genentech Inc, a Member of the Roche Group, South San Francisco, California (Brittain, Ferrara, Gray, Honigberg, Martin, Tong, Ehrlich); Johns Hopkins University School of Medicine, Baltimore, Maryland (Bressler); Editor, *JAMA Ophthalmology* (Bressler).

Author Contributions: Drs Gray and Bressler had full access to all the data in the study and take responsibility for the integrity of the data and the accuracy of the data analysis.
Study concept and design: Busbee, Chew, Mitchell, Brittain, Ferrara, Ehrlich, Bressler.
Acquisition, analysis, or interpretation of data: Holz, Sadda, Busbee, Chew, Tufail, Brittain, Ferrara, Gray, Honigberg, Martin, Tong, Ehrlich, Bressler.
Drafting of the manuscript: Busbee, Tufail, Brittain, Ferrara, Gray, Honigberg, Bressler.
Critical revision of the manuscript for important intellectual content: Holz, Sadda, Busbee, Chew, Mitchell, Brittain, Ferrara, Gray, Martin, Tong, Ehrlich, Bressler.
Statistical analysis: Gray, Martin, Tong.
Obtained funding: Ehrlich.
Administrative, technical, or material support: Brittain, Tong, Ehrlich.
Study supervision: Holz, Busbee, Mitchell, Brittain, Ferrara, Tong, Ehrlich, Bressler.

Conflict of Interest Disclosures: All authors have completed and submitted the ICMJE Form for Disclosure of Potential Conflicts of Interest. Dr Holz reported receiving consulting fees from Acucela, Allergan, Bayer, Genentech/Roche, GSK, Heidelberg Engineering, Merck, Novartis, and Thrombogenics. Dr Sadda reported serving as a consultant for Allergan, Carl Zeiss Meditec Inc, Centervue, F. Hoffmann-La Roche Ltd, Genentech Inc, Heidelberg Engineering, Iconic, Novartis, Optos PLC, and Thrombogenics; and receiving research support from Allergan, Carl Zeiss Meditec Inc, Genentech Inc, and Optos PLC. Dr Busbee reported serving as a consultant for Aerpio, Genentech Inc, and Valeant; and receiving royalties from Akorn. Dr Mitchell reported serving as a consultant for Abbott, Allergan, Bayer, Novartis, and Roche. Dr Tufail reported serving as a consultant for Allergan, Bayer, Genentech Inc, Genentech/Roche, GSK, Heidelberg Engineering, Novartis, and Thrombogenics; and receiving research support from Bayer and Novartis. Drs Brittain, Ferrara, Gray,

Honigberg, Martin, and Ehrlich are employees of Genentech Inc. Dr Tong reported being a former employee of Genentech Inc, and was an employee of Genentech Inc at the time of manuscript development. Dr Bressler reported serving as principal investigator of grants at Johns Hopkins University sponsored by the following entities (not including the National Institutes of Health): Bayer, Genentech Inc, Novartis, and Samsung. The Department of Ophthalmology, University of Bonn, has received nonfinancial support for supply of technical equipment by several imaging device manufacturers, including Centervue, Heidelberg Engineering, Optos, and Zeiss Meditec and has received research grants from Acucela, Alcon, Allergan, Bayer, Formycon, Genentech/Roche, Heidelberg Engineering, and Novartis. No other conflicts were reported.

Funding/Support: Funding was provided by F. Hoffmann-La Roche Ltd for third-party writing assistance, which was provided by Kathryn H. Condon, PhD, CMPP, Envision Pharma Group.

Role of the Funder/Sponsor: The funding source was involved in design and conduct of the study; collection, management, analysis, and interpretation of the data; preparation, review, or approval of the manuscript; and decision to submit the manuscript for publication.

Group Information: The Chroma Study Investigators include Federico Furno Sola, Grupo Laser Vision, Rosario, Argentina; Patricio Schlottmann, Organizacion Medica De Investigacion, Capital Federal, Argentina; Alberto Zambrano, Fundacion Zambrano, Caba, Argentina; Carlos Zeolite, Oftar, Mendoza, Argentina; Jennifer Arnold, Marsden Eye Research Centre, Parramatta, Australia; Mark Gillies, Save Sight Institute, Sydney, Australia; Alan Luckie, Eyeclinic Albury Wodonga, Albury, Australia; Paul Mitchell, Sydney West Retina, Westmead, Australia; Nicole Schneltzer, Kepler Universitätskliniken Gmbh-Med Campus Iii; Abt Für Augenheilkunde, Linz, Austria; Julie De Zaeytijd, Uz Gent, Gent, Belgium; Shelley Boyd, St Michael's Hospital, Toronto, Canada; Alan Cruess, Qeii-Hsc Department of Ophthalmology, Halifax, Canada; Peter Kertes, Sunnybrook Health Sciences Centre, Toronto, Canada; Laurent Lalonde, Institut De L'oeil Des Laurentides, Boisbriand, Canada; David Maberley, University of British Columbia, Vancouver, Canada; Caroline Laugesen, Sjællands Universitetshospital, Roskilde; Øjenafdelingen, Roskilde, Denmark; Bahram Bodaghi, Ch Pitie Salpetriere; Ophtalmologie, Paris, France; Salomon Yves Cohen, Centre Ophtalmologique; Imagerie et Laser, Paris, France; Catherine Francais, Centre Odeon; Exploration Ophtalmologique, Paris, France; Eric Souied, Chi De Creteil; Ophtalmologie, Creteil, France; Ramin Tadayoni, Hopital Lariboisiere; Ophtalmologie, Paris, France; Lebriz Altay, Universitätsklinikum Köln; Augenklinik, Köln, Germany; Nicole Eter, Universitätsklinikum Münster; Augenheilkunde, Münster, Germany; Nicolas Feltgen, Universitätsmedizin Göttingen Georg-August-Universität; Klinik Für Augenheilkunde, Göttingen, Germany; Carsten Framme, Medizinische Hochschule Hannover, Klinik Für Augenheilkunde, Hannover, Germany; Salvatore Grisanti, Universitätskliniikum Schleswig-Holstein, Campus Lübeck, Klinik Für Augenheilkunde, Lübeck, Germany; Frank Holz, Universitäts-Augenklinik Bonn, Bonn, Germany; Daniel Pauleikhoff, Augenabteilung Am St Franziskus-Hospital, Munster, Germany; András Seres, Budapest Retina Associates Kft., Budapest, Hungary; Attila Vajas, Debreceni Egyetem Klinikai Kozpont; Szemeszeti Klinika, Debrecem, Hungary; Balazs Varsanyi, Ganglion Medical Center, Pecs, Hungary; Francesco Boscia, Azienda Ospedaliero Universitaria Di Sassari; U. O. Oculistica, Sassari, Italy; Maria Cristina Parravano, Fondazione G. B. Bietti Per Lo Studio E. La Ricerca In Oftalmologia-Presidio Ospedaliero Britannico, Roma, Italy; Federico Ricci, Fondazione Ptv Policlinico Tor Vergata Di Roma; UOSD Patologie Renitiche, Roma, Italy; Francesco Viola, Fondazione IRCCS Ca' Granda Ospedale Maggiore Policlinico-Clinica Regina Elena; U. O. C. Oculistica, Milano, Italy; David Lozano Rechy, Macula Retina Consultores, Mexico, DF, Mexico; Virgilio Morales Canton, Hospital De La Ceguera Apec, Mexico, DF, Mexico; G. Dijkman, Leids Universitair Medisch Centrum, Leiden, Netherlands; Reinier Schlingemann, Academisch Medisch Centrum Universiteit Amsterdam, Amsterdam, Netherlands; Guillermo Reategui, Clinica Anglo Americana, Lima, Peru; Dorota Raczyńska, Optimum Profesorskie Centrum Okulistyki, Gdańsk, Poland; Bożena Romanowska-Dixon, Sp Zoz Szpital Uniwersytecki W Krakowie Oddział Kliniczny Okulistyki I Onkologii Okulistycznej, Krakow, Poland; Slawomir Teper, Gabinet Okulistyczny Prof Edward Wylegala, Katowice, Poland; Marek Kacerík, Fakultna Nemocnica Trencin Ocna Klinika, Trencin, Slovakia; Blandina Lipkova, Fakultna Nemocnica S Poliklinikou Zilina; Ocne Oddelenie, Zilina, Slovakia; Hedviga Mikova, Nemocnica Sv. Michala, AS, Bratislava, Slovakia; Javier Araiz, Instituto Clinico Quirurgico De Oftalmologia-Icqo, Bilbao, Spain; Luis Arias, Hospital Universitari De Bellvitge; Servicio De Oftalmologia, Hospitalet De Llobregat, Spain; Jorge Mataix, Fisabio. Fundación Oftalmologica Del Mediterraneo, Valencia, Spain; Jordi Mones, Institut De La Macula I La Retina, Barcelona, Spain; Javier Montero, Hospital Universitario Rio Hortega; Servicio De Oftalmologia, Valladolid, Spain; Laura Sararols, Hospital General De Catalunya, Sant Cugat Del Vallès, Spain; Stephan Michels, Stadtspital Triemli; Augenklinik, Zürich, Switzerland; Christopher Brand, Royal Hallamshire Hospital, Sheffield, UK; Baljean Dhillon, The Princess Alexandra Eye Pavilion, Edinburgh, UK; Anita Agarwal, Vanderbilt University, Nashville, Tennessee; Virgil Alfaro, Charleston Neuroscience Institute, Ladson, South Carolina; Brad Baker, Vitreo-Retinal Associates, PC, Worcester, Massachusetts; Brian Berger, Retina Research Center, Austin, Texas; Robert Bhisitkul, Ophthalmology, University of California San Francisco; Barbara Blodi, University of Wisconsin, Madison; David Boyer, Retina-Vitreous Associates Medical Group, Beverly Hills, California; H. Logan Brooks Jr, Southern Vitreoretinal Associates, Tallahassee, Florida; Stuart Burgess, Fort Lauderdale Eye Institute, Plantation, Florida; Brandon Busbee, Tennessee Retina PC, Nashville; Miguel Busquets, Associates in Ophthalmology, West Mifflin, Pennsylvania; David Callanan, Texas Retina Associates, Arlington; Clement Chan, Southern California Desert Retina Consultants, Palm Desert; Jeffrey Chang, Lahey Clinic Medical Center, Peabody, Massachusetts; Sanford Chen, Orange County Retina Medical Group, Santa Ana, California; James Combs, Eye Surgeons of Richmond Inc, Dba Virginia Eye Institute, Richmond; Dilsher Dhoot, California Retina Consultants, Bakersfield; Pravin Dugel, Retinal Research Institute LLC, Phoenix, Arizona; David Eichenbaum, Retina Vitreous Associates of Florida, Saint Petersburg; Richard Feist, University of Alabama at Birmingham Clinical Research Unit; Philip Ferrone, Long Island Vitreoretinal Consult, Great Neck, New York; Howard Fine, New Jersey Retina Research Foundation, Toms River; Jorge Fortun, Bascom Palmer Eye Institute, Palm Beach Gardens, Florida; Gregory A. Fox, Retina Associates, Shawnee Mission, Kansas; Arthur Fu, West Coast Retina Medical Group Inc, San Francisco, California; Ronald Gentile, New York Eye & Ear Infirmary, New York, New York; Ghassan Ghorayeb, West Virginia University Eye Institute, Morgantown; Manjot Gill, Northwestern Medical Group/Northwestern University, Chicago, Illinois; Victor Gonzalez, Valley Retina Institute PA, McAllen, Texas; Carmelina Gordon, Specialty Eye Institute, Jackson, Mississippi; Sunil Gupta, Retina Specialty Institute, Pensacola, Florida; Robert Hampton, Retina Vitreous Surgeons of Central New York, Syracuse; Jeffrey Heier, Ophthalmic Consultants of Boston, Boston, Massachusetts; Vrinda Hershberger, Florida Eye Associates, Melbourne; Patrick Higgins, Retina Center of New Jersey, Bloomfield; Darma Ie, Delaware Valley Retina Associates, Lawrenceville, New Jersey; Ricky Isernhagen, Retina Associates of Kentucky, Lexington; Randy Katz, Florida Eye Microsurgical Institute, Boynton Beach; Gregg Kokame, Retina Consultants of Hawaii, Aiea; Robert Kwun, Retina Associates of Utah, Salt Lake City; Paul Lee, Retina Consultants of Western New York, Orchard Park; Seong Lee, Strategic Clinical Research Group LLC, Willow Park, Texas; Sam Mansour, Virginia Retina Center, Warrenton; Dennis Marcus, Southeast Retina Center, Augusta, Georgia; Raj Maturi, Midwest Eye Institute Northside, Indianapolis, Indiana; Mark Michels, Retina Care Specialists, Palm Beach Gardens, Florida; Jeffrey Moore, Maine Eye Center, Portland; Jared Nielsen, Wolfe Eye Clinic, West Des Moines, Iowa; George Novalis, Retina Centers PC, Tucson, Arizona; Michael Ober, Retina Consultants of Michigan, Southfield; Karl Olsen, Retina Vitreous Consultants, Monroeville, Pennsylvania; Sunil Patel, Retina Research Institute of Texas, Abilene; Dante Pieramici, California Retina Consultants, Santa Barbara; Paul Raskauskas, National Ophthalmic Research Institute, Fort Myers, Florida; Soraya Rofagha, East Bay Retina Consultants, Oakland, California; Alan Ruby, Associated Retinal Consultants PC, Royal Oak, Michigan; Todd Schneiderman, Retina Center Northwest, Silverdale, Washington; Steven Schwartz, Jules Stein Eye Institute/University of California Los Angeles; Rajiv Shah, Wake Forest Baptist Health Eye Centre, Winston-Salem, North Carolina; Veeral Sheth, University Retina and Macula Associates PC, Oak Forest, Illinois; Lawrence Singerman, Retina Associates of Cleveland Inc, Beachwood, Ohio; Rishi Singh, Cleveland Clinic Foundation and Cole Eye Institute, Cleveland, Ohio; Raymond Sjaarda, Retina Specialists, Towson, Maryland; Glenn Stoller, Ophthalmic Consultants of Long Island, Lynbrook, New York; Robert Stoltz, Georgia Retina PC, Marietta; Ivan Suner, Retina Associates of Florida LLC, Tampa; Ali Tabassian, Retina Institute of Virginia, Richmond; Ryan Tarantola, Retina Specialty Institute, Pensacola, Florida; Allen Thach, Retina Consultants of Nevada, Henderson; Rafael Ufret-Vincenty, University of Texas Southwestern Medical Center at Dallas; Robert Wirthlin, Spokane

Eye Clinical Research, Spokane, Washington; Andre Witkin, Tufts Medical Center Research, Boston, Massachusetts; Robert Wong, Austin Retina Associates, Austin, Texas; Matthew Wood, Eye Surgical Associates, Lincoln, Nebraska; and Jeffrey Zheutlin, Vitreo-Retinal Associates, Grand Rapids, Michigan.

The Spectri Study Investigators include Arturo Alezzandrini, Oftalmos, Capital Federal, Argentina; Mauricio Martinez Cartier, Instituto De La Vision, Capital Federal, Argentina; Devinder Chauhan, Vision Eye Institute Eastern, Box Hill, Australia; Fred Chen, The Lions Eye Institute, Nedlands, Australia; Jagjit Gilhotra, Adelaide Eye and Retina Centre, Adelaide, Australia; Robyn Guymer, Royal Victorian Eye and Ear Hospital, East Melbourne, Australia; Anthony Kwan, Queensland Eye Institute, Brisbane, Australia; Ursula Schmidt-Erfurth, Medizinische Universität Wien; Universitätsklinik für Augenheilkunde und Optometrie, Vienna, Austria; Julie Jacob, Uz Leuven Sint Rafael, Leuven, Belgium; Laurence Postelmans, Chu Brugmann (Victor Horta), Brussels, Belgium; Michael Larsen, Glostrup Hospital, Øjenafdelingen, Forskningsafsnit Ø37, Glostrup, Denmark; Catherine Creuzot Garcher, Chu Bocage; Ophtalmologie, Dijon, France; Francois Devin, Centre Paradis Monticelli; Ophtalmologie, Marseille, France; Laurent Kodjikian, Hopital De La Croix Rousse; Ophtalmologie, Lyon Cedex, France; Jean Francois Korobelnik, Hopital Pellegrin; Ophtalmologie, Bordeaux, France; Saddek Mohand Said, CHNO des Quinze Vingts; Ophtalmologie, Paris, France; Michel Weber, Hopital Hotel Dieu Et Hme; Clinique Ophtalmologique, Nantes, France; Hansjurgen Agostini, Universitätsklinikum Freiburg, Klinik Für Augenheilkunde, Freiburg, Germany; Gerd Auffarth, Universitätsklinik Heidelberg; Augenklinik, Heidelberg, Germany; Ulrich Bartz-Schmidt, Universitätsklinikum Tübingen, Tübingen, Germany; Katharina Bell, Universitätsmedizin Der Johannes Gutenberg-Universität Mainz, Augenklinik Und Poliklinik, Mainz, Germany; Andreea Gamulescu, Universitätsklinikum Regensburg, Klinik & Poliklinik Für Augenheilkunde, Regensburg, Germany; Lars-Olof Hattenbach, Klinikum Der Stadt Ludwigshafen Am Rhein Ggmbh; Augenklinik, Ludwigshafen, Germany; Chris P. Lohmann, Klinikum Rechts der Isar der Tu München; Augenklinik, München, Germany; Armin Wolf, Lmu Klinikum der Universität, Augenklinik, München, Germany; Janos Nemeth, Semmelweis Egyetem Aok, Szemeszeti Klinika, Budapest, Hungary; Péter Vámosi, Peterfy Sandor Utcai Korhaz-Rendelointezet Es Baleseti Kozpont, Szemeszet Kr, Budapest, Hungary; Balazs Varsanyi, Ganglion Medical Center, Pecs, Hungary; Francesco Bandello, IRCCS Ospedale San Raffaele; U. O. Oculistica, Milano, Italy; Chiara Eandi, ASL To1 Presidio Ospedaliero Sperino Oftalmico, Torino, Italy; Paolo Lanzetta, AO Universitaria S. Maria Della Misericordia Di Udine; Clinica Oculistica, Udine, Italy; Massimo Nicolo, Universita' Degli Studi Di Genova-DiNOG; Clinica Oculistica, Genova, Italy; Giovanni Staurenghi, Asst Fatebenefratelli Sacco; Oculistica (Sacco), Milano, Italy; Gianni Virgili, Azienda Ospedaliero-Universitaria Careggi; SOD Oculistica, Firenze, Italy; Renata Garcia Franco, Instituto Mexicano De Oftalmologia I.A.P., Querétaro, Mexico; Juan Ramirez Estudillo, Hospital Nuestra Señora De La Luz, Mexico City, Mexico; Carel Hoyng, Radboud University Nijmegen Medical Centre; Ophthalmology, Nijmegen, Netherlands; Carlos Fernandez, Centro De Investigacion Oftalmolaser, Lima, Peru; Miguel Guzman, Tg Laser Oftalmica, Lima, Peru; Silvio Lujan, Mácula D&T, Lima, Peru; Ewa Herba, Szpital Specjalistyczny Nr 1; Oddzial Okulistyki, Bytom, Poland; Jozef Kaluzny, Oftalmika Sp Z. O. O., Bydgoszcz, Poland; Marta Misiuk-Hojło, Uniwersytecki Szpital Kliniczny; Klinika Okulistyki, Wrocław, Poland; Jerzy Nawrocki, Klinika Okulistyczna Jasne Błonia, Łódź, Poland; Angela Carneiro, Hospital De Sao Joao; Servico De Oftalmologia, Porto, Portugal; Joao Figueira, Espaco Medico Coimbra, Coimbra, Portugal; Rufino Silva, Aibili-Association for Innovation and Biomedical Research On Light, Coimbra, Portugal; Sara Vaz-Pereira, Hospital De Santa Maria; Servico De Oftalmologia, Lisboa, Portugal; Elmira Abdulaeva, Sahi "Republic Clinical Ophthalmological Hospial of Ministry of Heal of Tatarstan Republic", Kazan, Russian Federation; Valery Erichev, Fsbi "Scientific Research Institute of Eye Diseases" of Russian Academy of Medical Sciences, Moscow, Russian Federation; Andrey Zolotarev, St Educ Inst of High Prof Education "Samara State Medical University"; Chair of Ophathalmology, Samara, Russian Federation; Andrej Cernak, Univerzitna Nemocnica Bratislava, Nemocnica Sv Cyrila A. Metoda Ocna Klinika Szu a Unb, Bratislava, Slovakia; Marta Figueroa, Vissum Madrid Santa Hortensia, Madrid, Spain; Roberto Gallego-Pinazo, Hospital Universitario La Fe: Servicio De Oftalmologia, Valencia, Spain; Alfredo Garcia-Layana, Clinica Universitaria De Navarra; Servicio De Oftalmologia, Pamplona, Spain; Francisco Gomez Ulla, Instituto Oftalmologico Gomez Ulla, Santiago De Compostela, Spain; Rafael Navarro, Instituto De Microcirugia Ocular, Barcelona, Spain; Jose Manuel Ortiz, Hospital Perpetuo Socorro; Servicio De Oftalmología, Albacete, Spain; Ramon Torres Imaz, Hospital Universitario Clínico San Carlos; Servicio De Oftalmologia, Madrid, Spain; Anders Kvanta, St Eriks Eye Hospital, Stockholm, Sweden; Katja Hatz, Vista Klinik Binningen, Binningen, Switzerland; Sebastian Wolf, Inselspital Bern, Universitätsklinik Für Augenheilkunde, Bern, Switzerland; Bora Eldem, Hacettepe University Medical Faculty; Department of Ophthalmology, Ankara, Turkey; Nur Kir, Istanbul University Istanbul Medical Faculty; Department of Ophthalmology, Istanbul, Turkey; Jale Mentes, Ege University Medical Faculty; Department of Ophthalmology, Izmir, Turkey; Osman Saatci, Dokuz Eylul University Medical Faculty; Department of Ophthalmology, Izmir, Turkey; Gursel Yilmaz, Ankara Baskent University Medical Faculty; Department of Ophthalmology, Ankara, Turkey; Clare Bailey, Bristol Eye Hospital, Bristol, UK; Sanjiv Banerjee, University Hospital of Wales, Cardiff, UK; Andrew Browning, Royal Victoria Infirmary, Newcastle Upon Tyne, UK; Simona Esposti, Moorfields Eye Hospital NHS Foundation Trust, London, UK; Richard Gale, The York Hospital, York, UK; Faruque Ghanchi, Bradford Royal Infirmary, Bradford, UK; Tim Jackson, Kings College Hospital, London, UK; Andrew Lotery, Southampton General Hospital, Southampton, UK; Sajjad Mahmood, Macular Treatment Centre; Royal Eye Hospital, Manchester, UK; Quresh Mohamed, Gloucestershire Hospitals NHS Foundation Trust, Gloucester, UK; Niro Narendran, The Royal Wolverhampton Hospitals NHS Trust, Wolverhampton, UK; Ian Pearce, Royal Liverpool University Hospital; St Paul's Clinical Eye Research Centre, Liverpool, UK; Michael Williams, Royal Victoria Hospital, Belfast, UK; Prema Abraham, Black Hills Regional Eye Institute, Rapid City, South Dakota; Gary Abrams, Kresge Eye Institute, Detroit, Michigan; Sean Adrean, Retina Consultants of Orange County, Fullerton, California; Virgil Alfaro, Charleston Neuroscience Institute, Ladson, South Carolina; Andrew Antoszyk, Charlotte Eye Ear Nose & Throat Associates, Charlotte, North Carolina; Carl Baker, Paducah Retinal Center, Paducah, Kentucky; Richard Breazeale, Southeastern Retina Associates Chattanooga, Chattanooga, Tennessee; William Z. Bridges Jr, West Carolina Retinal Associates PA, Asheville, North Carolina; H. Logan Brooks Jr, Southern Vitreoretinal Associates, Tallahassee, Florida; David M. Brown, Retina Consultants of Houston, Houston, Texas; Jorge Calzada, Charles Retina Institute, Germantown, Tennessee; Peter Campochiaro, Wilmer Eye Institute, Baltimore, Maryland; Nauman Chaudhry, Retina Group of New England, New London, Connecticut; Lloyd Clark, Palmetto Retina Center, West Columbia, South Carolina; Brian Connolly, Retina Assoc of Western New York, Rochester; Karl Csaky, Texas Retina Associates, Dallas; Diana Do, University of Nebraska Medical Center Truhlsen Eye Institute, Omaha; Richard Dreyer, Retina Northwest, Portland, Oregon; William Durant, Sierra Eye Associates, Reno, Nevada; Alexander Eaton, Retina Health Center, Ft Myers, Florida; David Eichenbaum, Retina Vitreous Associates of Florida, St Petersburg; Leonard Feiner, Retina Associates of New Jersey, Teaneck; Henry Ferreyra, University of California San Diego Shiley Eye Center, La Jolla; Christina Flaxel, Oregon Health and Science University and Casey Eye Institute, Portland; Scott Foxman, Retinal & Ophthalmic Consultants PC, Northfield, New Jersey; K. Bailey Freund, Vitreous-Retina-Macula, New York, New York; Christine R. Gonzales, Retina & Vitreous Center of Southern Oregon, Ashland; Alan Gordon, Associated Retina Consultants, Phoenix, Arizona; Larry Halperin, Retina Group of Florida, Ft Lauderdale; Allen Ho, Mid-Atlantic Retina, Huntingdon Valley, Pennsylvania; Nancy Holekamp, Pepose Vision Institute, Chesterfield, Missouri; Deeba Husain, Massachusetts Eye and Ear Infirmary, Boston; Nieraj Jain, Emory University, Atlanta, Georgia; Cameron Javid, Retina Associates Southwest PC, Tucson, Arizona; Mark Johnson, University of Michigan, Kellogg Eye Center, Ann Arbor; Mark Johnson, Retina Group of Washington, Chevy Chase, Maryland; Szilard Kiss, New York Weil Cornell Medical Center, New York, New York; Eleonora Lad, Duke University Eye Center, Vitreoretinal, Durham, North Carolina; Theodore Leng, Byers Eye Institute at Stanford, Palo Alto, California; Mimi Liu, Colorado Retina Associates PC, Golden; Nikolas London, Retina Consultants, San Diego, California; Brian Madow, University of South Florida, Tampa; Daniel Miller, Cincinnati Eye Institute, Cincinnati, Ohio; Lawrence Morse, University of California, Davis, Eye Center, Sacramento; Jared Nielsen, Wolfe Eye Clinic, West Des Moines, Iowa; Matthew Ohr, Ohio State University Eye Physicians & Surgeons, Columbus; Scott Oliver, University of Colorado, Aurora; Sunil Patel, Retina Research Institute of Texas, Abilene; Joel Pearlman, Retinal Consultants Medical Group, Sacramento, California; Dante Pieramici, California Retina Consultants, Santa Barbara; Subhransu K. Ray, Bay Area Retina Associates, Walnut Creek, California; Carl Regillo, Mid Atlantic Retina, Philadelphia, Pennsylvania; Robert Rosa, Scott and White Hospital, Temple, Texas; Philip Rosenfeld,

Bascom Palmer Eye Institute, Miami, Florida; David Saperstein, Vitreoretinal Associates of Washington, Bellevue; David Sarraf, Jules Stein Eye Institute/University of California Los Angeles; Yevgeniy Shildkrot, University of Virginia Ophthalmology, Charlottesville; Raymond Sjaarda, Retina Specialists, Towson, Maryland; Eric Suan, The Retina Care Center, Baltimore, Maryland; Paul Weishaar, Vitreo Retinal Consultants, Wichita, Kansas; Mark Wieland, Northern California Retina Vitreous Associates, Mountain View; David Williams, Vitreoretinal Surgery, Edina, Minnesota; Jonathan Williams, Retina Consultants of Southern Colorado, Colorado Springs; and Charles C. Wykoff, Retina Consultants of Houston, The Woodlands, Texas.

Disclaimer: Dr Bressler is the editor of *JAMA Ophthalmology* but was not involved in the editorial review or the decision to accept the manuscript for publication.

Previous Presentation: This study was presented at the 2018 Association for Research in Vision and Ophthalmology Annual Meeting; May 2, 2018; Honolulu, Hawaii.

REFERENCES

1. Flaxman SR, Bourne RRA, Resnikoff S, et al; Vision Loss Expert Group of the Global Burden of Disease Study. Global causes of blindness and distance vision impairment 1990-2020: a systematic review and meta-analysis. *Lancet Glob Health*. 2017;5(12):e1221-e1234.

2. Rudnicka AR, Kapetanakis VV, Jarrar Z, et al. Incidence of late-stage age-related macular degeneration in American whites: systematic review and meta-analysis. *Am J Ophthalmol*. 2015;160(1):85-93.e3.

3. Wong WL, Su X, Li X, et al. Global prevalence of age-related macular degeneration and disease burden projection for 2020 and 2040: a systematic review and meta-analysis. *Lancet Glob Health*. 2014;2(2):e106-e116.

4. Brown DM, Kaiser PK, Michels M, et al; ANCHOR Study Group. Ranibizumab versus verteporfin for neovascular age-related macular degeneration. *N Engl J Med*. 2006;355(14):1432-1444.

5. Heier JS, Brown DM, Chong V, et al; VIEW 1 and VIEW 2 Study Groups. Intravitreal aflibercept (VEGF trap-eye) in wet age-related macular degeneration. *Ophthalmology*. 2012;119(12):2537-2548.

6. Rosenfeld PJ, Brown DM, Heier JS, et al; MARINA Study Group. Ranibizumab for neovascular age-related macular degeneration. *N Engl J Med*. 2006;355(14):1419-1431.

7. Age-Related Eye Disease Study Research Group. A randomized, placebo-controlled, clinical trial of high-dose supplementation with vitamins C and E, beta carotene, and zinc for age-related macular degeneration and vision loss: AREDS report no. 8. *Arch Ophthalmol*. 2001;119(10):1417-1436.

8. Age-Related Eye Disease Study 2 Research Group. Lutein + zeaxanthin and omega-3 fatty acids for age-related macular degeneration: the Age-Related Eye Disease Study 2 (AREDS2) randomized clinical trial. *JAMA*. 2013;309(19):2005-2015.

9. Brown JC, Goldstein JE, Chan TL, Massof R, Ramulu P; Low Vision Research Network Study Group. Characterizing functional complaints in patients seeking outpatient low-vision services in the United States. *Ophthalmology*. 2014;121(8):1655-62.e1.

10. Sunness JS, Rubin GS, Applegate CA, et al. Visual function abnormalities and prognosis in eyes with age-related geographic atrophy of the macula and good visual acuity. *Ophthalmology*. 1997;104(10):1677-1691.

11. Sunness JS, Rubin GS, Zuckerbrod A, Applegate CA. Foveal-sparing scotomas in advanced dry age-related macular degeneration. *J Vis Impair Blind*. 2008;102(10):600-610.

12. Klein R, Meuer SM, Knudtson MD, Klein BE. The epidemiology of progression of pure geographic atrophy: the Beaver Dam Eye Study. *Am J Ophthalmol*. 2008;146(5):692-699.

13. Lindblad AS, Lloyd PC, Clemons TE, et al; Age-Related Eye Disease Study Research Group. Change in area of geographic atrophy in the Age-Related Eye Disease Study: AREDS report number 26. *Arch Ophthalmol*. 2009;127(9):1168-1174.

14. Sunness JS. Reading newsprint but not headlines: pitfalls in measuring visual acuity and color vision in patients with bullseye maculopathy and other macular scotomas. *Retin Cases Brief Rep*. 2008;2(1):83-84.

15. Fleckenstein M, Mitchell P, Freund KB, et al. The progression of geographic atrophy secondary to age-related macular degeneration. *Ophthalmology*. 2018;125(3):369-390.

16. Sadda SR, Chakravarthy U, Birch DG, Staurenghi G, Henry EC, Brittain C. Clinical endpoints for the study of geographic atrophy secondary to age-related macular degeneration. *Retina*. 2016;36(10):1806-1822.

17. Ricklin D, Hajishengallis G, Yang K, Lambris JD. Complement: a key system for immune surveillance and homeostasis. *Nat Immunol*. 2010;11(9):785-797.

18. Walport MJ. Complement: second of two parts. *N Engl J Med*. 2001;344(15):1140-1144.

19. Ambati J, Atkinson JP, Gelfand BD. Immunology of age-related macular degeneration. *Nat Rev Immunol*. 2013;13(6):438-451.

20. Fritsche LG, Fariss RN, Stambolian D, Abecasis GR, Curcio CA, Swaroop A. Age-related macular degeneration: genetics and biology coming together. *Annu Rev Genomics Hum Genet*. 2014;15:151-171.

21. Boyer DS, Schmidt-Erfurth U, van Lookeren Campagne M, Henry EC, Brittain C. The pathophysiology of geographic atrophy secondary to age-related macular degeneration and the complement pathway as a therapeutic target. *Retina*. 2017;37(5):819-835.

22. Seddon JM, Cote J, Page WF, Aggen SH, Neale MC. The US twin study of age-related macular degeneration: relative roles of genetic and environmental influences. *Arch Ophthalmol*. 2005;123(3):321-327.

23. Seddon JM, Silver RE, Kwong M, Rosner B. Risk prediction for progression of macular degeneration: 10 common and rare genetic variants, demographic, environmental, and macular covariates. *Invest Ophthalmol Vis Sci*. 2015;56(4):2192-2202.

24. Lesavre PH, Müller-Eberhard HJ. Mechanism of action of factor D of the alternative complement pathway. *J Exp Med*. 1978;148(6):1498-1509.

25. Volanakis JE, Narayana SV. Complement factor D, a novel serine protease. *Protein Sci*. 1996;5(4):553-564.

26. Volanakis JE, Barnum SR, Giddens M, Galla JH. Renal filtration and catabolism of complement protein D. *N Engl J Med*. 1985;312(7):395-399.

27. Katschke KJ Jr, Wu P, Ganesan R, et al. Inhibiting alternative pathway complement activation by targeting the factor D exosite. *J Biol Chem*. 2012;287(16):12886-12892.

28. Loyet KM, Good J, Davancaze T, et al. Complement inhibition in cynomolgus monkeys by anti-factor D antigen-binding fragment for the treatment of an advanced form of dry age-related macular degeneration. *J Pharmacol Exp Ther*. 2014;351(3):527-537.

29. Yaspan BL, Williams DF, Holz FG, et al; MAHALO Study Investigators. Targeting factor D of the alternative complement pathway reduces geographic atrophy progression secondary to age-related macular degeneration. *Sci Transl Med*. 2017;9(395):eaaf1443. doi:10.1126/scitranslmed.aaf1443

30. World Medical Association. WMA Declaration of Helsinki—ethical principles for medical research involving human subjects. https://www.wma.net/policies-post/wma-declaration-of-helsinki-ethical-principles-for-medical-research-involving-human-subjects/. Accessed October 25, 2017.

31. International Conference on Harmonisation of Technical Requirements for Registration of Pharmaceuticals for Human Use. ICH harmonised tripartite guideline: guideline for good clinical practice E6(R1). https://www.ich.org/fileadmin/Public_Web_Site/ICH_Products/Guidelines/Efficacy/E6/E6_R1_Guideline.pdf. Published June 10, 1996. Accessed April 12, 2018.

32. Medical Dictionary for Regulatory Activities, version 20.0. https://www.meddra.org. Published March 2017. Accessed April 12, 2018.

33. Busbee BG, Ho AC, Brown DM, et al; HARBOR Study Group. Twelve-month efficacy and safety of 0.5 mg or 2.0 mg ranibizumab in patients with subfoveal neovascular age-related macular degeneration. *Ophthalmology*. 2013;120(5):1046-1056.

34. Sunness JS, Gonzalez-Baron J, Bressler NM, Hawkins B, Applegate CA. The development of choroidal neovascularization in eyes with the geographic atrophy form of age-related macular degeneration. *Ophthalmology*. 1999;106(5):910-919.

35. Holz FG, Bindewald-Wittich A, Fleckenstein M, Dreyhaupt J, Scholl HP, Schmitz-Valckenberg S; FAM-Study Group. Progression of geographic atrophy and impact of fundus autofluorescence patterns in age-related macular degeneration. *Am J Ophthalmol*. 2007;143(3):463-472.

36. Macular Photocoagulation Study Group. Risk factors for choroidal neovascularization in the second eye of patients with juxtafoveal or subfoveal choroidal neovascularization secondary to age-related macular degeneration. *Arch Ophthalmol*. 1997;115(6):741-747.

37. Solomon SD, Jefferys JL, Hawkins BS, Bressler NM, Bressler SB; Submacular Surgery Trials Research Group. Risk factors for second eye progression to advanced age-related macular

degeneration: SST report No. 21 Submacular Surgery Trials Research Group. *Retina*. 2009;29(8):1080-1090.

38. Apellis Pharmaceuticals. Apellis Pharmaceuticals announces that APL-2 met its primary endpoint in a phase 2 study in patients with geographic atrophy, an advanced form of age-related macular degeneration. http://apellis.com/pdfs/Press%20Release%20FILLY%2012%20Month%20Results%20FINAL%20FINAL%2017082З.pdf. Published August 24, 2017. Accessed February 16, 2018.

39. ClinicalTrials.gov. CLG561 proof-of-concept study as a monotherapy and in combination with LFG316 in subjects with geographic atrophy (GA). https://clinicaltrials.gov/ct2/show/NCT02515942. Accessed December 6, 2017.

40. Ophthotech. Ophthotech provides update on Zimura complement programs for treatment of eye diseases. http://investors.ophthotech.com/news-releases/news-release-details/ophthotech-provides-update-zimurar-complement-programs-treatment. Published September 19, 2017. Accessed February 16, 2018.

41. Yehoshua Z, de Amorim Garcia Filho CA, Nunes RP, et al. Systemic complement inhibition with eculizumab for geographic atrophy in age-related macular degeneration: the COMPLETE study. *Ophthalmology*. 2014;121(3):693-701.

42. Zamiri P. Complement C5 inhibition for AMD. Paper presented at: Angiogenesis; February 6, 2016; Miami, FL.

43. Wurzelmann JI, Lopez FJ, Fries M, et al. SNPs associated with complement factor I do not predict 4-month lesion growth rate in geographic atrophy [ARVO abstract]. *Invest Ophthalmol Vis Sci*. 2015;56(7):2850.

44. Yehoshua Z, de Amorim Garcia Filho CA, Nunes RP, et al. Association between growth of geographic atrophy and the complement factor I locus. *Ophthalmic Surg Lasers Imaging Retina*. 2015;46(7):772-774.

45. Grassmann F, Fleckenstein M, Chew EY, et al. Clinical and genetic factors associated with progression of geographic atrophy lesions in age-related macular degeneration. *PLoS One*. 2015;10(5):e0126636.